



100 Years of Earth System Model Development

David A. Randall*

Department of Atmospheric Science, Colorado State University, Fort Collins, Colorado

80523-1371

Cecilia M. Bitz

Department of Atmospheric Sciences, University of Washington, Seattle, Washington 98195

Gokhan Danabasoglu

National Center for Atmospheric Research, Boulder, Colorado 80307-30000

A. Scott Denning

Department of Atmospheric Science, Colorado State University, Fort Collins, Colorado

80523-1371

Peter R. Gent

National Center for Atmospheric Research, Boulder, Colorado 80307-30000

Andrew Gettelman

National Center for Atmospheric Research, Boulder, Colorado 80307-30000

Stephen M. Griffies

Geophysical Fluid Dynamics Laboratory, Princeton, New Jersey 08540

18

Peter Lynch

19

University College Dublin, Dublin, Ireland

20

Hugh Morrison

21

National Center for Atmospheric Research, Boulder, Colorado 80307-3000

22

Robert Pincus

23

University of Colorado/CIRES, Boulder, Colorado

24

John Thuburn

25

University of Exeter, Exeter EX4 4QF, United Kingdom

26 **Corresponding author address:* Department of Atmospheric Science, Colorado State University,

27 Fort Collins, Colorado 80523-1371

28 E-mail: david.randall@colostate.edu

ABSTRACT

29 Today's global Earth System Models began as simple regional models of tro-
30 pospheric weather systems. Over the past century, the physical realism of the
31 models has steadily increased, while the scope of the models has broadened
32 to include the global troposphere and stratosphere, the ocean, the vegetated
33 land surface, and terrestrial ice sheets. This chapter gives an approximately
34 chronological account of the many and profound conceptual and technolog-
35 ical advances that made today's models possible. For brevity, we omit any
36 discussion of the roles of chemistry and biogeochemistry, and terrestrial ice
37 sheets.

38 1. Introduction

39 The development of models for numerical simulation of the atmosphere and oceans was one
40 of the great scientific triumphs of the twentieth century. The models have added enormously to
41 our *understanding* of the diverse and complex processes at work in the Earth system, and to our
42 ability to produce realistic *simulations* of both near-future weather and the longer-term future of
43 the climate system. Understanding and simulation are the two broad goals of model development.

44 Today's global atmospheric models are commonly coupled with ocean models, sea ice models,
45 and land-surface models that include representations of terrestrial vegetation and the carbon cycle.
46 Because of the diversity of processes represented, it is becoming more common to refer to these
47 large coupled models as "Earth System Models," especially when the carbon cycle is included.
48 In ESMs, the atmosphere, ocean, sea ice, and land surface models are included as sub-models,
49 which can be viewed as components of the larger coupled model. Some ESMs also include com-
50 ponents representing atmospheric and marine chemistry, terrestrial ice sheets, ocean biology, and
51 biogeochemistry, but we will not discuss those topics in this chapter. The atmosphere and ocean
52 sub-models of ESMs are often referred to as global circulation models, or "GCMs."

53 Each component of an ESM includes exchanges of mass, momentum and energy with one or
54 more of the other components. The atmosphere model is the only component of an ESM that
55 carries out exchanges with *all* of the other components.

56 The air, water, and ice are in constant motion. In the atmospheric component of an ESM,
57 the adiabatic terms of the equation of motion, the thermodynamic equation, and the continuity
58 equations for dry air, moisture, and chemical species are solved on a three-dimensional grid¹
59 using what is called a "dynamical core"². The horizontal and vertical grid spacings determine the

¹Spectral models are discussed later.

²"Dycore" for the enthusiasts.

60 spatial “resolution” of the model. This chapter includes an overview of the evolution of dynamical
61 cores for global models of the atmosphere and ocean.

62 Atmospheric models also include parametric representations, called “parameterizations,” that
63 are designed to represent the transports by radiation, precipitation, and the unresolved or “subgrid-
64 scale” motions of the air, as well as the phase changes of water, averaged up to the grid scale. This
65 chapter includes a selective overview of the evolution of the parameterizations used in global
66 atmospheric models. All of the parameterized processes are formulated in terms of the fields that
67 are resolved by the model’s dynamical core. A fundamental issue in parameterization development
68 is that the atmosphere and ocean contain eddies on all scales. Early studies aimed to choose the
69 grid spacing so that it coincided with meteorologically inactive scales (e.g., Fiedler and Panofsky
70 1970), but it soon became clear that there is no such “spectral gap;” eddies exist on all scales (e.g.,
71 Nastrom et al. 1984), although of course some are more consequential than others.

72 The dynamical cores of ocean models are designed to cope with the complex geometry of the
73 ocean basins. Numerical modeling of the ocean began somewhat later than numerical modeling
74 of the atmosphere, but has today reached a comparable level of intellectual maturity. This chapter
75 discusses the history of the hydrostatic primitive-equation ocean models used as components of
76 ESMs. Ocean models include parameterizations of the fluxes associated with unresolved motions
77 of the water. We focus on dynamical and numerical aspects, and do not discuss regional and
78 coastal ocean applications, biogeochemistry, or process modeling. Further discussion of ocean
79 physics and dynamics is given in the chapter by Carl Wunsch and colleagues, in this volume.

80 Even sea ice and terrestrial ice sheet models can be said to have dynamical cores, in the sense
81 that they include dynamical equations that govern the motions of the ice. Prior to 1950, there were
82 no publications about sea ice models in English – possibly none at all – and few scientists had
83 ever seen sea ice. Nevertheless, long before weather and climate models simulated the mass or

84 momentum balance of sea ice, scientists recognized the importance for the climate system of the
85 high albedo of sea ice. Early climate modelers used energy balance models with an ice-albedo
86 feedback parameterized by raising the surface albedo when the surface temperature dropped be-
87 low a critical value (Budyko 1969; Sellers 1969). When subjected to climate forcing, such as a
88 reduction in the solar radiation, the energy balance models respond with cooling that is strongest
89 in the high latitudes — a phenomenon now widely known as polar amplification.

90 Land-surface models have no dynamical cores; in that sense, they are “all parameterization.”
91 We humans live on the land surface, so it is hardly surprising that our science has spent a lot
92 of effort to understand and predict conditions there. From the point of view of the atmosphere,
93 the land is merely a lower boundary condition, but it’s also where we grow most of our food,
94 build our cities, and live our lives. Quantitative modeling of land surface processes goes back
95 well over 100 years, primarily with applications to agriculture and water resources. The land
96 surface is an important mediator in the flows of energy, water, carbon, and momentum. The
97 albedo of the land surface is highly variable. Ordinarily, most net radiative energy absorbed by
98 the surface is transferred to the atmosphere as turbulent fluxes of sensible and latent heat, with
99 only a small residual driving changes of heat storage in the soil. These turbulent energy fluxes are
100 important drivers of atmospheric energetics and circulation. Water from precipitation can infiltrate
101 the surface or run off, and infiltrated water is stored and can be released later as vapor. The land
102 surface is a strong sink of atmospheric momentum, and the friction arising from the land surface
103 is felt throughout the atmospheric boundary layer and sometimes far beyond. The topography of
104 the land surface has an enormous impact on the circulation of the atmosphere. Critically, much of
105 the land surface is alive. It is inhabited by vegetation and by microbes in the soil, whose biological
106 processes mediate the partition between turbulent fluxes of sensible and latent heat and regulate
107 the ability of the atmosphere to extract water from beneath the ground. Vegetation is an important

108 determinant of the surface albedo and surface friction. The responses of plants and soil microbes
109 to changes in atmospheric conditions can dramatically affect the surface fluxes.

110 The purpose of this chapter is to give an account of the century or so of *development* work
111 that led to today's ESMs, starting from the early years of the 20th century. Model development
112 involves scientific analysis of how nature works, so that the model can work in the same way as
113 far as possible. Some engineering is also involved, especially to achieve optimal performance on
114 the available computers.

115 In writing this chapter, we have assumed that the readers have some familiarity with numerical
116 modeling of the Earth system, but of course we have tried to avoid unnecessary technical details.
117 Our chapter contains no equations. Applications of the models are briefly mentioned, but not
118 emphasized. The story of the development of ESMs is huge and complicated, and our version
119 of it is unavoidably incomplete. Space limitations make it impossible for us to mention all of
120 the important contributions. We acknowledge our debt to earlier accounts, including those of
121 Smagorinsky (1983); Wiin-Nielsen (1991); Arakawa (2000); Lynch (2006); Washington (2007);
122 Edwards (2010, 2011); Weart (2010); Donner et al. (2011); Harper (2012); Bauer et al. (2015) and
123 Fleming (2016).

124 The chapter is organized chronologically, to the extent possible. The first section deals with
125 the gestational period from about 1900 to 1950. Then, starting with the 1950s, the sections are
126 organized by decade, but with some exceptions to maintain narrative continuity. We tell the story
127 of each decade using several subsections, some of which are focused on particular ESM compo-
128 nents. We have attempted to interweave our accounts of the developments of numerical methods,
129 radiative transfer, turbulence and cloud parameterizations, ocean and sea ice modeling, and land-
130 surface modeling, because of course that's the way it really happened. The all-important and
131 rapidly evolving "supercomputers" needed to run the models are also mentioned in several places.

132 Our chapter inevitably infringes on the subject of numerical weather prediction, which is a major
133 focus of a separate chapter in this volume by Stanley Benjamin and colleagues.

134 **2. Before the Beginning**

135 *a. Early work on dynamical cores*

136 Concepts fundamental to Earth system modeling were developed in the early years of the twen-
137 tieth century. Three visionary scientists played particularly central roles (Fig. 1). The great
138 American meteorologist Cleveland Abbe recognized that meteorology is essentially the applica-
139 tion of hydrodynamics and thermodynamics to the atmosphere (Abbe 1901), and he identified
140 the system of mathematical equations that govern the evolution of the atmosphere (Willis and
141 Hooke 2006). The Norwegian scientist Vilhelm Bjerknes undertook a more explicit analysis of
142 the weather prediction problem from a scientific perspective (Bjerknes 1904). His stated goal was
143 to make meteorology an exact science, a true physics of the atmosphere. He argued that it should
144 be possible to predict changes in the weather by solving systems of partial differential equations,
145 which is exactly what we do today.

146 The English Quaker mathematician, Lewis Fry Richardson, went further. He wanted a worked
147 example for his book “Weather Prediction by Numerical Processes” (Richardson 1922). Partly to
148 create such an example, he attempted what is now called numerical weather prediction (NWP): a
149 direct (but approximate) solution of the equations of motion. The result was his famous “failed”
150 numerical forecast (actually a hindcast) for May 20, 1910. He carried out the calculations by hand,
151 in the intervals between driving for the Friends Ambulance Unit during the war in France (Ashford
152 1985; Lynch 2006). Although his results were not realistic, his achievement was heroic, and his
153 book was remarkably prescient. His overall approach bears a striking resemblance to that used in

154 modern weather and climate models, and he appreciated many of the issues that still preoccupy
155 modelers today. In particular, he understood that the large-scale dynamics of the atmosphere would
156 be resolved, while other processes, such as radiation, boundary layer turbulence, and cloud pro-
157 cesses, would have to be parameterized. He used what we now call the quasi-static approximation.
158 In order to obtain approximate solutions of the differential equations of the model, he proposed
159 a method based on finite differences, a technique that he had devised and previously applied to
160 stresses in a masonry dam (Richardson 1911). He discretized his domain on a longitude-latitude
161 grid or “lattice” that covered part of western Europe, with five layers to represent the atmosphere’s
162 vertical structure. He understood that a staggered arrangement of variables on the grid could im-
163 prove the accuracy of finite differences, and he used what we would now recognize as a pair of
164 C-grids (Lynch 2006; Arakawa and Lamb 1977). He also foresaw that his proposed grid would
165 present difficulties in the polar regions. His model included equations for predicting soil moisture
166 based on empirical work by hydrologists in the mid-19th century. He knew that the weather is
167 influenced by terrestrial vegetation, which had already been appreciated by Von Humboldt et al.
168 (1859), and he understood the role of plant physiology in regulating the extraction of water from
169 the soil (transpiration). Finally, he provided suggestions for initializing and integrating his model.

170 Richardson’s hindcast gave a totally unrealistic rate of change of the surface pressure: 145 hPa
171 over a six-hour period. The full story of Richardson’s work, the reason for his disappointing
172 numerical results and a complete reconstruction of the forecast are described by Lynch (2006).
173 When, in a later retrospective recreation, Richardson’s initial data were dynamically balanced, the
174 initial tendency of surface pressure was reduced to a reasonable value of less than 1 hPa over six
175 hours, confirming that his unrealistic prediction was due to the dynamical imbalance of the initial
176 data that he used. Details are presented in Lynch (2006).

177 Richardson's forecasting scheme was quite impractical in the pre-computer era, but he was un-
178 daunted, speculating that "some day in the dim future it will be possible to advance the compu-
179 tations faster than the weather advances." In fact, developments on several fronts were necessary
180 before NWP could be put into practice. First, a more complete understanding of atmospheric
181 dynamics allowed the development of simplified but sufficiently general systems of equations.
182 Advances in what used to be called "physical meteorology" pointed the way to useful statistical
183 representations of the effects of unresolved physical processes on the resolved scales. Regular
184 observations of the free atmosphere provided the initial conditions needed for numerical weather
185 prediction; accurate and stable discretization schemes were developed. Finally, increasingly pow-
186 erful digital computers provided a practical means of carrying out the prodigious calculations
187 needed to forecast changes in the weather.

188 At the time of the First World War, computational weather forecasting was impractical for at
189 least four reasons. First, the observations of the three-dimensional structure of the atmosphere
190 were available only on a very occasional basis, with inadequate coverage, and never in real time.
191 The registering balloons had to be recovered and the recordings analyzed to obtain the data, a pro-
192 cess that took days or even weeks. Second, the numerical algorithms for solving the atmospheric
193 equations were subject to instabilities that were not understood. Because of this, the numerical
194 solution might bear little or no resemblance to the solution of the continuous equations. Third, the
195 nearly balanced (e.g., nearly geostrophic) nature of atmospheric flow was not yet understood, and
196 the imbalances arising from observational and analysis errors confounded Richardson's forecast.
197 Fourth, the massive volume of computation required to advance the numerical solution could not
198 be carried out, even by a huge team of human computers. In reality, Richardson's estimate that
199 64,000 human computers would be needed to do the calculations for a useful forecast in real time,
200 was a gross under-estimate. It has been reckoned that closer to one million people would have

201 been required for the task (Lynch et al. 1993). It seems fair to say that what Richardson devised
202 was a “method without a means.”

203 In the ensuing decades, a variety of key developments prepared the way for progress. Theo-
204 retical developments provided crucial understanding of atmospheric dynamics, in particular the
205 approximate balance of the large-scale atmospheric state and the means of eliminating spurious
206 high-frequency gravity-waves. This led to the quasi-geostrophic equations, which filter gravity
207 waves and describe the large-scale motions of atmosphere away from the Equator. Advances in
208 numerical analysis led to the design of stable algorithms that faithfully replicated the true solution
209 provided that certain restrictions on the size of the time step were respected. Timely observations
210 of the three-dimensional atmosphere became available following the invention of the radiosonde
211 in 1927. This provided real-time measurements of pressure, temperature, humidity and winds
212 through a vertical column of the atmosphere. Finally, the development of digital computers pro-
213 vided a way of attacking the enormous computational task of weather forecasting.

214 The Electronic Numerical Integrator and Computer (ENIAC), an electronic computer commis-
215 sioned by the United States Army for calculating the paths of projectiles, was completed in 1945.
216 It was the first programmable electronic digital computer ever built. The gigantic machine used
217 18,000 thermionic tubes, filled a large room, and consumed 140 kW of power (Fig. 2). Both input
218 and output were by means of punched cards. McCartney (1999) provides an absorbing account of
219 the origins, design, development and legacy of ENIAC.

220 In the late 1940s, the mathematician John von Neumann recognized that weather forecasting, a
221 problem of both great economic and military importance, and strong intrinsic scientific interest, is
222 an ideal application for a digital computer. He established a Meteorology Project at the Institute
223 for Advanced Study in Princeton, and recruited meteorologist Jule Charney to lead it. The project
224 created a model in which the atmosphere was treated as a single layer, represented by conditions at

225 the 500 hPa level. ENIAC was used to time-step the barotropic vorticity equation, which expresses
226 the conservation of absolute vorticity following the flow, and filters out gravity-wave solutions.
227 Centered-in-space finite differences were used to evaluate the vorticity transport, and leapfrog
228 time-differencing was used. A Poisson equation was solved obtain the geopotential height from
229 the predicted vorticity. Fortunately, Charney and his colleagues were aware of the work of Courant
230 et al. (1928, 1967), which showed that in order for their explicit time-stepping method to be stable,
231 the size of the time step cannot exceed the grid size divided by the signal speed, a constraint
232 that we now call the CFL (Courant-Friedrichs-Lewey) criterion.³ With the barotropic vorticity
233 equation, the relevant signal speed is the wind speed; in a system that permits gravity waves the
234 signal speed would be the much faster speed of wave propagation, and as a result the time step
235 would have to be much smaller to satisfy the CFL criterion for stability. The initial data for the
236 forecasts were prepared manually from standard operational 500 hPa analysis charts produced by
237 the U.S. Weather Bureau. The heights were held constant on the outer boundaries of the domain,
238 throughout each 24-hour integration.

239 The resulting numerical predictions, carried out on ENIAC, were truly ground-breaking. Four
240 24-hour forecasts were carried out, and the results clearly showed that the large-scale features
241 of the mid-tropospheric flow could be predicted numerically with a reasonable resemblance to
242 reality. The forecasts were described in a seminal paper by Jule Charney, Ragnar Fjørtoft and
243 John von Neumann (Charney et al. 1950). The success of the ENIAC forecasts had an electrifying
244 effect on the meteorological community, world-wide. Several baroclinic (multi-level) models were
245 developed in the following years. All of them were based on the filtered or quasi-geostrophic
246 system of equations. Later, models using the more accurate primitive equations were introduced.

³More generally, a necessary condition for stability is that the domain of dependence of the numerical solution at any point should contain the corresponding physical domain of dependence.

247 Charney had anticipated this as a necessary step, and indeed André Robert later identified it as a
248 key development in numerical weather prediction (see Lin et al. 1997).

249 Charney et al. (1950) noted that the computation time for a 24-hour forecast was about 24 hours.
250 In other words, the team could just keep pace with the weather, provided that the ENIAC did
251 not fail. The computation time included off-line operations, such as the reading, punching, and
252 interfiling of punch cards. Lynch and Lynch (2008) recreated the ENIAC integrations using a
253 programmable cell phone, which they called the “Portable Hand-Operated Numerical Integrator
254 and Computer,” or PHONIAAC. In this recreation, PHONIAAC executed the main loop of the 24-hour
255 forecast in less than one second.

256 *b. Early work on radiative transfer*

257 Thanks to astronomers, methods that can be used for calculating radiative heating rates and
258 fluxes in the Earth’s atmosphere have been available since the first half of the twentieth century.
259 Astronomers developed the two-stream methods used to compute the fluxes of radiation (Schuster
260 1905; Eddington 1916). The idea of collecting together parts of the spectrum with similar amounts
261 of absorption, which forms the basis of the k -distribution technique now used in ESMs, was orig-
262 inally proposed by Ambartsumian (1936). The theory describing the scattering of light by round
263 particles like cloud drops is usually attributed to Mie (1908).

264 Radiative transfer is fundamentally important for ESMs because radiation is (almost) the only
265 mechanism by which the Earth can exchange energy with the rest of the universe, and because
266 motions of the atmosphere are fundamentally driven by spatial gradients in the electromagnetic
267 radiation emitted by the Earth, its atmosphere, and the Sun. The same gradients also play a key role
268 in determining the thermal structure of the atmosphere. The deep convective clouds of the tropics
269 arise from a rough balance between destabilization by radiative cooling and the response of deep

270 convection, for example, while the planetary-scale Hadley circulation is driven by the gradient
271 in absorbed sunlight between the equator and higher latitudes. Models of atmospheric motion
272 therefore need to represent the flow of radiation through the atmosphere, especially the radiative
273 flux divergences within the atmosphere that give rise to heating and cooling, and the fluxes of
274 radiation that are absorbed (and emitted) by the surface. Models that are aimed at understanding
275 climate (as opposed to weather) must accurately compute the net energy input at the top of the
276 atmosphere.

277 The practical calculations needed to advance an atmospheric model are daunting, even today.
278 The underlying reason is that the solution to the radiative transfer equation is non-linear in the
279 parameters used in the equation (optical depth τ , single-scattering albedo ω_0 , and some measure
280 of the scattering phase function, often the asymmetry parameter g). These parameters are quite
281 variable in the earth's atmosphere. For clear skies the primary problem is that the extinction, the
282 differential value of τ , of gases varies by many orders of magnitude in very small spectral regions
283 around each of the thousands to millions of absorption lines associated with each gas. Clouds
284 present a different class of problem. Compared to the optical depths of gases, the optical depth of
285 clouds varies far more smoothly with wavelength and by only three or four orders of magnitude
286 overall, but much more rapidly in time and space.

287 The history of radiative transfer parameterizations for ESMs is about maximizing the utility
288 of available computational power by focusing our scientific thinking on specific, motivating prob-
289 lems. One theme that emerges is that computational challenges have, over the last century, sparked
290 useful insights and novel methods. A second is that the collective efforts to understand parameteri-
291 zation errors by comparison to reference line-by-line models have been instrumental in identifying
292 the sources and magnitudes of those errors and pointing to possible solutions.

293 *c. Where things stood in 1950*

294 As the 1940s came to an end, new data sources were being used to carry out pioneering obser-
295 vational studies of the global circulation of the atmosphere, notably by Victor Starr's group at the
296 Massachusetts Institute of Technology (MIT; Starr 1948; Starr and White 1951), Eric Palmén and
297 colleagues in Finland and at the University of Chicago (Palmén 1948; Palmén and Riehl 1957),
298 and Jacob Bjerknes (the son of Vilhelm Bjerknes, who was mentioned earlier) and Yale Mintz at
299 the University of California at Los Angeles (UCLA; Mintz and Bjerknes 1951; Bjerknes 1955).
300 These observations proved to be both a motivation for and a basis for evaluation of the global
301 atmospheric models that were soon to follow.

302 **3. The 1950s**

303 The 1950s saw some major advances in our understanding of the global circulation. For exam-
304 ple, Edward Lorenz (1955) of MIT published the first of his most influential papers, which defined
305 and analyzed available potential energy, and provided important insights into the atmospheric en-
306 ergy cycle. At the University of Chicago, David Fultz carried out rotating annulus experiments that
307 reproduced some of the observed characteristics of the global circulation of the atmosphere (Fultz
308 et al. 1959). Both of these studies (and many others) influenced the development of atmospheric
309 numerical models during the 1950s.

310 *a. Progress with dynamical cores*

311 The landmark NWP success of Charney et al. (1950) was soon emulated in several other places
312 around the world (e.g., Persson 2005b). As the 1950s unfolded, operational numerical weather
313 prediction began in Sweden (1954; Bolin 1955), the United States of America (1955), and Japan
314 (1959; Lynch 2006; Persson 2005a,c), though none of those early models were global or even

315 hemispheric. During this period, experiments began with three-dimensional models that could
316 supplant the barotropic vorticity equation. At first, these continued to use filtered systems of equa-
317 tions that have no gravity-wave solutions, but more accurate systems were needed. Early baroclinic
318 models were developed by Charney and Phillips (1953), and experimental forecasts with the prim-
319 itive equations were carried out by Hinkelmann (1951). Later, Charney (1962) experimented with
320 both the primitive and balance equations. The forecasts produced using three-dimensional filtered
321 models were not much better than those produced using the barotropic vorticity equation, and
322 this motivated more work on hydrostatic primitive equation models (e.g., Shuman and Hovermale
323 1968; Bushby and Timpson 1967). Because the primitive equations support rapidly propagating
324 gravity waves, a shorter time step is needed to ensure computational stability. In compensation,
325 primitive-equation models do not need the expensive elliptic solvers of the quasigeostrophic and
326 balanced models.

327 Early model builders had to make some very basic choices that are still under discussion today.
328 An example is the choice of how the different variables in the model should be arranged in the
329 vertical. Charney and Phillips (1953) offset the thermodynamic variable, potential temperature θ ,
330 relative to the horizontal wind components u and v , because this arrangement is natural to capture
331 hydrostatic and thermal wind balance. Lorenz (1960), on the other hand, placed θ at the same
332 levels as u and v (Fig. 3), because that arrangement is advantageous for conservation of total
333 energy.

334 Subsequent applications of the Charney-Phillips and Lorenz vertical grids with more complete
335 equation sets showed that the Charney-Phillips grid better captures wave motions that depend on
336 buoyancy (e.g., Thuburn and Woollings 2005, and references therein). It also showed that the
337 Lorenz grid possesses a computational mode—a pattern of perturbations in the model variables
338 that is invisible to the numerical method and consequently behaves unphysically, for example by

339 failing to propagate (Tokioka 1978; Arakawa and Moorthi 1988). However, a satisfactory scheme
340 for achieving energy conservation with a Charney-Phillips grid has proved elusive. For many
341 years, Lorenz's choice was almost universally adopted, but the relative merits of the Charney-
342 Phillips and Lorenz grids were revisited several decades later (Arakawa and Moorthi 1988). Some
343 recently developed models use the Charney-Phillips grid (e.g., Girard et al. 2014; Wood et al. 2014)
344 while others use the Lorenz grid (e.g., Untch and Hortal 2004; Satoh et al. 2008a; Skamarock et al.
345 2012a; Zängl et al. 2015). The debate continues.

346 The dynamical simulation of climate using numerical models can be said to have started in 1956,
347 when Norman Phillips carried out the first extended-range simulation of the global circulation
348 of the atmosphere (Phillips 1956; Lewis 1998). The model predicted the winds at two vertical
349 levels with, naturally, the Charney-Phillips vertical grid, which means that there was only one
350 prognostic temperature, in the middle troposphere. The model was quasi-geostrophic, on a beta-
351 plane channel, with just 16 x 17 grid columns. It was driven by a specified meridionally varying
352 distribution of heating and cooling. Because the temperature was predicted at only one level, the
353 static stability had to be prescribed; a smaller-than-observed value was used to mimic the effects
354 of moist convection. Starting from a zonal flow with small random perturbations, a disturbance
355 with a wavelength of 6000 km developed. It had the characteristic westward tilt with height of
356 a developing baroclinic wave. Phillips examined the energy transformations associated with the
357 developing wave, and found good qualitative agreement with observations of baroclinic systems
358 in the atmosphere.

359 His simulation broke down after a few simulated weeks, due to a previously unknown form of
360 numerical instability (Phillips 1959). It was not of the sort of instability that results from violation
361 of the CFL criterion; instead, it turned out to be an inherently nonlinear instability in which the
362 spatial scale of nonlinear terms is misrepresented ('aliased') by the finite-resolution grid, leading

363 to feedback and the growth of small-scale noise (Phillips 1959). This type of instability can occur,
364 in principle, even in a time-continuous model. Arakawa (1966) reasoned that if the Jacobian term
365 could be computed in such a way as to conserve either energy or enstrophy then there would be
366 “no room for nonlinear computational instability.” Moreover, conservation of *both* energy and
367 enstrophy would prevent an unrealistic downscale cascade of energy. This motivated Arakawa to
368 develop his energy- and enstrophy-conserving finite-difference Jacobian. The value of numerical
369 methods that conserve physically important quantities emerged as a major theme in later work
370 (e.g., Thuburn 2008).

371 Von Neumann was tremendously impressed by Phillips’ work. To explore its implications, he
372 arranged a conference at Princeton University in October 1955 on “Application of Numerical In-
373 tegration Techniques to the Problem of the General Circulation.” The workshop had a galvanizing
374 effect on the meteorological community. Within ten years, there were several major research
375 groups modeling the global circulation of the atmosphere. The first sign of these impending de-
376 velopments was Smagorinsky’s two-level model, formulated using a zonal channel on the sphere
377 (Smagorinsky 1958).

378 In a further important advance, Norman Phillips proposed the use of the terrain-following σ
379 coordinate (Phillips 1957a), which greatly simplifies the lower boundary conditions of atmospheric
380 models. Variations of the σ coordinate are still very widely used today. Phillips’ invention of the
381 σ coordinate marks the beginning of a multi-decadal search for the *optimal* vertical coordinate
382 systems for use in both atmosphere and ocean models. We return to that story later in this chapter.

383 *b. Early work on parameterizations of the boundary layer, the land surface, clouds, and cumulus*
384 *convection*

385 The exchanges of momentum, sensible heat, and moisture between the atmosphere and the lower
386 boundary are fundamental to understanding the Earth system. In a key development of the 1950s,
387 the Russian scientists Monin and Obukhov formulated a similarity theory for the “surface layer,”
388 which is the lower portion of the atmospheric boundary layer (Monin and Obukhov 1954; Foken
389 2006). They showed how the surface fluxes of sensible heat and momentum are related to the
390 near-surface profiles of temperature and wind. Later their ideas were extended to include the
391 surface moisture flux over the oceans and other water surfaces. Two decades later the similarity
392 functions described by Monin and Obukhov were measured in famous field experiments carried
393 out in Kansas (Businger et al. 1971; Haugen et al. 1971) and Minnesota (Izumi and Caughey 1976).
394 Today, Monin-Obukhov similarity theory is used to determine the surfaces fluxes of sensible heat,
395 momentum, and moisture in virtually all atmospheric models. Further discussion is given in the
396 chapter in this volume on *100 years of progress in boundary-layer meteorology*, by Margaret
397 LeMone and colleagues.

398 The 1950s produced major advances in understanding the atmospheric boundary layer and cu-
399 mulus clouds. Joanne Starr Malkus Simpson and colleagues carried out pioneering observations
400 of turbulence and cumulus convection over the tropical and subtropical oceans, and developed
401 simple and insightful theories of cumulus updrafts and downdrafts (Bunker et al. 1949; Malkus
402 1952; Starr Malkus 1954, 1955; Simpson et al. 1965; Simpson and Wiggert 1969). Their ideas
403 played crucial roles in the subsequent development of parameterizations of the boundary layer
404 and cumulus convection. It is an interesting fact that the concept of cumulus entrainment, which

405 plays an important role in those parameterizations, was first discussed by *oceanographer* Henry
406 Stommel (1951).

407 Riehl and Malkus (1958) used the (relatively meager) observations of their time to analyze
408 the flows of energy through what we now call the Intertropical Convergence Zone (ITCZ). They
409 drew the fundamentally important conclusion that thunderstorms strongly transport energy upward
410 through the depth of the tropical troposphere, and that at some levels the upward energy flux is
411 against the gradient. Their study motivated the representation of cumulus updrafts as penetrative
412 “hot towers” that act like express elevators, carrying energy and other quantities upward through
413 the troposphere in an hour or less. As we will see, these ideas were widely used in cumulus
414 parameterizations during the 1960s and later.

415 Cloud microphysics deals with cloud and precipitation particles, including their formation and
416 the processes governing their evolution such as condensation, evaporation, melting and freezing.
417 Since these processes act at the microscale (smaller than a micron to centimeters), they cannot be
418 resolved and must be parameterized in all weather and climate models, now and for the foreseeable
419 future. The parameterizations must describe the net effects of interactions between sub-grid scale
420 microphysical processes and the grid-scale temperature, water vapor, and winds. The parameter-
421 ization of microphysics plays an essential role in quantitative precipitation forecasting, coupling
422 with the model dynamics through latent heating and the condensate weight, radiative transfer, and
423 coupling with aerosols and chemistry. While the roots of cloud microphysics extend back several
424 centuries, quantitative understanding was not established until fairly recently. A rapid acceleration
425 of microphysics research began abruptly around 1940, coinciding with growing military interest
426 in cloud processes, the development of new observational techniques including radar, and a hope
427 that it might be possible to modify precipitation production through artificial means (Pruppacher
428 and Klett 1997). Cloud microphysics, and moist physics more generally, had a limited role in the

429 early development of weather and climate models, because extreme simplicity was required. We
430 will return to the subject of cloud physics later in this chapter. For a more thorough discussion
431 of the history of cloud physics research, see the chapter in this volume by Sonia Kreidenweis and
432 colleagues.

433 Modern land-surface models also draw on important ideas from the 1950s. Soil temperature as
434 a function of depth can be modeled as thermal diffusion of heat in the vertical, given estimates
435 of heat capacity and thermal diffusivity (Lettau 1954). The vertical heat flux through the soil
436 column is determined by the temperature difference between the air and the soil surface. Penman
437 (1948) derived a simple parameterization for the rate of evaporation from a wet surface based on
438 vapor pressure, wind speed, and net radiation. The chapter in this volume by Christa Peters-Lidard
439 and colleagues summarizes 100 years of progress in hydrology, which is an important aspect of
440 land-surface modeling.

441 *c. Approaching 1960*

442 As the 1950s drew to a close, the International Geophysical Year raised the profile of the Earth
443 sciences (Sullivan 1961). Major technological innovations were also occurring. Digital computers
444 were becoming more powerful, easier to program, and much more widely available. Beginning
445 with Sputnik in 1957, artificial satellites were launched into orbit, soon to be followed by quan-
446 titative satellite-based observations of the Earth. In the following decades, both of these new
447 technologies had major impacts on the development and applications of ESMs.

448 **4. Model development in the Age of Aquarius**

449 The culturally, scientifically, and technologically tumultuous 1960s produced multiple landmark
450 advances in the development of ESMs, including the creation of several now-legendary “ances-

451 tral” models, which were aimed mainly at climate simulation rather than weather prediction. In
452 many cases, the earliest versions of the ancestral models were not truly global, and used simplified
453 geography. They incorporated simple parameterizations of surface fluxes, radiation, cumulus con-
454 vection and stratiform or “large-scale” clouds, and they were coupled to very simple land-surface
455 models. With one important exception they used prescribed sea surface temperatures (SSTs),
456 rather than coupling with an ocean model.

457 *a. The GFDL model*

458 Joseph Smagorinsky was the first director of the Geophysical Fluid Dynamics Laboratory
459 (GFDL) of the National Oceanographic and Atmospheric Administration. His vision was to re-
460 cruit a team of scientists focused on the multi-decadal task of using numerical models as an aid to
461 understanding the global circulation of the atmosphere (Lewis 2008). GFDL’s atmosphere model
462 was developed by Smagorinsky, Syukuro Manabe, and collaborators (Smagorinsky et al. 1965;
463 Manabe and Smagorinsky 1967). Early versions covered only the northern hemisphere, with a
464 stereographic map projection, and used idealized geography. The GFDL model used the σ co-
465 ordinate of Phillips (1957a). Some versions used “reduced grids” with fewer grid points around
466 latitude circles near the poles (Kurihara 1965). By 1965, the GFDL model had relatively high
467 vertical resolution for the time, with nine glorious layers.

468 During the 1960s, the GFDL modeling team achieved many important firsts, including a very
469 influential parameterization for the horizontal diffusion of momentum (Smagorinsky 1963), the
470 first radiation parameterization (Manabe and Möller 1961a; Manabe and Strickler 1964a), the first
471 cumulus parameterization (Smagorinsky 1963; Smagorinsky et al. 1965; Manabe et al. 1965), and
472 the first land-surface model (Budyko and Zubenok 1961; Manabe 1969a). Fig. 4 schematically
473 summarizes the formulation of the early GFDL model (Manabe 1969b).

474 Smagorinsky addressed the parameterization of precipitation from stratiform clouds (Smagorin-
475 sky and Collins 1955; Smagorinsky 1960), but he did not propose methods to represent cumulus
476 convection or the radiative effects of the clouds. The cumulus problem was tackled by Manabe
477 et al. (1965), who developed what is widely known as “moist convective adjustment.” Before the
478 implementation of moist convective adjustment, the GFDL atmosphere model produced unrealistic
479 results in humid regions with steep lapse rates. Manabe et al. (1965) wrote that

480 “...Because of convective instability, intense grid-scale convection develops exponen-
481 tially in the area where the lapse rate is unstable. ...Therefore, it is desirable to design a
482 scheme of convection such that the grid-scale convection does not develop....We used a
483 very simple scheme of convective adjustment depending upon both relative humidity and
484 the lapse rate and successfully avoided the abnormal growth of grid-scale convection.”

485 Moist convective adjustment was designed to remove convective instability by adjusting the lapse
486 rate back to “moist neutral,” and limiting the relative humidity to 100% or less, while minimizing
487 complexity. Moist convective adjustment couples neighboring layers of a model, pairwise. It does
488 not try to represent the penetrative nature of deep convection, which had been emphasized by Riehl
489 and Malkus (1958). Moist convective adjustment is still being used in some of today’s models.

490 Early results from the GFDL atmosphere model were published by Smagorinsky (1963) and
491 Manabe et al. (1965). The primary application of the GFDL model was climate simulation, but
492 Miyakoda et al. (1969) also used versions of the model in experimental NWP.

493 GFDL scientists also developed a simple but explicit representation of the surface energy bal-
494 ance over land. The bulk aerodynamic formula of Penman (1948) had been extended by Monteith
495 (1965), who combined the constraints of surface energy balance with the conservation of wa-
496 ter through turbulent transport. The combined Penman-Monteith equation includes the effect of

497 surface or stomatal resistance to evapotranspiration. Stomata are microscopic pores on the under-
498 side of plant leaves through which water evaporates, whose apertures provide the physiological
499 mechanism for control of evapotranspiration. The Penman-Monteith equation has long been used
500 by farmers and engineers to estimate the evapotranspiration, but the estimation of stomatal con-
501 ductance remains entirely empirical. Budyko and Zubenok (1961) suggested that physiological
502 control ratio of the ratio of actual evapotranspiration to the potential evapotranspiration could be
503 usefully approximated by a linear ramp between 0 and 1 as soil moisture varied from the wilting
504 point to field capacity. The linear ramp was adapted by Manabe (1969a), who represented soil
505 hydrology by analogy to a bucket of water. Rainfall is added to the soil bucket, whose capacity is
506 arbitrarily set to 15 cm. Adding additional rainfall when the bucket is full leads to runoff. Evap-
507 otranspiration removes water from the bucket at a rate β times the potential evapotranspiration
508 rate, where β is just the ratio of the current contents of the bucket to its capacity. The linear ramp
509 incorporated through β represents the well-known tendency of vegetation to take up less and less
510 water as root-zone soil moisture is depleted.

511 The origins of numerical ocean circulation modeling can also be traced to GFDL. Smagorin-
512 sky recognized the importance of developing a World Ocean circulation model, and in 1960 he
513 hired Kirk Bryan to lead GFDL's ocean modeling project. It was a massive undertaking, believed
514 by many to be a fool's mission with extensive known and unknown scientific and engineering
515 challenges. There were prominent naysayers in the community who felt that such efforts were
516 ill-advised at best. Fortunately, Bryan was able to leverage from GFDL's work on atmospheric
517 numerical models. Mike Cox was an additional member of the ocean modeling team, whose pio-
518 neering scientific programming skills proved critical to the success of the project (Bryan 1991).

519 Bryan and Cox made assumptions to allow for efficient numerical integration using the com-
520 puters available in the 1960s. One of these assumptions was a rigid lid for the upper boundary of

521 the ocean. A rigid lid eliminates fast external gravity waves (effectively making their speed infi-
522 nite), and converts a hyperbolic problem for surface gravity waves into an elliptic boundary value
523 problem for the barotropic (depth integrated) streamfunction of the circulation. This innovation al-
524 lowed for the use of relatively long time steps, thus enabling the century-long integrations needed
525 for climate studies. An additional key element of the model was a momentum advection scheme
526 based on the approach of Arakawa (1966) to remove nonlinear instabilities that had plagued mod-
527 els at that time (Bryan 1966). Bryan chose the Arakawa B-grid (Arakawa and Lamb 1977) for
528 staggering of tracer and velocity variables. This choice rendered a relatively accurate numerical
529 calculation of geostrophically balanced motions using the coarse resolution allowed by computers
530 of the day. Bryan and Cox completed their prototype World Ocean model in the mid-1960s (Bryan
531 and Cox 1967). Their pioneering work has now been followed by nearly 50 years of enhancements
532 and refinements. The further evolution of the Bryan-Cox code is discussed in Section 5 e.

533 Bryan's ocean model was soon coupled to GFDL's global atmosphere model to create the world's
534 first global coupled atmosphere-ocean model (Manabe and Bryan 1969), although with idealized
535 geography. The fundamental importance of ocean-atmosphere interactions for climate makes it
536 reasonable to say that the model of Manabe and Bryan (1969) was the first true climate model – a
537 major milestone.

538 The GFDL ocean model was coupled with a sea ice model (Manabe 1969b; Bryan 1969a), which
539 treated the sea ice as a slab of uniform thickness in each grid cell, with all-or-nothing coverage.
540 The temperature profile of the sea ice was assumed to be linear and the effects of salt trapped in
541 the sea ice were neglected. Sea ice less than 3 m thick was advected at the speed of ocean currents
542 averaged over the upper 100 m, while thicker ice was assumed to be locked in place, so it could

543 not converge indefinitely and build to excess. This method for treating sea ice motion came to be
544 known as “free-drift with stoppage⁴.”

545 The domain and geography of the GFDL model were gradually made more realistic. First results
546 from a global version of the model, with realistic topography, were published by Holloway and
547 Manabe (1971).

548 *b. Leith’s model*

549 Starting in 1960, the Livermore model (Leith 1965a,b, 1988; Michael 1996) was developed
550 single-handedly by Cecil “Chuck” Leith of the Lawrence Radiation Laboratory.⁵ Leith’s model ran
551 on the Livermore Automatic Research Calculator (LARC), which was one of the first computers
552 to use transistors rather than vacuum tubes. At first the model represented only the northern
553 hemisphere up to 60° north, but a later version was truly global. It used a spherical grid based
554 on longitude and latitude, with a grid spacing of 5° in each direction, but with fewer grid points
555 around latitude circles near the poles. It had five layers, and used pressure as its vertical coordinate
556 – the only numerical model of the atmosphere ever to do so, as far as we know. The surface
557 pressure was predicted. The effects of mountains were not included. The model predicted water
558 vapor, and included the warming effects of latent heat release, as well as precipitation, but had no
559 parameterization of cumulus convection. It did include a parameterization of radiative transfer,
560 including the diurnal cycle, but neglected the radiative effects of clouds. Leith’s dynamical core
561 needed very strong damping to maintain numerical stability. His model had a relatively short
562 lifetime, because his interests shifted towards two-dimensional turbulence. In 1968, he relocated
563 to the National Center for Atmospheric Research (NCAR), which, as discussed below, had its
564 own global modeling project. After moving to NCAR, Leith continued his studies of large-scale

⁴Which sounds like some sort of plumbing problem.

⁵The Lawrence Radiation Laboratory was later renamed as the Lawrence Livermore National Laboratory.

565 atmospheric turbulence, but he was only peripherally involved in the development of NCAR's
566 global atmospheric model.

567 *c. The UCLA model*

568 Beginning in 1961, the UCLA model (Arakawa et al. 1968; Langlois and Kwok 1969; Arakawa
569 1972) was developed by Akio Arakawa and collaborators, including Yale Mintz, at the University
570 of California at Los Angeles. It was the only one of the four ancestral models to be developed at
571 a university. A detailed first-person account of the project is given by Arakawa (2000). The early
572 two-level version of the model, which was finished in 1963, did not predict water vapor, but it was
573 global and had a realistic (but low-resolution) land-sea distribution and topography. Results from
574 this version were published by Mintz (1968).

575 The UCLA model brought several important innovations. Its dynamical core used what are now
576 called “finite-volume” methods for both advection and the horizontal pressure-gradient force. It
577 was designed with an emphasis on conservation of mass, energy (Arakawa 1966; Lilly 1997;
578 Arakawa 1972) and other important quantities. These conservation properties were achieved
579 through what are now called “mimetic” discretization methods (Hyman and Shashkov 1997). The
580 model's dynamical core was designed to optimally simulate the propagation of inertia-gravity
581 waves, including the shortest waves that could be represented on the grid (Arakawa and Lamb
582 1977).

583 The cumulus parameterization of the early UCLA model made use of the entraining-plume ideas
584 advocated by Stommel (1951), Riehl and Malkus (1958), and Simpson and Wiggert (1969). It al-
585 lowed multiple “types” of cumulus clouds; the number of cloud types was determined by the
586 number of layers used, which was three at the time. The UCLA model was the first to use the
587 “mass flux” approach for parameterizing convection (Arakawa 1969), which has now been almost

588 universally adopted. The closure used in the cumulus parameterization removed convective insta-
589 bility, but allowed a less-than-saturated relative humidity. The model's radiation parameterization
590 (Katayama 1967, 1972) included the diurnal cycle and the radiative effects of the predicted clouds.

591 *d. The NCAR model*

592 NCAR's first global atmospheric model was developed by Akira Kasahara, Warren Washington,
593 and David Williamson. The earliest version had two levels (Kasahara and Washington 1967;
594 Washington and Kasahara 1970; Olinger et al. 1970). It had no orography, and water vapor was
595 assumed to be at its saturation value throughout the atmosphere, so that latent heat was released
596 wherever and whenever the air moved upward. The NCAR model was the first (and so far only)
597 quasi-static global model to use constant-height surfaces as its vertical coordinate. Richardson's
598 equation was solved to determine the vertical velocity. Kasahara and Washington (1969), Kasahara
599 and Washington (1971) and Washington and Williamson (1977) described a later six-level version
600 of the model, which included the effects of mountains and predicted clouds. It was coupled to a
601 simple land-surface model. The radiation parameterization was developed by Sasamori (1968).

602 *e. Additional advances during the 1960s*

603 Radiation parameterizations for atmospheric models need to account for heating and cooling
604 by gases that vary in concentration within the atmosphere, notably water vapor and ozone. Early
605 models focused on the impacts of individual gases (carbon dioxide, ozone, and especially wa-
606 ter vapor) on radiation and heating rates within the atmosphere, exploiting the fact that each gas
607 affects a different spectral region. Some approaches used gas amounts as a function of tempera-
608 ture to compute a broadband emissivity (Elsasser and Culbertson 1960) by fitting to observations
609 and/or laboratory data. Emissivity could be used to compute heating rates from a spectrally inte-

610 grated equation describing flux (e.g. Sasamori 1968). Others used band models (Curtis and Goody
611 1954, is one example) in which an assumed distribution of absorption line shapes, strengths, and
612 relative positions determines the average transmission of a model layer as a function of absorber
613 amount, temperature, and pressure within some finite spectral region. The absorption features of
614 each gas were assumed to be spectrally independent so that the total transmission is the product of
615 the transmission due to each gas. Total fluxes and heating rates can then be computed by adding up
616 contributions from each spectral region. Longwave cooling calculations were typically expressed
617 as matrix problems, following Curtis (1956) and Rodgers and Walshaw (1966). This approach
618 describes the exchange of radiation between pairs of not necessarily contiguous layers, and be-
619 tween each layer and the upper and lower boundary (space and the surface, respectively). Such a
620 calculation scales as the number of layers squared times the number of spectral intervals, but the
621 relatively coarse vertical and spectral resolutions of the time made it practical.

622 A desire to simulate the global circulation of the atmosphere on a more or less homogeneous grid
623 motivated some early interest in quasi-uniform spherical grids, including overset grids (Phillips
624 1957b), icosahedral grids (Williamson 1968; Sadourny et al. 1968), and cubed spheres (Sadourny
625 1972). The first results with these methods were not very encouraging, however, and with the
626 emergence of the spectral transform method around that time (Eliassen et al. 1970; Orszag 1970),
627 interest waned until the 1990s. Both quasi-uniform spherical grids and the spectral method are
628 discussed further later in this chapter.

629 The U.S. National Meteorological Center developed the first operational NWP model to incor-
630 porate precipitation and the effects of latent heating at (Shuman and Hovermale 1968). The model
631 predicted the precipitable water, i.e., the total amount of water vapor in each atmospheric column,
632 and instantaneously converted vapor to surface precipitation when the precipitable water in a grid
633 cell exceeded 0.8 times the value that would occur if the air was saturated at all levels. An ad-

634 hoc approach was used to distribute the corresponding latent heating vertically, and there was no
635 explicit representation of microphysical processes. This parameterization was used operationally
636 starting in March 1967. A similar approach was used in many operational weather forecast models
637 over the next two to three decades.

638 H. L. Kuo (1965) proposed the first cumulus parameterization to use an entraining plume to
639 represent the cumulus updrafts (see also Kuo 1974). He assumed (incorrectly) that the environ-
640 ment of the cumulus clouds was warmed by outward diffusion of enthalpy from the updrafts rather
641 than by convective fluxes. Kuo determined the intensity of convection based on the tendency of
642 water vapor due to low-level convergence and surface evaporation. This moisture-convergence
643 “closure” was widely used for many years (e.g., Anthes 1977; Tiedtke 1989), but later fell out of
644 favor (Emanuel 1991; Arakawa 2004).

645 Cumulus convection was not the only important cloud type to receive close attention during the
646 1960s. Douglas Lilly published an elegant, insightful, and (ultimately) very influential analysis of
647 marine subtropical stratocumulus clouds (Lilly 1968). He emphasized the importance of cloud-
648 top processes, including radiative cooling, entrainment, and the evaporation of cloud water, for the
649 evolution of stratiform cloud systems. Over a period of decades, Lilly’s 1968 paper has exerted a
650 major impact on parameterizations of both clouds and boundary-layer turbulence.

651 During the 1960’s and into the 1970s global atmospheric models predicted water vapor dis-
652 tributions including the effects of precipitation and moist convection, but most specified a fixed
653 distribution of clouds from observations for interaction with radiation (e.g., Manabe et al. 1965;
654 Washington and Kasahara 1970). The UCLA model was an exception.

655 In the late 1950’s and 1960’s efforts were made to theoretically interpret cloud and precipitation
656 observations. This work coincided in particular with the development and use of radar and other
657 observational advances and was largely independent of weather and climate model developments

658 at the time. Pioneering work in this area was conducted by Edwin Kessler. As a doctoral student
659 at MIT and later as a researcher at the Weather Radar Branch at Great Blue Hill, Massachusetts
660 and director of the Atmospheric Physics Division at the Travelers Research Center in Hartford,
661 Kessler recognized the utility of analyzing data using simplified water mass continuity equations.
662 As he wrote (Kessler 1995):

663 I worked with a strong sense for interactions among processes as discussed here, and in
664 expectation that their study would be facilitated by simple means to portray microphysi-
665 cal processes. The first process to be considered was conversion of cloud to precipitation.
666 How to portray it? I did little more than observe in the literature and with my own eyes
667 that thin water clouds seem to be persistent, and that rain falls from dense clouds.

668 This behavior was captured by continuity equations for cloud water and rain mass that were
669 developed and initially applied in a kinematic flow model (Kessler 1969). Conversion processes
670 between cloud and rain were represented by “autoconversion” using a threshold cloud mass mixing
671 ratio above which conversion occurred, and “accretion” which represented the growth of existing
672 raindrops by collection of cloud. Rain was allowed to evaporate and sediment and the precipitation
673 rate was calculated explicitly from the predicted rain field. A diagram of the scheme is shown in
674 Fig. 5 a. This was a major advance, and it still provides a general framework for almost all bulk
675 microphysics schemes used in weather and climate models up to the present day.

676 From the late 1950s to the early 1980s, the first attempts were made to simulate turbulence and
677 cumulus clouds using high-resolution numerical models with relatively small domains (Malkus
678 and Witt 1959; Lilly 1962; Ogura 1962; Deardorff 1964, 1972b, 1974, 1980; Moeng 1984). To-
679 day we speak of models for “large eddy simulation” (LES), and cloud-resolving models. Such
680 models are now extensively used for developing and testing global models, and for determining

681 the numerical values of parameters used in subgrid-scale parameterizations for lower-resolution
682 models.

683 Lorenz’s landmark paper on deterministic nonperiodic flow (Lorenz 1963) revolutionized our
684 understanding of the limits of deterministic weather prediction, and eventually led to ensemble
685 forecasting (Lewis 2005). Motivated by Lorenz’s discovery, Charney (1966) used early versions
686 of the Livermore, UCLA, and GFDL models to investigate the sensitivity of the atmospheric cir-
687 culation to small perturbations. This work by Charney and colleagues could perhaps be viewed as
688 the first model intercomparison study.

689 *f. Where things stood at the end of the 1960s*

690 It is interesting to list some of the ways in which the global modeling arena of the 1960s differed
691 from today’s. First, all of the global atmosphere and ocean models of the 1960s were devel-
692 oped in the USA, although Japanese immigrants to the USA (Akio Arakawa, Akira Kasahara, and
693 Syukuru Manabe) played key roles in the development of three of the models. All of the lead
694 developers were men. The motivations for developing the models were purely academic, in the
695 sense that the primary focus was improved understanding, rather than immediate practical appli-
696 cations. The funding that supported the modeling work was modest by today’s standards. The
697 modeling teams were small and informally organized, in contrast to today’s much larger and more
698 bureaucratic enterprises. All of the models used “grid-point” methods with spherical (longitude-
699 latitude) coordinates, and all of them used the quasi-static primitive equations. The atmospheric
700 models simulated only the troposphere, with the exception of an early experiment by Manabe and
701 Hunt (1968). Although, as discussed above, the 1960s did see some early work on models of
702 the ocean, sea ice, and the land surface, by far the largest effort was aimed at developing atmo-

703 spheric models. Finally, and importantly, the model-users of the 1960s were mostly the same as
704 the model-developers, whereas today users vastly outnumber developers.

705 **5. The 1970s**

706 *a. More modeling groups*

707 During the 1970s, more global modeling projects started up, in various places around the world,
708 including at the United Kingdom Meteorological Office in Bracknell (Gilchrist et al. 1973; Rowntree
709 tree 1976; Corby et al. 1977; Rowntree and Walker 1978), and the Laboratoire de Météorologie
710 Dynamique (LMD) in Paris (Laval and Sadourny 1979; Laval et al. 1981b,a; Sadourny 1984). In
711 the U.S., the National Aeronautics and Space Administration (NASA) was motivated to enter the
712 global modeling arena by a desire to maximize the meteorological utility of satellite data. Data
713 assimilation is a process that combines new observations with pre-existing information (often in
714 the form of previous short-term forecasts), to provide an optimal estimate of the state of the at-
715 mosphere. Weather forecasts use data assimilation to create the “initial conditions” used to start a
716 forecast. In work carried out at NASA’s Goddard Institute for Space Studies (GISS), in New York
717 City, Charney et al. (1969) pointed to data assimilation, and especially the assimilation of satel-
718 lite data, as an important new application of numerical models. To enable NASA’s work on data
719 assimilation, a version of the UCLA model was provided to GISS in the early 1970s (Somerville
720 et al. 1974). Data assimilation is of course now key to operational NWP, and to the production of
721 “reanalyses,” which are discussed later in this chapter. See the chapter in this volume by Stanley
722 Benjamin and colleagues for a more complete discussion of data assimilation.

723 GISS was originally organized to study astronomical problems, in which radiative transfer is of
724 course central. Radiative transfer studies at GISS were strongly influenced by methods that had

725 been developed by the planetary atmospheres community, and these were adapted for use in global
726 atmospheric models. For example, the adding method for computing the transport of radiation in
727 scattering atmospheres is attributed by Lacis and Hansen (1974) to papers describing gamma-ray
728 transfer, although the atmospheric formulation arose from a collaboration between James Hansen
729 and Hendrik van de Hulst (Andrew Lacis, *pers. comm.*, 2017) . GISS was the first modeling
730 center to use a k -distribution to model the spectral variation in optical depth (Somerville et al.
731 1974; Hansen et al. 1983). In a k -distribution, spectral regions with each band are ordered by
732 extinction absorption coefficient, so that the integral over wavelength becomes smooth and just a
733 few quadrature points provide high accuracy.

734 Notably, the 1970s saw the beginning of operational *global* numerical weather prediction (Stack-
735 pole 1978; Woods 2006), and the founding of the European Centre for Medium Range Weather
736 Forecasts (ECMWF; Woods 2006), which quickly established itself as the most skillful of the
737 operational centers.

738 *b. Atmospheric dynamical cores*

739 1) THE SPECTRAL METHOD BECOMES POPULAR

740 During the 1970s and early 1980s, the global spectral ⁶ method (Silberman 1954; Robert 1966;
741 Baer 1972; Bourke 1974) became widely used in the dynamical cores of atmospheric models.
742 In this approach, the horizontal distribution of model fields is represented by an expansion in
743 spherical harmonics (Fig. 6). The spectral representation allows horizontal derivatives to be cal-
744 culated very accurately and, with a triangular truncation of the expansion, gives homogeneous
745 and isotropic resolution. Moreover, a spectral dynamical core that solves the barotropic vortic-

⁶To avoid confusion: The spectral method used in dynamical cores is a mathematical technique based on functional expansions, and has nothing to do with the electromagnetic spectrum that is dealt with by radiation parameterizations, or the apocryphal spectral energy gap mentioned earlier.

746 ity equation conserves energy and enstrophy, as in the continuous system. The calculation of
747 quadratic nonlinear terms directly from the spectral representation using interaction coefficients
748 was prohibitively expensive, and for other types of nonlinearity even more so. This barrier to the
749 use of the spectral method was removed with the introduction of the spectral transform method
750 by Eliassen et al. (1970) and Orszag (1970). In the spectral transform method, the nonlinear ad-
751 vection terms, along with any terms based on physical parameterizations, are computed in grid
752 space, and efficient transforms are used to go back and forth between grid space and the spectral
753 representation (Jarraud and Simmons 1983).

754 A further important advantage of the spectral method is that it greatly facilitates the use of a
755 semi-implicit time integration scheme. An implicit treatment of the terms responsible for fast
756 gravity waves effectively enlarges the domain of dependence of the numerical solution, allowing
757 the CFL criterion to be satisfied with larger time steps. The price to pay was the re-appearance
758 of an elliptic problem to be solved at each time step⁷. Inspired by the work of Marchuk, semi-
759 implicit schemes were proposed for both gridpoint models (Kwizak and Robert 1971; Robert et al.
760 1972) and spectral models (Robert 1969; Bourke 1974; Hoskins and Simmons 1975). A major
761 advantage of the spectral method is that it allows fast (i.e., computationally inexpensive) solution
762 of the semi-implicit elliptic problem that arises with semi-implicit time-differencing. This, in turn,
763 allows spectral models to use long time steps, which enhances their computational speed.

764 As a result of these strengths of the spectral method, it was soon adopted by GFDL, NCAR,
765 and ECMWF, and it dominated atmospheric modeling efforts around the world for the next two
766 decades (see the review by Williamson 2007). It is still used today at several major modeling
767 centers.

⁷As mentioned above, elliptic problems arise in the solution of the earlier quasi-geostrophic and balanced models.

768 2) IMPROVEMENTS TO GRID-POINT MODELS

769 For the modeling centers that persevered with grid-point methods, important progress was made
770 along two lines. One was the understanding that, in order to adequately capture geostrophic bal-
771 ance, it is necessary to adequately simulate the adjustment towards balance that occurs through the
772 radiation of gravity waves. Ideally, non-propagating computational modes should be avoided and
773 the entire wave spectrum should have group velocities of the correct sign. These properties de-
774 pend crucially on the staggering of variables on the grid, and systematic study (Winninghoff 1968;
775 Arakawa and Lamb 1977; Randall 1994) concluded that the B-grid (for large $\Delta x/L_R$), C-grid (for
776 small $\Delta x/L_R$), and Z-grid (for all $\Delta x/L_R$) horizontal staggerings perform best (Figure 3). Here Δx
777 is the grid spacing and L_R is a key dynamical length scale called the Rossby radius of deformation.

778 Another line of progress built upon Arakawa's Jacobian work (Arakawa 1966) to develop
779 schemes that conserve energy, enstrophy, or angular momentum for more complete equation
780 sets. These developments involved both horizontal (Sadourny 1975; Burridge and Haseler 1977;
781 Arakawa and Lamb 1981) and vertical (Arakawa and Lamb 1977; Simmons and Burridge 1981)
782 discretizations.

783 The improved dynamical cores had to adapt to changing computer architectures. The most im-
784 portant architectural change during the 1970s was the introduction of "vector" computing, which
785 became available to many scientists when a Cray-1 computer was delivered to NCAR in 1976. A
786 vector computer can perform arithmetic on lists of numbers (called vectors) much faster than con-
787 ventional machines.⁸ In order to take advantage of the increased speed of the vector hardware, the
788 computer codes of the models had to be rewritten; this entailed a significant amount of program-
789 ming work, but had many beneficial side effects in addition to the direct benefit of faster-running
790 models.

⁸Vector computing is not to be confused with parallel computing, which came later.

791 *c. Adding the stratosphere*

792 During the 1970s, some global atmospheric models were extended upward to include the strato-
793 sphere. The earliest such model was described by Manabe and Hunt (1968). Later studies include
794 those of Manabe and Mahlman (1976), Schlesinger (1976), and Schlesinger and Mintz (1979).
795 With support from the Climate Impact Assessment Program (CIAP) of the U. S. Department of
796 Transportation, some of the models were used to simulate the effects of supersonic airliners on
797 stratospheric ozone (Johnston 1971; Grobecker et al. 1974; National Research Council Climatic
798 Impact Committee 1975; Morrisette 1989). This was the first time that agency funding was made
799 available specifically for the application of global atmospheric models to investigate anthropogenic
800 effects on the climate system. It can perhaps be viewed as a loss of innocence.

801 The temperature structure of the stratosphere is dominated by radiative processes, so includ-
802 ing this layer motivated developments in radiative transfer parameterizations. At GFDL, Steven
803 Fels had an insight that pointed the way to more accurate calculations without large increases
804 computational expense. As Green (1967) showed in a crisp two-page note, the radiative cooling
805 calculation at any level in the atmosphere can be expressed as the sum of exchanges between the
806 level in question and every other level, plus one more term representing the energy lost to the infi-
807 nite heat sink of the rest of the universe – the cooling-to-space term. Temperatures throughout an
808 atmospheric column, and hence the emitted longwave fluxes, vary by much less than the contrast
809 between the atmosphere and outer space, so that when the cool-to-space term is non-zero it is
810 usually much larger than the exchange term. Faced with the limited power of early computers Fels
811 and Schwarzkopf (1975) exploited this asymmetry in the Simplified Exchange Approximation,
812 the heart of which is a spectrally detailed, and hence more accurate, treatment of cooling to space,
813 and a spectrally coarse treatment of regions in which intra-atmospheric exchanges dominate. The

814 approach is one of the first in which a focus on a specific problem – for the Simplified Exchange
815 Approximation, the computation of heating rates within the atmosphere – allows for algorithms
816 that save time by targeting that calculation. The parameterization was quickly adopted by the
817 radiation community, and incorporated into GFDL’s SkiHi model in 1979.

818 *d. Boundary layer and cloud parameterizations during the 1970s*

819 1) BOUNDARY LAYER PARAMETERIZATIONS

820 The early ECMWF model used a surface-flux parameterization developed by Louis (1979). It
821 was based on Monin-Obukhov similarity theory, but with some modifications to facilitate use in
822 atmospheric models. The Louis parameterization is still very widely used today.

823 During the 1960s, a new approach to turbulence parameterization, called “higher-order closure,”
824 emerged within the engineering community (Glushko 1966; Bradshaw et al. 1967; Beckwith and
825 Bushnell 1968; Donaldson and Rosenbaum 1969). A few years later, an essay by Donaldson
826 (1973) introduced higher-order closure to the atmospheric sciences. Soon thereafter, Mellor and
827 Yamada (1974) proposed a detailed hierarchical approach for the application of higher-order clo-
828 sure to atmospheric modeling. Miyakoda and Sirutis (1977) were the first to test higher-order
829 closure in a global atmospheric model. Higher-order closure has been of lasting and recently
830 increasing importance for atmospheric modeling, so we devote some space to it here.

831 Higher-order closure uses the equations that govern selected “moments” of the subgrid-scale
832 variables. The first moments are the grid-cell-averaged values of the primary variables, which
833 might include the liquid water potential temperature, θ_l , total water mixing ratio, q_{tot} , and the
834 three velocity components u , v , and w . These grid-cell-averages are directly predicted by the
835 model’s dynamical core. Second moments (computed in terms of departures from the means)
836 include variances and fluxes, e.g., $\overline{(\theta'_l)^2}$ and $\overline{w'\theta'_l}$. Here a prime denotes a departure from a grid-

837 cell average. Third moments include fluxes of second moments, such as $\overline{w'w'\theta'_l}$. A model that uses
838 the equations for selected second moments but parameterizes the third moments is called a second-
839 order closure model. A model that uses the equations for selected second and third moments but
840 parameterizes the fourth moments is called a third-order closure model. Closures beyond third
841 order are impractical.

842 Higher-order closure models need closures for four things:

- 843 1. the effects of higher moments that are not predicted, e.g., as mentioned above, the third
844 moments in a second-order closure model;
- 845 2. moments involving the pressure, which occur in the equations for the moments that involve
846 velocity components;
- 847 3. dissipation terms, which are especially important in the equations governing variances; and
848 4. moments involving heating, precipitation, and other diabatic processes.

849 At first, it was hoped that second-order closure models would succeed in realistically representing
850 the clear convective boundary layer. Experience showed, however, that second-order closures do
851 not transport turbulence kinetic energy (TKE) realistically. As a result, the boundary layer deep-
852 ens too slowly in second-order closure models Mellor and Yamada (e.g., 1974). This discovery
853 motivated the development of third-order closure models (e.g., André et al. 1976), which more
854 realistically transport TKE.

855 Ever since the 1970s, the literature on higher-order closure has been closely linked with the lit-
856 erature on cloud parameterizations, which were receiving greater attention in part because of more
857 and better satellite observations of the atmosphere (e.g., Stowe et al. 1988; Schiffer and Rossow
858 1983). An important advance came when the equations of higher-order closure were applied to

859 parameterize fractional cloudiness. Sommeria and Deardorff (1977) and Mellor (1977) indepen-
860 dently proposed combining higher-order closure with *assumed* probability density functions. See
861 also Manton and Cotton (1977) and Chen (1991). The idea of is that within the small grid cells of a
862 large-eddy simulation (LES), the θ_l and q_{tot} can be assumed to have a joint Gaussian distribution.
863 Sommeria, Deardorff, and Mellor showed how this assumption can be used to diagnose the frac-
864 tional cloudiness from the means, variances and covariance of θ_l and q_{tot} . Their approach was to
865 predict the variances and covariance using second-order closure, and then use the predicted (first
866 and) second moments to determine the parameters of the assumed joint Gaussian for each grid
867 cell of a model. The joint distribution could then be used to diagnose the fractional cloudiness,
868 and also the liquid water content of the clouds. As discussed in section 7 e, more highly evolved
869 parameterizations based on assumed distributions with higher-order closure are now increasingly
870 being used in global atmospheric models.

871 2) CUMULUS PARAMETERIZATIONS

872 Cumulus parameterization underwent major theoretical advances during the 1970s, supported
873 by new field observations. Arakawa and Schubert (1974, hereafter AS) proposed a very influential
874 cumulus parameterization with several important new ideas. First, following Arakawa (1969), they
875 allowed a spectrum of cumulus cloud sizes, distinguished by their fractional entrainment rates, and
876 each with its own mass flux. Second, they determined the intensity of convective activity using
877 the hypothesis of “quasiequilibrium,” which asserts that the cumulus clouds consume convective
878 available potential energy (almost) as rapidly as it is generated by other processes. Third, they
879 included a very simple but explicit representation of the interactions between the cumulus clouds
880 and the subcloud boundary layer. Finally, AS allowed the cumulus updrafts to detrain liquid water
881 and ice (and also water vapor) into the environment, thus providing a “hook” that can be used in a

882 parameterization of convectively generated stratiform clouds. It is noteworthy that AS cited a total
883 of nine papers that were authored or co-authored by Joanne Simpson.

884 Although AS appreciated that stratiform clouds often form in the outflows from cumulus clouds,
885 modeling research at the time emphasized the role of convection, and tended to treat stratiform
886 clouds as having significance only for their radiative effects. This paradigm was challenged by
887 Houze (1977), who used an analysis of tropical field data to demonstrate that about 40% of the
888 precipitation in a tropical convective system is stratiform in nature. Stratiform clouds received
889 increased attention in subsequent model development efforts. Models also used the mass-flux
890 approach to include convective momentum transport by both updrafts and downdrafts, with the
891 simplifying assumption that horizontal momentum is conserved within updrafts and downdrafts
892 except for the effects of entrainment.

893 AS also neglected the effects of convective downdrafts, which had been recognized in observa-
894 tional studies (Starr Malkus 1955). Johnson (1976) proposed a way to include downdrafts in a cu-
895 mulus parameterization, and more such work followed (e.g., Emanuel 1981; Cheng and Arakawa
896 1997).

897 *e. The GFDL-based family of ocean models*

898 Here we depart from the decade-by-decade organization of this chapter to describe a “family
899 tree” of ocean models that sprang from the Bryan (1969b) model, which was developed during
900 the 1960s. The tree began to grow during the 1970s, and continues to put out new branches in the
901 twenty-first century.

902 1) DESCENDANTS OF THE BRYAN (1969B) OCEAN MODEL

903 As mentioned in Section 4 a, GFDL developed the Bryan-Cox ocean model during the 1960s.
904 The model underwent extensive further development during the 1970s, and beyond. Figure 8
905 shows a flow diagram illustrating the lineage of ocean circulation models originating from the
906 Bryan-Cox code. In addition to details offered in the extended figure caption, we highlight certain
907 elements of the developments in the main text. The Bryan-Cox code was enhanced by Albert
908 J. Semtner, Jr., who joined the global modeling group at UCLA after completing his Ph.D. at
909 Princeton (Semtner and Mintz 1977). Semtner's version of the code incorporated arbitrary land-
910 sea masking (allowing for more realistic domains) and upgrades to the computational efficiency on
911 vector machines (Semtner 1974). Semtner's enhancements were incorporated into the Cox (1984)
912 code, thus initiating a practice of sharing algorithmic upgrades among a community of developers.
913 The Killworth et al. (1991) algorithm to include a free-surface option was also incorporated into
914 the code. The Bryan-Cox-Semtner code was used for the first simulations of the global ocean at
915 $1/2^\circ$ resolution (Semtner and Chervin 1992). These simulations ushered in the era of global ocean
916 models that admit transient mesoscale eddy activity (see Thomas et al. 2008, for a more recent
917 compendium).

918 The Bryan-Cox-Semtner code was also used in the Parallel Ocean Climate Model (POCM)
919 developed at NCAR during the 1990s. POCM was one of the first ocean models to make efficient
920 use of the massively parallel computer architectures that are now standard in the community.

921 In 1989, Mike Cox died at a relatively young age⁹, at which point Ron Pacanowski, Keith Dixon,
922 and Tony Rosati at GFDL took charge of the GFDL ocean model. Their efforts led to the first
923 version of the Modular Ocean Model (MOM1), thus furthering the GFDL lineage that continues
924 to this day with MOM6. MOM1 was the ocean component of many global climate models in the

⁹See Bryan (1991) for a summary of Cox's impacts on oceanography.

925 1990s, such as the first climate model developed by the United Kingdom Meteorological Office
926 (Murphy 1995), and the second version of the Canadian Climate Center model (Flato et al. 2000).
927 Climate models in Germany, Japan, and Australia also made use of MOM1.

928 2) SUPPORT FOR A COMMUNITY OF NUMERICAL MODELERS

929 The Semtner (1974) code and technical report were made available to other ocean modelers,
930 which led to a much wider use of the GFDL code, especially in the USA and the UK. This idea
931 of sharing code was then formalized in 1984 when Mike Cox made the GFDL ocean code freely
932 available to the public (Cox 1984). The code could be configured to suit the scientific interests of
933 the investigators. This promoted its use as an experimental tool for scientific investigation. Use
934 of the Bryan-Cox-Semtner code thus spread through the ocean and climate modeling community
935 worldwide. These efforts at community development are widespread in today's world of open-
936 source code development, but they were unique in the late 1970s and early 1980s. In addition to the
937 Fortran code, Cox provided an updated technical manual describing the mathematical equations
938 and numerical methods that formed the basis for the code. The Semtner (1974) technical report and
939 the Cox (1984) manual proved extremely valuable in communicating the scientific and engineering
940 rationales for various features of the model. As a result, the code was readily understandable by a
941 broad community of oceanographers and numerical algorithm specialists.

942 These pioneering efforts at building a community of informed users paved a path towards en-
943 hancing the scientific integrity, transparency, and reproducibility of ocean model codes and the
944 simulations produced with them (a formidable task to this day!). It also fostered several allied
945 efforts to use the Bryan-Cox-Semtner code for a suite of scientific applications, and to enhance the
946 physical parameterizations, numerical methods, and computational efficiency of the models.

947 3) OCEAN CODES INSPIRED BY MOM

948 The Parallel Ocean Program (POP) is a direct descendant of the Bryan-Cox-Semtner code. It was
949 developed in the early 1990s for the Connection Machine by Rick Smith, John Dukowicz, and Bob
950 Malone at Los Alamos National Laboratory (LANL; Smith et al. 1992). An implicit-free-surface
951 formulation and other numerical improvements were added by Dukowicz and Smith (1994). Later,
952 the capability for general orthogonal coordinates for the horizontal mesh was implemented (Smith
953 et al. 1995). See also Murray (1996) for efforts with the Bryan-Cox-Semtner code and Madec
954 et al. (1997) for efforts with the Océan PARallélisé (OPA) model in France. In 2001, POP was
955 adopted as the ocean component of the Community Climate System Model (CCSM) based at
956 NCAR. Substantial efforts at both the LANL and NCAR have gone into adding various features
957 to meet the needs of the CCSM climate model (Smith et al. 2010; Danabasoglu et al. 2006, 2012).
958 The POP code has been used as the ocean component of the CCSM, and versions 1 and 2 of the
959 Community Earth System Model (Hurrell et al. 2013).

960 Upon the release of the Cox code in 1984, scientists around the world had access to the fruits of
961 more than 20 years of focused efforts at GFDL. Nonetheless, as scientists are prone to do, many
962 arrived at distinct ideas for how best to go about developing numerical models. One such effort
963 is the ocean component of the Nucleus for European Modelling of the Ocean (NEMO). This code
964 was developed from the OPA model, release 8.2; (Madec et al. 1997). The NEMO code has been
965 used for a wide range of applications, both regional and global, as a forced ocean model and as a
966 component of a climate model. In particular, it is used today in the global models of the United
967 Kingdom Meteorological Office, the European Centre for Medium Range Weather Forecasting,
968 and the French National Centre for Scientific Research.

969 The Max Planck Institute ocean model (MPIOM) is the ocean-sea ice component of the MPI
970 Earth System Model. MPIOM is a primitive equation model (C-grid, z-coordinates, free surface)
971 with the hydrostatic and Boussinesq assumptions. It includes a bottom boundary layer scheme for
972 the flow across steep topography, and uses a curvilinear orthogonal grid which allows for a variety
973 of configurations. A description of MPIOM can be found in Marsland et al. (2003). A list of model
974 development efforts that is current up to the year 2000 can be found in Griffies et al. (2000). Any
975 list is incomplete, and we do not attempt an update here.

976 *f. Sea ice advances during the 1970s and 1980s*

977 The 1970s and 1980s were a golden age for the development of sea ice models, with major
978 advances in the treatment of sea ice thermodynamics and the emergence of models that simulate
979 sea ice dynamics, in which mechanical failure causes ridging and rafting among floes and also
980 creates openings between floes known as leads. The regional jumble of sea ice caused by the
981 interplay of deformation, growth, and melt results in a distribution of thicknesses that modelers
982 wanted to simulate in order to capture the highly nonlinear thickness-dependence on compressive
983 stress and growth.

984 Observations and scientific understanding of sea ice had recently expanded as a result of the
985 International Geophysical Year (IGY) in 1957-1958. Norbert Untersteiner spent a year on the sea
986 ice as chief scientist of an IGY field camp. In the decade that followed he published a series of
987 papers that established the basic principles that govern a numerical model of sea ice thermody-
988 namics. Together with graduate student Gary Maykut of University of Washington, he assembled
989 a sea ice model that treated the surface energy budget and sea ice growth and melt with the unique
990 dependence on sea ice brine pockets (Maykut and Untersteiner 1971). The concentration of brine
991 in the pockets varies with heat stored in the sea ice. The temperature and brine concentration

992 were simulated in 10-cm layers that absorbed sunlight and conducted heat between ocean and
993 atmosphere. The physical interactions were so complex that their model was limited to just the
994 vertical-dimension, and because of its computational expense no climate or weather model adopted
995 the Maykut and Untersteiner model of brine-pocket dynamics until the 21st century.

996 The RAND Corporation sought to create a simpler thermodynamic sea ice model to couple to
997 early ocean models. RAND commissioned Bert Semtner to reduce the complexity of the Maykut
998 and Untersteiner model. Semtner did so by developing a very simple one-layer model of sea ice
999 alone and an innovative three-layer model (two layers of sea ice and one of snow) with a reservoir
1000 of interior solar heating to mimic the effect of brine pockets and shift the timing of the surface
1001 melt season in a semi-realistic way (Semtner 1976). These two reduced-complexity models by
1002 Semtner were the basis for sea ice thermodynamics in global climate models for decades.

1003 In the fall of 1976, sea ice scientist William Hibler became the 25th visitor to GFDL. He was
1004 impressed by the practical issues of sea ice modeling in a global climate model. He learned how
1005 ocean models were formulated from his host Frank Bryan, who inspired him to simplify the sea
1006 ice model from the Arctic Ice Dynamics Joint Experiment (AIDJEX, Coon et al., 1974), which
1007 employed a constitutive law for plastic behavior to simulate the dependence of the stress tensor on
1008 the velocity field, allowing for material failure and deformation. Hibler (1979) greatly reduced the
1009 numerical complexity of the AIDJEX model by formulating a nonlinear viscous-plastic rheology
1010 for sea ice. He demonstrated the scheme in an 8-year simulation of the Arctic basin. The AIDJEX
1011 model and Hibler's viscous-plastic scheme remain the basis for the dynamics in most sea ice
1012 models used in climate models today, though many climate models, including GFDL's, used highly
1013 idealized methods such as free-drift with stoppage to model sea ice dynamics for several more
1014 decades as efforts continued to further reduce the computation demands of the viscous-plastic
1015 dynamics.

1016 As Hibler and other sea ice modelers explored methods to simulate sea ice dynamics, the need
1017 for a sub-grid scale parameterization to simulate the distribution of sea ice thicknesses arose. An
1018 equation to describe the ice-thickness distribution was developed by Alan Thorndike with other
1019 colleagues at the University of Washington (Thorndike et al. 1975). Hibler soon implemented an
1020 ice-thickness distribution scheme in his Arctic Basin model (Hibler 1980).

1021 The advanced sea ice models developed during the 1980s were used only in experimental ap-
1022 plications, occasionally coupled to an ocean model. They were not coupled to an atmosphere
1023 model for another decade. One reason is that climate modeling centers considered advanced sea
1024 ice models to be too computationally demanding. Another factor was that the focus of global cli-
1025 mate modeling remained primarily on the tropics and northern midlatitudes until the twenty-first
1026 century.

1027 *g. Simulations of global warming*

1028 Manabe and Möller (1961b) demonstrated that radiation is roughly balanced by convection
1029 (Manabe and Strickler 1964b).¹⁰ The GFDL team performed pioneering one-dimensional sim-
1030 ulations of “radiative-convective equilibrium” (RCE; Manabe and Strickler 1964a; Manabe and
1031 Wetherald 1967), an idealization that continues to be useful today (e.g., Wing et al. 2018). To
1032 mention one very important example, the study of Manabe and Wetherald (1967) pointed to the
1033 importance of the water vapor feedback for climate change. As noted by Manabe and Strickler
1034 (1964b) in a paper describing single-column modeling of RCE, “one of the major purposes of our
1035 study is the construction of a model of radiative transfer simple enough to be incorporated into a
1036 general circulation model of the atmosphere.”

¹⁰That radiation and convection balance each other was appreciated before 1964, as is made clear by George Simpson’s comments on the paper of Guy Callendar (1938).

1037 During the 1960s, Manabe and Wetherald (1967) had already studied the effects of increasing
1038 atmospheric carbon dioxide concentrations on the “climate” of a one-dimensional RCE model, and
1039 this work pointed to the importance of the water-vapor feedback on climate change. But the first
1040 simulation of global warming with a true climate model was reported by Manabe and Wetherald
1041 (1975). Their model was idealized through the use of a limited computational domain, simplified
1042 topography, no energy transport by the oceans, no seasonal or diurnal cycles, and fixed cloudiness.
1043 It is remarkable that this first simulation with a simplified model, more than forty years ago,
1044 predicted many changes that have now been observed in the real atmosphere, including a warming
1045 troposphere with greater warming near the pole, a cooling stratosphere, stronger precipitation, and
1046 increased atmospheric water vapor. The successful strategy of Manabe and Wetherald (1975),
1047 Manabe and Stouffer (1980), and Manabe and Wetherald (1980) was to explore the possibility of
1048 anthropogenic climate change using the relatively simple models available at the time, rather than
1049 waiting for the more complete models of the future.

1050 **6. The 1980s**

1051 *a. Community modeling gets under way*

1052 In 1983, NCAR released the “Community Climate Model” (CCM) (Pitcher et al. 1983;
1053 Williamson 1983; Williamson et al. 1983; Kiehl et al. 1998). Initially, the CCM was essentially an
1054 atmosphere model with a simple land-surface model attached. It lacked a coupled ocean model,
1055 so calling it a “climate model” was a bit of an exaggeration. The CCM was widely used because
1056 it was freely available and fully documented.

1057 During the 1980s, Washington and Meehl (1983), Washington and Meehl (1984) and Washing-
1058 ton and Meehl (1989) used versions of the CCM to perform increasingly detailed simulations of

1059 anthropogenic greenhouse warming. In the late 1990s, Washington et al. (2000) developed the
1060 Parallel Climate Model (PCM). The atmosphere component was the CCM3 at T42 resolution, and
1061 the ocean component was the POP model at about 0.5-degree resolution. The PCM was one of
1062 the first models designed to run very efficiently on the parallel computers that were emerging at
1063 that time. The PCM was subsequently used to run ensembles of 20th century simulations forced
1064 by the individual climate forcings, such as greenhouse gases, aerosols and solar variability, rather
1065 than their combined effects. The interesting results are presented in Meehl et al. (2003).

1066 The CCM matured through a series of releases. During the 1990s, a sophisticated land model
1067 (Bonan 1998) was added (Kiehl et al. 1998). In 1996, CCM was coupled to an ocean and was
1068 able to run without flux adjustments through the introduction of the so-called Gent-McWilliams
1069 ocean mixing parameterization (Gent and McWilliams, 1990). The entire model was renamed as
1070 the Community Climate System Model (CCSM) in 2004, and then renamed again as the Com-
1071 munity Earth System Model (CESM) in 2010; the Community Atmosphere Model (CAM) is the
1072 atmosphere component of the CESM.

1073 *b. Atmospheric dynamical cores in the 1980s*

1074 Although the semi-implicit method allowed the CFL criterion to be satisfied for gravity waves,
1075 and truncation errors were generally thought to be dominated by the space discretization, model
1076 time steps were still limited by the CFL criterion for explicit Eulerian advection. This motivated
1077 Robert (1981, 1982) to propose a semi-implicit semi-Lagrangian method of integrating the model
1078 equations. In the semi-Lagrangian method time derivatives are expressed as derivatives along fluid
1079 parcel trajectories. Fluid parcel trajectories arriving at model grid points are traced backwards over
1080 one or two time steps, and the required fields are interpolated to the trajectory departure points. In
1081 this way the CFL criterion for advection is satisfied and significantly longer time steps are possible.

1082 The first semi-implicit semi-Lagrangian schemes used three time levels, but more efficient two-
1083 time-level versions were soon formulated (Temperton and Staniforth 1987; McDonald and Bates
1084 1987), and ways of handling the poles in spherical geometry were worked out (Ritchie 1991; Bates
1085 et al. 1990). The resulting efficiency gains meant the method was soon adopted at a number of
1086 operational centers (Ritchie 1991; Ritchie et al. 1995).

1087 *c. Radiative transfer work in the 1980s*

1088 Stephens (1984) provides a useful view of the state of radiation parameterization in the early
1089 1980s. Although more parameterizations were available than during the 1960s and 1970s
1090 (Stephens describes six), the ideas can all be traced back to the earliest treatments. One sig-
1091 nificant change was the addition of a wider range of gases, especially in models devoted to longer
1092 climate simulations as opposed to short-term weather forecasts. As Ramaswamy explained,

1093 “In the eighties, the so-called OTGs, the other trace gases became very popular and
1094 well-known, particular following Ramanathan’s and Hansen’s papers (Ramanathan et al.
1095 1983; Hansen et al. 1983) . We [GFDL] felt that to create proper energy balance, espe-
1096 cially when doing climate calculations, you needed to have methane, nitrous oxide, and
1097 chlorofluorocarbons.” (*Interview with Ramasawmy, 28 Nov 2017*)

1098 As Stephens (1984) notes, the treatment of interactions between clouds and radiation in global
1099 models in the mid-1980s was fairly rudimentary. Cloud properties were almost universally pre-
1100 scribed, perhaps as a function of relative humidity but frequently as a function of location and
1101 season, with limited spectral information. Methods for more sophisticated treatments were al-
1102 ready in place, with insights from work on planetary atmosphere (Hansen and Travis 1974) in-
1103 forming complete parameterizations in both spectral regions (Stephens 1978; Roach and Slingo

1104 1979; Slingo and Schrecker 1982). The delta-scaling method for treating the sharp forward peaks
1105 in the scattering phase function of clouds had been developed (Potter 1970; Joseph et al. 1976)
1106 and the variety of proposed two-stream methods had been unified by Meador and Weaver (1980)
1107 and Zdunkowski et al. (1980). These tools were in place as models began to make more detailed
1108 calculations of cloud properties (section 6 d), although treatments of “cloud overlap” i.e. how
1109 radiation was partitioned between clear and cloudy skies in the vertical, remained simple.

1110 The move to better prediction of cloud properties was partly motivated by recognition of the role
1111 of cloud-radiation interactions in shaping the large-scale circulation including tropical convection.
1112 One example came from a small group working with the UCLA/GLA (Goddard Laboratory for At-
1113 mospheres) GCM, who demonstrated that predicting cloud properties and allowing those variable
1114 properties to influence the radiation field (Harshvardhan et al. 1987) had tremendous impacts on
1115 the global distribution of cloudiness and the resulting energy budget (Randall et al. 1989; Harsh-
1116 vardhan et al. 1989).

1117 The importance of radiation for short-term weather forecasts was also becoming clear. Jean-
1118 Jacques Morcrette, now retired from ECMWF, recalled how more accurate (but more computa-
1119 tionally expensive) radiation calculations helped to increase forecast skill:

1120 . . . I got the feeling that at least part of the problem might be in the clear-sky longwave
1121 cooling of the descending branch of the Hadley circulation (Now it is easy to state it so
1122 simply, at the time it was not so clear-cut.) The temperature dependence of the longwave
1123 absorption is very different in my band models (Morcrette 1990, 1991) from that in the
1124 then-current ECMWF scheme (essentially from Geleyn and Hollingsworth 1979). It
1125 took me till April 1989 to convince people that some revised version of the Lille codes
1126 [from which Morcrette’s codes have been adapted] were better overall even if they were

1127 less computer-efficient. The main impact is a much more stable maintenance of the
1128 Hadley circulation, which previously tended to weaken with the length of the forecast,
1129 and an increased geographical contrast in cloud forcing. (Jean-Jacques Morcrette, *pers.*
1130 *comm.*, 2017)

1131 The many independent spectral calculations required for broadband calculations, and the usual
1132 desire to compute fluxes with and without clouds to help understand the role of clouds in the
1133 Earth's energy budget, make radiation a computationally large burden. In most models, tendencies
1134 due to radiation are computed less frequently in time than other physical processes, but the need for
1135 computational efficiency has motivated other interesting compromises. Two approaches at NASA
1136 GISS do not seem to have been reported in the literature although they have been used since the
1137 original models described by Hansen et al. (1983).

1138 The first is that the sampling in time is often done at intervals that are not divisors of the daily
1139 cycle, so that the entire diurnal cycle is eventually sampled. Andrew Lacis described how this
1140 arose:

1141 "... [when sampling the diurnal cycle regularly] you get beat frequencies in there – pres-
1142 sure waves building up and stuff like that. When you make that odd fraction it would
1143 eliminate some of that type of noise. The other thing we did to speed up the radiation
1144 was sampling – we did every other grid box. So with sampling every 2 and a half hours
1145 and every other gridbox I think radiation might've been taking maybe 25 percent of the
1146 computing time." (*Interview with Andrew Lacis, 26 Oct 2017*)

1147 The second is that fractional cloudiness is treated by sampling in time:

1148 "... so if this cloud has a 50 percent chance of being there we'll draw a random number,
1149 and if it's bigger than a half we'll call it clear and smaller than a half we'll call it cloudy.

1150 That idea might've come from Larry Travis, at least according to Bill Rossow. The
1151 rationale for doing that came from Charney, who basically said that random errors in
1152 climate model don't matter that much but systematic errors do." (*ibid*)

1153 The 1980s also saw the development of widely available reference models and data for making
1154 radiative transfer calculations. For problems in clear-sky radiative transfer, this included the pub-
1155 lication of spectroscopic databases covering an increasingly broad set of gases (e.g., HITRAN;
1156 Rothman et al. 1987) and the development of line-by-line models (e.g., LBLRTM; Clough et al.
1157 1992) capable of computing optical depths given the state of the atmosphere. Calculations in-
1158 volving clouds were made more tractable by the widespread availability of codes for doing Mie
1159 calculations (Wiscombe 1980) for single-scattering properties and discrete-ordinates calculations
1160 (Stamnes et al. 1988) to obtain the angularly resolved radiation field.

1161 The wide-spread availability of these codes provided an opportunity to test parameterizations
1162 against reference results. The first of such efforts was the InterComparison of Radiation Codes
1163 used in Climate Models (ICRCCM; see Ellingson and Fouquart 1991; Ellingson et al. 1991;
1164 Fouquart et al. 1991). ICRCCM argued for the use of reference models, rather than direct ob-
1165 servations, as the standard for radiation intercomparisons, given the difficulties in making simulta-
1166 neous comparable measurements at the bottom and top of the atmosphere. The broad lesson from
1167 the intercomparison effort (Fig. 9) was that line-by-line models agreed to within a few percent
1168 (unsurprisingly, given that many use the same underlying spectroscopic information) but that
1169 parameterizations used in weather and climate models could be substantially in error, especially
1170 with respect to radiative forcing, i.e., the sensitivity of changes in fluxes to changes in composi-
1171 tion. The profiles used in ICRCCM were quite idealized, however, making it difficult to estimate

1172 the magnitude of errors in weather forecasting or climate projection applications, a problem that
1173 persists in more recent assessments (Oreopoulos et al. 2012; Pincus et al. 2015).

1174 *d. Boundary layer and cloud parameterizations during the 1980s*

1175 Deardorff (1972a) emphasized the importance and highly variable nature of the depth of the
1176 boundary layer, especially over land. He proposed a boundary-layer parameterization in which the
1177 depth of the boundary layer is an explicit prognostic (i.e., time-stepped) variable of the model.
1178 Deardorff's idea was implemented in the UCLA model by Randall (1976) and Suarez et al.
1179 (1983). A parameterization of stratocumulus clouds was included following Lilly (1968), and
1180 the boundary-layer parameterization was coupled with the cumulus parameterization of Arakawa
1181 and Schubert (1974) by allowing the cumulus clouds to remove mass from the boundary layer.
1182 The model's vertical coordinate system was modified to make the boundary-layer top an internal
1183 coordinate surface. With this approach, the model layers below the boundary-layer top comprised
1184 the boundary layer, and the depth of the boundary layer could change in response to mass fluxes
1185 across the boundary-layer top due to entrainment and cumulus convection. Randall et al. (1985)
1186 analyzed seasonal simulations with the model, and reported the results of some numerical experi-
1187 ments, including one in which the boundary-layer depth was artificially held constant, and another
1188 in which the diurnal cycle of solar radiation was replaced by daily-mean insolation. The results
1189 showed the importance of variations of the boundary-layer depth for precipitation over land and
1190 for determining the amount of low-level clouds.

1191 We mention four advances in cumulus parameterization during the 1980s. Emanuel developed
1192 a similarity theory of convective downdrafts (Emanuel 1981). (Raymond and Blyth 1986) pro-
1193 posed that mixed parcels created through entrainment migrate to their levels of neutral buoyancy.
1194 This idea, called "buoyancy sorting," has been very influential. The Betts-Miller parameteriza-

1195 tion (Betts 1986; Betts and Miller 1986), developed at ECMWF, used an adjustment to empiri-
1196 cally determined soundings of both temperature and water vapor. Finally, the Tiedtke convection
1197 parameterization (Tiedtke 1989) was implemented in the ECMWF model. Tiedtke's parameter-
1198 ization used the moisture-convergence closure developed by Kuo (1965). Later, the version of
1199 Tiedtke's parameterization used by the Max Planck Institute for Meteorology was modified to use
1200 a buoyancy closure (Nordeng 1994).

1201 Cloud microphysics parameterizations began to appear in global atmospheric models during
1202 the 1980s. The earliest low-resolution mesoscale models developed in the 1970's used the grid-
1203 scale saturation removal method for calculating surface precipitation, similar to what was done in
1204 early operational NWP models. However, cloud-scale models around this time quickly adopted
1205 a Kessler-like approach with separate equations for cloud and rain mass (e.g, Klemp and Wil-
1206 helmson 1978). By the early to mid 1980's many mesoscale models had also adopted this type of
1207 approach (e.g, Hsie et al. 1984). Around this time both mesoscale and cloud models also began in-
1208 corporating ice microphysics; commonly used schemes included those from Lin et al. (1983) and
1209 Rutledge and Hobbs (1984). These schemes generally assumed two or three ice categories (cloud
1210 or small ice, snow, and graupel or hail) and included conversion processes between the categories
1211 analogous to the Kessler approach for liquid microphysics. Beginning in the late 1960s and 1970s
1212 detailed bin microphysical schemes that explicitly evolved the particle size or mass distributions
1213 by predicting the total water mass in size or mass bins were also developed (e.g., Bleck 1970;
1214 Berry and Reinhardt 1974), but computational cost precluded their wider use in models until the
1215 1990s and 2000s.

1216 As noted above, larger-scale NWP models at operational centers through the 1970's and 1980's
1217 continued to convert water vapor to surface precipitation when the water vapor mixing ratio ex-
1218 ceeded some threshold value. Microphysical processes were not considered in this approach. By

1219 the late 1990's, the operational Eta Model at the U.S. National Centers for Environmental Predic-
1220 tion (NCEP) adopted a prognostic cloud scheme that explicitly included evolution equations for
1221 cloud condensate and a diagnostic treatment of precipitation from the predicted cloud fields (Zhao
1222 et al. 1997). Both the cloud fraction and predicted cloud water content were accounted for in
1223 the radiation parameterization. Some forecast models with prognostic cloud condensate included
1224 more detailed representations of sub-grid scale condensation for both stratiform and convective
1225 clouds (Sundqvist et al. 1989) as well as prognostic cloud fraction (Tiedtke 1993). These models
1226 typically partitioned condensate as liquid or ice according to temperature. These were important
1227 advances for operational forecast models, but the representation of microphysics was still highly
1228 simplified compared to contemporaneous finer mesh mesoscale and cloud models that employed
1229 several prognostic categories of cloud and precipitation water.

1230 The representation of the hydrologic cycle in global climate models in the 1970's through the
1231 1990's was generally at a similar level of complexity to that of operational NWP at the time, but
1232 with more sophisticated diagnostic parameterizations to represent the cloud fraction and optical
1233 properties. The diagnostic schemes of the 1980s were used to predict the occurrence and radiative
1234 properties of clouds based on the relative humidity, vertical velocity, temperature, and/or precipi-
1235 tation rate (e.g., Slingo 1985; Wetherald and Manabe 1988).

1236 The 1980s brought an increased emphasis on the radiative effects of clouds, for which greatly
1237 improved observations were becoming available (Schiffer and Rossow 1983; Barkstrom 1984; Ra-
1238 manathan et al. 1989). Cloud feedback became an important focus of climate change simulations
1239 with global models (Charney et al. 1979; Hansen et al. 1984; Wetherald and Manabe 1988). The
1240 model intercomparison organized by Cess et al. (1989) pointed to the importance of cloud feed-
1241 backs for climate change. The intercomparison of (Cess et al. 1989) marked the beginning of
1242 increased communication and cooperation among the world's modeling groups. It had an imme-

1243 diate influence on the formulations of some of the participating models. For example, comparison
1244 of results from different models led to the discovery of some coding errors!

1245 Starting in the 1980s, cloud-parameterization testing became organized on an international scale,
1246 beginning with NASA’s FIRE Program¹¹ during the 1980s (Cox et al. 1987), and continuing in the
1247 1990s and beyond with DOE’s ARM Program¹² (Stokes and Schwartz 1994; Turner and Ellingson
1248 2017) and the GCSS¹³ activities (GEWEX Cloud System Science Team 1993; Randall et al. 2003).
1249 The radiation intercomparisons mentioned in subsection c are important ways of testing radiation
1250 parameterizations. One strategy for testing the parameterizations of a model as a coupled set
1251 is to drive both the parameterized column physics of a GCM and a high-resolution CRM (e.g.,
1252 Krueger 1988; Khairoutdinov and Randall 2003) or LES model with “forcing” data based on field
1253 observations, and then compare the results of the two models with each other and with additional
1254 observations from the field (Randall et al. 1996b). The column-physics is called a “single-column
1255 model.” The high-resolution models are called “process models.”

1256 *e. Momentum transport by gravity waves*

1257 Eliassen (1960) analyzed the vertical fluxes of energy and momentum associated with internal
1258 gravity waves excited by the wind blowing over mountain ranges. The importance of such fluxes
1259 for the global circulation began to be appreciated about twenty years later (Lindzen 1981). Since
1260 the mid-1980s, there has been a lot of interest in the effects of gravity wave momentum fluxes on
1261 the global circulation of the atmosphere; because the waves act to decelerate the mean flow, these
1262 interactions are referred to as “gravity-wave drag” (Palmer et al. 1986; McFarlane 1987). At the
1263 beginning, most of the discussion was about gravity waves forced by flow over topography, but

¹¹FIRE stands for the First ISCCP Regional Experiment; ISCCP is the International Satellite Cloud Climatology Project.

¹²ARM stands for Atmospheric Radiation Measurements.

¹³GCSS stands for the GEWEX Cloud Systems Study; GEWEX is the Global Energy and Water Experiment.

1264 later gravity waves forced by convective storms were also recognized as important (e.g., Fovell
1265 et al. 1992; Richter et al. 2014).

1266 Ocean models are also parameterizing momentum transport and mixing due to internal gravity
1267 waves, as discussed in section 8 d 3.

1268 *f. Land-surface modeling during the 1980s*

1269 During the 1980s methods were developed to relate evapotranspiration on the land surface to the
1270 actual physiology of plant stomates. In a key paper, Jarvis (1976) used laboratory measurements to
1271 derive empirical functions that related stomatal conductance to light, humidity, and temperature.
1272 Plants actively control the aperture of their stomates in response to these three environmental
1273 variables. Light triggers photosynthesis, during which stomates must open to let CO₂ diffuse into
1274 their tissues. The rate of transpiration through open stomates depends on the humidity of the
1275 environmental air, so plants close their stomates in very dry air to prevent desiccation. Finally,
1276 stomates tend to close when conditions are either too hot or too cold.

1277 These ideas were combined with previous work in land surface modeling to create compre-
1278 hensive schemes aimed at fulfilling Richardson's vision of realistic land-surface boundary con-
1279 ditions for atmospheric models. Examples of such models were the work of Deardorff (1978),
1280 the Biosphere-Atmosphere Transfer Scheme (BATS; Dickinson et al. 1986), the Simple Biosphere
1281 Model (SiB; Sellers et al. 1986), and the model of Noilhan and Planton (1989). These models were
1282 fully coupled to atmospheric global circulation models and provided interactive lower boundary
1283 conditions for the exchange of radiation, heat, water, and momentum. They included two-stream
1284 canopy radiative transfer for the calculation of leaf and soil temperatures and albedo. They prog-
1285 nosed soil moisture and temperature and diagnosed the temperature of vegetation, and turbulent
1286 fluxes of sensible and latent heat as well as ground heat flux. Surface parameters such as rough-

1287 ness, radiative properties, and soil hydraulic properties were prescribed as global maps derived
1288 from many disparate sources.

1289 Turbulent fluxes in these models were represented using a network of nodes and resistors (Fig-
1290 ure 10) using an “electrical analogy” to Ohm’s Law, which was first introduced by Richardson
1291 (1922). Temperature and water vapor are treated as potentials, the fluxes of sensible and latent
1292 heat among model components as resulting currents proportional to the difference in potentials,
1293 and the proportionality coefficients as variable resistors. Ohm’s Law is thus simply analogous to
1294 diffusion, with diffusivity at the molecular scale for transpiration through plant stomates and at
1295 turbulent scales elsewhere in the model. BATS (Dickinson et al. 1986) used a single plant canopy
1296 layer, whereas SiB (Sellers et al. 1986) introduced a sub-canopy or “understory” of grass or shrubs
1297 beneath a taller tree canopy.

1298 Simulation experiments revealed important modes of interaction between the vegetated land
1299 surface and the atmosphere that can affect climate. Charney (1975) showed that land clearing
1300 and overgrazing could lead to drought through a feedback between surface albedo and enhanced
1301 atmospheric subsidence. Shukla and Mintz (1982) demonstrated that evapotranspiration from
1302 land exerted a profound influence on the Earth’s hydrologic cycle and climate. Dickinson and
1303 Henderson-Sellers (1988) used a coupled land-atmosphere GCM to explore the consequences of
1304 tropical deforestation. They manipulated model surface parameters to simulate the conversion of
1305 the Amazon rainforest to grassland, which resulted in substantial surface warming due primarily
1306 to changes in albedo and roughness.

1307 Land surface modelers recognized the very substantial mismatch in spatial scales between mi-
1308 croscopic stomata, macroscopic plant canopies, and GCM grid cells that were hundreds of km
1309 across. Jarvis and McNaughton (1986) recognized that under low-wind conditions evapotranspi-
1310 ration from vegetation acted to humidify the air near the surface, reducing the vapor pressure

1311 gradient and thereby shifting the energy balance toward sensible heat. They introduced the idea of
1312 estimating surface energy fluxes at landscape scales as a continuum between physiological control
1313 by stomates and environmental control by radiation, atmospheric humidity, and wind speed. They
1314 introduced a coupling coefficient to represent this continuum, and showed that at larger scales
1315 transpiration is influenced less by stomata and more by radiation.

1316 Besides the leaf-to-canopy conundrum, scaling local fluxes to GCM grid cells was also problem-
1317 atic because the coupling may include dynamical processes above heterogeneous surfaces which
1318 are distributed at sub grid scale. These are very common, arising from juxtaposed farms and cities,
1319 forests and pastures, or even locations with and without antecedent rain. Anthes (1984) showed
1320 that mesoscale circulations induced by strong gradients in temperature and sensible heat fluxes
1321 above wet and dry patches in semiarid regions acted like inland sea breezes to enhance convection
1322 along the boundaries between patches. These circulations can interact with both the atmospheric
1323 and land states to create mesoscale energy and water fluxes that can't be obtained by linear aver-
1324 aging of surface fluxes in isolation (Avisar and Pielke 1989; Pinty et al. 1989; Pielke et al. 1991).
1325 Pielke et al. (1991) used limited area coupled models and found that they could be significant
1326 under conditions of large patches and low mean wind speeds.

1327 Another key development in the 1980s was global mapping of vegetation properties using satel-
1328 lite imagery. Chlorophyll and other pigments absorb strongly in visible wavelengths to drive pho-
1329 tosynthesis, but they are highly reflective in the near infrared part of the solar spectrum (Tucker
1330 1979). A series of polar-orbiting weather satellites maintained by the National Oceanographic and
1331 Atmospheric Administration to monitor cloud properties produced near daily global coverage of
1332 a quantity called the Normalized Difference Vegetation Index or NDVI. The NDVI was shown to
1333 be highly correlated with plant growth and CO₂ uptake (Tucker et al. 1986; Fung et al. 1987). Al-
1334 gorithms were developed to derive self-consistent vegetation parameters for land surface models

1335 from satellite imagery (Sellers 1985). These began to replace the ad-hoc and often inconsistent
1336 sets of global parameter maps.

1337 *g. Reanalysis*

1338 Improved global observations of the atmosphere and the Earth's surface, especially from satel-
1339 lites, made global weather analyses a realistic possibility (Bengtsson et al. 1982). Global models
1340 and their associated data assimilation systems were essential for the production of these analyses.
1341 "Reanalysis" of historical data using a the best available global model was advocated by Bengts-
1342 son et al. (1982), and soon became a reality (Kalnay et al. 1996; Uppala et al. 2005; Saha et al.
1343 2010a; Onogi et al. 2007; Schubert et al. 1993; Rienecker et al. 2011; Gibson 1997; Dee et al.
1344 2011). Reanalysis uses a fixed but up-to-date forecast model and data assimilation system to pro-
1345 cess historical observations over a long record. Fixing the systems avoids some of the temporal
1346 discontinuities that occur in a series of routine operational analyses, though not discontinuities
1347 caused by large changes in the available observations. Reanalyses have now become essential for
1348 atmospheric science research. The application of global ocean models to the reanalysis of ocean
1349 observations is at an earlier stage of development (Schiller et al. 2008; Balmaseda et al. 2013),
1350 but reanalyses of the coupled ocean-atmosphere system are beginning to appear (Laloyaux et al.
1351 2018).

1352 *h. Global warming becomes a societal concern*

1353 During the 1960s, climate scientists were aware of the possibility of anthropogenic climate
1354 warming due to increasing greenhouse gas concentrations, but the issue had not yet reached the
1355 public consciousness. This changed during the 1980s, as observations showed continuing in-
1356 creases in CO₂ concentrations, and the United States Congress and other governmental bodies

1357 began to take an interest (Shabecoff 1988; Weart 2008). More simulations of anthropogenic cli-
1358 mate change were appearing in the literature (e.g., Hansen et al. 1981; Washington and Meehl
1359 1989). Today, ESM development is increasingly driven by the global warming issue.

1360 **7. The 1990s**

1361 *a. New models, and new interactions among modeling groups*

1362 During the 1990s, important new models were created, and modeling groups began interacting
1363 in important new ways.

1364 In 1990 the Met Office Hadley Centre was opened (Folland et al. 2004), creating a dedicated
1365 center for research on the Earth's climate (e.g., Senior and Mitchell 2000; Mitchell et al. 1995b).
1366 The Hadley Centre's Unified Model (Cullen 1993b; Cullen et al. 1997; Davies et al. 1998) is
1367 designed for use in both operational NWP and climate simulation. This has the advantage that
1368 operational NWP is an excellent way to test a climate model (e.g., Palmer et al. 2008; Senior et al.
1369 2010).

1370 A version of the ECMWF forecast model was modified to create ECHAM (Roeckner et al. 1989;
1371 Simmons et al. 1989; Stevens et al. 2013), a climate model in use at the Max Planck Institute for
1372 Meteorology in Hamburg, Germany. More recently, the center is using a new global atmosphere
1373 model called ICON, which is based on a geodesic grid, and which has been developed in a part-
1374 nership with the German Weather Service (Wan et al. 2013; Giorgetta et al. 2018). Here again we
1375 see a single model being used for both operational NWP and climate simulation.

1376 As mentioned in section 6 d, Cess et al. (1989) organized an intercomparison of results from
1377 many modeling groups. Additional intercomparisons proliferated during the 1990s. An important
1378 example is the Atmospheric Model Intercomparison Project (AMIP; Gates 1992). AMIP was

1379 presaged by the study of Lau (1985), who showed that the atmosphere responds strongly and
1380 predictably to prescribed observed interannual changes in sea surface temperatures. An AMIP
1381 simulation uses an atmospheric model (coupled to a land-surface model) with prescribed observed
1382 sea surface temperatures for a sequence of real years. An AMIP simulation can be used to test
1383 the ability of a global atmospheric model to respond realistically to interannual variability of sea
1384 surface temperatures such as that associated with El Niño. The experimental design is similar to
1385 that developed earlier by Lau (1985), but follows a formal protocol. AMIP simulations continue to
1386 be a valuable and widely used method to test global atmospheric models (e.g., Eyring et al. 2016).
1387 Intercomparisons have also been crucial for the work of the Intergovernmental Panel on Climate
1388 Change (IPCC), which issued its first assessment report in 1990 (IPCC 1990) and continues its
1389 work today (e.g., Stocker et al. 2013). The IPCC is a truly historic enterprise that is strongly
1390 reliant on results from ESMs. The Coupled Model Intercomparison Project (CMIP) has been
1391 particularly central to the work of the IPCC (Meehl et al. 2000; Covey et al. 2003; Eyring et al.
1392 2016).

1393 Operational seasonal prediction with coupled ocean-atmosphere models began during the 1990s,
1394 and has gradually been maturing since (Palmer et al. 2000; Kanamitsu et al. 2002; Woods 2006;
1395 Kirtman and Pirani 2009).

1396 *b. Atmospheric dynamical cores*

1397 During the 1990s spectral semi-implicit semi-Lagrangian models were well-established. It was
1398 shown that the East-West density of grid points could be reduced near the poles (giving a ‘reduced
1399 grid) with negligible loss in accuracy (Hortal and Simmons 1991; Courtier and Naughton 1994).
1400 Also, since the advective nonlinearity was now handled by the semi-Lagrangian advection, the
1401 extra grid resolution needed to avoid aliasing of quadratic nonlinear terms was no longer necessary,

1402 and a coarser ‘linear grid’ could be used (Côté and Staniforth 1988; Williamson 1997). Both of
1403 these ideas led to further significant efficiency gains. An additional motivation for the adoption of
1404 semi-Lagrangian advection was that spectral advection of water vapor proved to be problematic
1405 (Williamson and Rasch 1994).

1406 Around this time interest was growing in global nonhydrostatic models. This stemmed partly
1407 from a desire for unified modeling systems that could operate either globally or at nonhydrostatic
1408 scales (Cullen et al. 1997) and partly from an ambition for global modeling that resolved nonhydro-
1409 static scales, which growing computer power would soon permit (Qian et al. 1998; Yeh et al. 2002;
1410 Satoh et al. 2008a; Matsuno 2016). The fully compressible equations support acoustic waves, and
1411 the CFL criterion for an explicit treatment of their vertical propagation would be very restrictive.
1412 Therefore, inspired by earlier work on small-scale nonhydrostatic models, one of four options
1413 was generally adopted. The first was a fully three-dimensional semi-implicit treatment of acoustic
1414 waves (Tapp and White 1976; Cullen et al. 1997; Qian et al. 1998; Yeh et al. 2002); a variety of
1415 solution methods for the resulting elliptic problem were tried. The second was a split-time-step
1416 method in which acoustic wave propagation was treated via shorter substeps. The third approach
1417 is to use a horizontally explicit but vertically implicit (“HEVI”) time-differencing scheme (Klemp
1418 and Wilhelmson 1978; Satoh et al. 2008a; Weller et al. 2013). This is motivated by the fact that
1419 vertical grid spacing is typically much finer than horizontal grid spacing, so that it is the verti-
1420 cally propagating sound waves that place the most severe limit on a model’s time step. The fourth
1421 approach is to use a sufficiently accurate set of equations that filters vertically propagating sound
1422 waves (Arakawa and Konor 2009), thus eliminating the problem before discretization begins.

1423 Semi-Lagrangian schemes proved to be very effective for weather forecasting, but for longer cli-
1424 mate simulations they were limited by their lack of conservation. This prompted the development
1425 of several conservative large-time-step advection schemes (e.g., Harris et al. 2011, and references

1426 therein), some of which were eventually incorporated into operational models (Lauritzen and Nair
1427 2008; Wood et al. 2014).

1428 *c. The evolution of the vertical coordinates used in atmosphere and ocean models*

1429 The vertical coordinate is a fundamental algorithmic choice for atmosphere and ocean models.
1430 It determines how subgrid-scale parameterizations manifest and what parameterizations are ap-
1431 propriate. A comprehensive discussion of vertical coordinate systems for hydrostatic atmospheric
1432 models was published by Kasahara (1974). For ocean models, the vertical coordinate determines
1433 representations of the upper-ocean and bottom boundary layers and the stratified ocean interior as
1434 well as their interactions with each other and with the solid-earth (Griffies et al. 2000). Vertical
1435 coordinates for numerical modeling of the atmosphere and ocean have been under study at least
1436 since the 1950s, and work continues today. We choose to summarize the topic in this section of
1437 our chapter because many important ideas emerged during the 1990s.

1438 1) QUASI-EULERIAN VERTICAL COORDINATES

1439 As mentioned earlier, both pressure and height were used as vertical coordinates in early global
1440 atmospheric models. These choices are both problematic (especially pressure), in part because the
1441 coordinate surfaces intersect the lower boundary. The terrain-following σ coordinate of Phillips
1442 (1957a) solves that problem by conforming to the lower boundary, but it leads to difficulty in the
1443 accurate computation of the horizontal pressure-gradient force above steep topography (Smagorin-
1444 sky et al. 1967; Kurihara 1968; Sundqvist 1975). The problem arises because with the sigma co-
1445 ordinate the horizontal pressure-gradient force is the sum of two terms. Over steep topography,
1446 these two terms are individually large and of opposite sign, and the horizontal pressure-gradient
1447 force is the relatively small difference between them. Mesinger (1982) and Mesinger and Janjić

1448 (1985) proposed a modified σ coordinate system, which they called η . The η coordinate elim-
1449 inates the problem with the horizontal pressure-gradient force near steep terrain by introducing
1450 “step mountains” that come in discrete sizes, like off-the-rack clothing. The sizes of the moun-
1451 tains are chosen to match the specified thicknesses of the model layers. For about 25 years, the
1452 η coordinate was used in the operational ETA Model used for regional prediction by the U.S.
1453 National Centers for Environmental Prediction (Janjić 1994); this was mentioned in Section 6 d.
1454 Simmons and Burridge (1981) suggested a different way to address the problem with the horizon-
1455 tal pressure-gradient force near steep terrain, through the use of a hybrid vertical coordinate that
1456 behaves like σ near the lower boundary but like pressure aloft. Their hybrid approach has been
1457 very widely used.

1458 For most applications of large-scale basin and global ocean circulation modeling, the vertical
1459 coordinate is based on geopotential (or depth). Similar but more flexible “quasi-Eulerian” ap-
1460 proaches have been developed (Adcroft and Hallberg 2006). They can be used with ocean models
1461 that retain the traditional Bryan (1969b) algorithmic architecture, in which the vertical vertical
1462 motion crossing coordinate surfaces (i.e., vertical velocity) is diagnosed through mass continu-
1463 ity in non-Boussinesq models or volume continuity in Boussinesq models. Of particular note for
1464 global climate efforts is the rescaled geopotential coordinate z^* , which allows more flexibility with
1465 realistic undulations of the ocean free surface than the traditional geopotential (z -coordinate) mod-
1466 els (Stacey et al. 1995). The z^* coordinate was first implemented in the MITgcm by Adcroft and
1467 Campin (2004), and has been used for climate applications with MOM4.1 and MOM5 (Griffies
1468 et al. 2005).

1469 Another advance was made by Marshall et al. (2004), who made use of an isomorphism between
1470 pressure coordinate non-Boussinesq (compressible) fluids and geopotential coordinate Boussinesq
1471 (incompressible) fluids. This made it straightforward to incorporate compressible dynamics into

1472 formerly incompressible ocean models. Doing so allows ocean models to include a full representa-
1473 tion of oceanographic processes impacting the model’s sea level, including the global thermosteric
1474 effects that are missing from Boussinesq models (Griffies and Greatbatch 2012).

1475 The σ coordinate has also been adapted for use in ocean models, for example by Lemarié et al.
1476 (2012). Their work, implemented in the Regional Ocean Modeling System (ROMS; Shchepetkin
1477 and McWilliams 2005), bridges the gap between regional and global modeling applications. The
1478 Russian Institute of Numerical Mathematics Ocean Model (INMOM; Volodin et al. 2010) also
1479 uses a global, σ coordinate model as the ocean component of an ESM.

1480 2) QUASI-LAGRANGIAN METHODS

1481 Quasi-Lagrangian methods have also been used in both atmosphere and ocean models. In these
1482 methods, the vertical “layers” of a model are bounded by surfaces that move with the fluid, as
1483 nearly as possible, so that little or no mass crosses layer edges. For atmospheric models, one ap-
1484 proach is to use potential temperature, θ , as a vertical coordinate; in the absence of heating, the
1485 “vertical velocity” vanishes with the θ coordinate. For ocean models, the corresponding isopy-
1486 cnal approach is to use potential density as the vertical coordinate, so that the vertical velocity
1487 vanishes in the absence of diapycnal diffusion (Adcroft and Hallberg 2006). Isopycnal ocean
1488 models have the advantage of naturally including advection along potential density surfaces in
1489 the quasi-adiabatic ocean interior below the strongly mixed upper ocean. However, they are at a
1490 disadvantage at high latitudes where their vertical resolution declines because of the very small
1491 density difference between the surface and deep ocean.

1492 The utility of θ coordinates for observational analyses was appreciated very early, by Rossby
1493 (1937) and Starr (1945). It was further developed by Johnson (1989), and by Hoskins et al. (1985),
1494 who emphasized the dynamical importance of the isentropic potential vorticity. Early atmospheric

1495 models based on θ coordinates were developed by Eliassen and Raustein (1968) and Bleck (1973).
1496 More recently, the merits of models based on θ coordinates have been discussed by Hsu and
1497 Arakawa (1990), Johnson (1997) and Benjamin et al. (2004), among others.

1498 An issue with the use of θ coordinates in models is that θ surfaces intersect the Earth's surface.
1499 This has motivated numerous proposals for hybrid σ - θ coordinates (e.g., Johnson and Uccellini
1500 1983; Zhu et al. 1992; Bleck and Benjamin 1993; Zapotocny et al. 1994; Konor and Arakawa 1997;
1501 Benjamin et al. 2004; Bleck et al. 2010a). An alternative is the "Arbitrary Lagrangian-Eulerian"
1502 (ALE) approach (Bleck and Benjamin 1993; Bleck et al. 2010a), which allows deviations from
1503 strict θ coordinates on the basis of a set of "rules." For example, a rule might enforce a minimum
1504 pressure difference across a model layer (Toy and Randall 2009), or it might periodically "remap"
1505 the edges of quasi-Eulerian layers to pre-specified target values of the σ coordinate (Lin 2004).
1506 The ALE method allows for a mapping to an arbitrary vertical surface, such as geopotential, σ ,
1507 potential temperature (or potential density), or even coordinates with no explicit mathematical
1508 definition.

1509 Isopycnal ocean models were pioneered by Rainer Bleck at the University of Miami with the Mi-
1510 ami Isopycnic Coordinate Ocean Model (MICOM), a well used community layered model (Bleck
1511 and Boudra 1986; Sun and Bleck 2001). A version of MICOM has been developed by Helge
1512 Drange and colleagues at the University of Bergen, and is the ocean component of the Norwegian
1513 Earth System Model (Bentsen et al. 2013). Dunne et al. (2012) used a layered isopycnal model
1514 developed at GFDL for use in climate (General Ocean Layer Dynamics; GOLD).

1515 The quasi-Lagrangian approach used in isopycnal models provides a useful starting point for
1516 efforts to implement the Arbitrary Lagrangian-Eulerian (ALE) methods (Donea et al. 2004) in
1517 ocean models (Bleck 2002). The ALE method provides a natural framework for wetting and
1518 drying, such as for studies of coastal inundation and moving ice shelf grounding lines (Goldberg

1519 et al. 2012). HYbrid Coordinate Ocean Model (HYCOM) made use of ALE to blend an isopycnal
1520 coordinate in the deeper ocean with a depth coordinate in the strongly mixed upper ocean, with
1521 terrain following coordinates along the shelves. HYCOM became the ocean component of the
1522 Goddard Institute for Space Sciences climate model (Sun and Bleck 2006).

1523 The ALE approach is now spreading throughout the ocean modeling community to codes such
1524 as Model for Prediction Across Scales Ocean (MPAS-O; Ringler et al. 2013) and MOM6 (Adcroft
1525 and Hallberg 2006). Similar methods are also becoming more fully realized in the atmospheric
1526 modeling community (Bleck et al. 2015, 2010b; Sun et al. 2018).

1527 *d. Radiative transfer modeling in the 1990s: Unification*

1528 The errors evident in many radiation codes used in weather and climate models in the early
1529 1990s prompted the development of new codes with a close link to reference models. Mlawer et al.
1530 (2016) describes the development of one such code: RRTM (Mlawer et al. 1997).¹⁴ RRTM imple-
1531 ments a correlated k -distribution (Goody et al. 1989; Lacis and Oinas 1991; Fu and Liou 1992), an
1532 extension of the original k -distribution technique to vertically inhomogeneous atmospheres. The
1533 code was originally developed as an offline column model aimed at reproducing line-by-line cal-
1534 culations (themselves tightly constrained by a new wealth of observations, as Mlawer et al. (2016)
1535 describes), but soon included an offshoot with reduced spectral resolution (RRTMG) for use in
1536 atmospheric models.

1537 The UK Met Office undertook a similar effort aimed at their new Unified Model (Cullen 1993a),
1538 the first to be used to make both routine weather forecasts and climate projections. The Edwards-
1539 Slingo code (Edwards and Slingo 1996) stressed flexibility: the correlated k -distribution is spec-
1540 ified at run time, allowing for different spectral resolutions and computational costs for different

¹⁴The acronym stands for “Rapid Radiative Transfer Model.”

1541 applications and for easy integration of new spectroscopic knowledge. Each k -distribution can
1542 be traced back to and assessed against a line-by-line calculation. Clouds are treated consistently
1543 across the longwave and shortwave spectrum; this includes treating scattering by clouds in long-
1544 wave calculations. John Edwards attributes many of these design decisions to Tony Slingo:

1545 Tony Slingo was the one who had the who had the vision for it, and a couple of things
1546 that he wanted very strongly. One was, because it was to be used in climate, we really
1547 wanted to get the forcings right, and so having the ability to run at different spectral
1548 resolutions and have, as far as possible, traceability from precise comparisons with line-
1549 by-line, was seen as very important. Another thing was that we wanted the same cloud
1550 overlap assumptions in long-wave and short-wave so we'd be doing cloud radiative effect
1551 consistently between the two spectral regions (*interview with John Edwards, 20 October*
1552 *2017*).

1553 *e. Boundary layer, cloud, and aerosol parameterizations during the 1990s*

1554 As discussed in section 5 d 1, Sommeria and Deardorff (1977) used higher-order closure with an
1555 assumed bivariate Gaussian distribution for (roughly speaking) temperature and moisture to deter-
1556 mine the fractional cloudiness and liquid water mixing ratio. This approach can be called Assumed
1557 Distributions with Higher-Order Closure (ADHOC). The intended application of Sommeria and
1558 Deardorff (1977) was large-eddy simulation, with grid cells less than 100 m across. Much later,
1559 Lewellen and Yoh (1993) suggested using a pair of joint Gaussians instead of one. This approach
1560 is more appropriate for larger grid cells that contain many clouds. In such larger grid cells, one
1561 of the Gaussians can represent the cloudy part of the domain, while the other represents the clear
1562 spaces between the clouds.

1563 Randall (1987), Randall et al. (1992), and Lappen and Randall (2001) added vertical velocity to
1564 the mix, so that vertical fluxes of temperature and moisture could be computed from the param-
1565 eters of the resulting trivariate distribution. Following the mass flux approach, they used a pair
1566 of delta functions, one representing turbulent updrafts and the other representing downdrafts. Fi-
1567 nally, Golaz et al. (2002b) combined the approaches of Lappen and Randall (2001) and Lewellen
1568 and Yoh (1993), resulting in a pair of trivariate Gaussians. This method has been used by Bogen-
1569 schutz and Krueger (2013), Bogenschutz et al. (2013), and Thayer-Calder et al. (2015). It has now
1570 been implemented in version 6 of the Community Atmosphere Model, with encouraging results
1571 (Bogenschutz et al. 2018).

1572 Increasingly detailed microphysics parameterizations have also been incorporated into global
1573 atmospheric models. Beginning in the early 1990's, climate models began to adopt prognostic
1574 equations for cloud water following the approach of Sundqvist et al. (1989), sometimes with sep-
1575 arate equations for liquid and ice (e.g., Ose 1993; Lohmann and Roeckner 1996; Rotstayn et al.
1576 2000). The fraction of cloud water present as liquid or ice is critical for cloud radiative properties.
1577 These schemes typically employed diagnostic precipitation schemes (e.g., Ghan and Easter 1992),
1578 while others adopted prognostic equations for both cloud and precipitation similar to mesoscale
1579 models developed in the 1980's and 1990's employing Kessler-like parameterizations (e.g., Fowler
1580 et al. 1996).

1581 The value of predicting two characteristics or moments of the cloud and precipitation size dis-
1582 tributions, namely the number and mass, has been recognized since at least the 1970s (Koenig
1583 and Murray 1976). Such "two-moment" parameterizations allow independent evolution of bulk
1584 mass and mean size, which improves the physical realism for processes such as size sorting (the
1585 preferential fallout of larger and heavier particles). The prediction of cloud particle number by
1586 these schemes also allows explicit coupling with chemistry and aerosols through activation of

1587 cloud condensation and ice nuclei, allowing climate models to simulate aerosol indirect effects
1588 on clouds. Two-moment schemes were developed and applied in a few cloud-scale models in the
1589 1980's (e.g., Ziegler 1985), but came into widespread use for cloud and mesoscale modeling in the
1590 mid 1990s through the 2000s (e.g., Schoenberg Ferrier 1994; Cohard and Pinty 2000; Seifert and
1591 Beheng 2001).

1592 Starting in the 1990s, the development of aerosol representations for use in global climate mod-
1593 els was motivated by a need to study the direct effects of aerosols on radiative forcing (e.g., Kiehl
1594 and Briegleb 1993; Taylor and Penner 1994; Mitchell et al. 1995a; Haywood et al. 1997). Dur-
1595 ing this time, climate models also began to simulate the indirect effects of aerosols on radiation
1596 through their influence on clouds, by diagnostically relating droplet number to aerosol properties
1597 (e.g., Boucher and Lohmann 1995).

1598 *f. Land-surface modeling during the 1990s*

1599 With the availability of fully coupled global land-atmosphere models and the widespread recog-
1600 nition of the problems of scale, a series of ambitious field experiments were undertaken to evaluate
1601 models by quantifying regional land-atmosphere interactions in nature. These included the First
1602 ISLSCP Field Experiment (FIFE) over the Kansas prairie (Hall and Sellers 1995); the Hydrologic
1603 Atmospheric Pilot Experiment (HAPEX) in the African Sahel (Prince et al. 1995); the Boreal
1604 Ecosystem-Atmosphere Study (BOREAS) in central Canada (Sellers et al. 1997); and the Large-
1605 Scale Biosphere-Atmosphere Experiment in Amazonia (LBA) in Brazil (Keller et al. 2004). Each
1606 of these experiments involved simultaneous measurements of both atmospheric and surface con-
1607 ditions at a range of spatial scales from individual leaves and soil probes to regional footprints
1608 meant to represent entire GCM grid cells. The pioneering field experiments made extensive use
1609 of new satellite data sets and provided a huge resource for both testing models derived from lo-

1610 cal relationships and especially for learning how scales of land-atmosphere interaction worked in
1611 nature.

1612 During the 1990s, many studies used coupled models to analyze land-atmosphere interactions in
1613 nature (e.g., Betts et al. 1996). In particular, comparisons of models and observations showed that
1614 soil moisture could act as a long-memory component in the climate system to amplify or extend the
1615 duration of droughts and rainy periods (Oglesby and Erickson III 1989; Lean and Rowntree 1993;
1616 Dirmeyer 1994; Milly and Dunne 1994; Brubaker and Entekhabi 1996; Diedhiou and Mahfouf
1617 1996; Trenberth and Guillemot 1996; Eltahir 1998; Fennessy and Shukla 1999; Douville et al.
1618 2001). Precipitation recycling of water through evapotranspiration was recognized as a major
1619 process at regional scales (Trenberth 1999). By this time, land-atmosphere coupling had also
1620 been adopted in numerical weather forecasting (Viterbo and Beljaars 1995). Interactive land-
1621 atmosphere models were used to analyze the role of the land surface in amplifying or extending
1622 the duration of droughts and rainy periods. Beljaars et al. (1996) used coupled models to analyze
1623 the effect of anomalies in soil moisture on persistent atmospheric circulation patterns associated
1624 with major drought and floods. They found that forecasts of the summer US drought in 1988
1625 and the Mississippi River floods in 1993 were dramatically improved when they initialized their
1626 coupled model with realistic soil moisture.

1627 An innovative approach to the problem of subgrid-scale heterogeneity at the land surface was
1628 developed by Koster and Suarez (1992), in which many instances of the land parameterization are
1629 coupled to a single overlying atmosphere. The separate instances, or “tiles” have different proper-
1630 ties such as assemblages of vegetation or soils, or may represent separate hydrologic catchments
1631 within a larger GCM grid cell. Separate calculations of prognostic soil temperature and mois-
1632 ture are done for each tile, and then the energy fluxes of each are weighted by their subgrid-scale
1633 fractional area before being passed to the atmospheric component. This approach has since been

1634 widely adopted to represent heterogeneity. Unlike the mesoscale flux experiments discussed above
1635 with limited area models (e.g., Pielke et al. 1991), tiling is tractable in global models because the
1636 computational expense of multiple instances of the land model is modest.

1637 Plant physiologists worked with climate modelers to improve the biological realism of parame-
1638 terized stomatal resistance. Rather than the simple empirical functions relating stomatal aperture
1639 to radiation, humidity, and temperature (Jarvis 1976; Dickinson et al. 1986), a new generation of
1640 models coupled stomatal function with photosynthesis. The new approach recognized that stom-
1641 atal conductance solves an optimization problem in which plants evolved physiological mecha-
1642 nisms to maximize carbon gain under the constraint of minimizing water loss. Sellers et al. (1992)
1643 introduced the calculation of photosynthetic carbon assimilation using enzyme kinetic relation-
1644 ships previously studied in the laboratory (Farquhar et al. 1980). High rates of photosynthesis
1645 require highly conductive (open) stomates, which also allow transpiration. This simultaneously
1646 depletes CO₂ and enhances vapor pressure at the leaf surface, which feeds back on both photosyn-
1647 thesis and stomatal conductance (Ball 1988). An additional node was inserted between stomatal
1648 pores and the canopy air space to the resistance network in previous models. This laminar bound-
1649 ary layer at the leaf surface may be only a few millimeters thick, but maintains higher vapor
1650 pressure in immediate contact with stomatal pores and retards the upward flow of water vapor by
1651 turbulent exchange. Adding this extra resistance largely solved the coupling problem previously
1652 highlighted by Jarvis and McNaughton and allowed a greater degree of biophysical realism (Col-
1653 latz et al. 1991). The models were iterated to solve simultaneously for the stomatal conductance
1654 and the rates of photosynthesis and transpiration.

1655 Research continued into the critical problem of scaling physiological processes from stomates
1656 to grid cells. Sellers et al. (1992) showed that a simultaneous solution for canopy-scale transpira-
1657 tion could be obtained from leaf-level parameters by assuming that (1) the progressive downward

1658 attenuation of solar radiation through vegetation canopies followed an exponential decay with cu-
1659 mulative leaf area (Beers' Law); and that (2) plants have evolved to redistribute scarce resources
1660 (primarily nitrogen) according to the time-mean vertical distribution of light. These two assump-
1661 tions allowed leaf-level equations for stomatal conductance and the rates of photosynthesis and
1662 transpiration to be integrated vertically in closed form.

1663 Leaf area index is the area of leaves in a canopy per unit area of ground, and Sellers et al. (1992)
1664 used the cumulative leaf area index above a point in the canopy as a vertical coordinate. Integrat-
1665 ing assimilation (photosynthesis) rate from the top of the canopy to the ground, and assuming that
1666 photosynthesis decreases exponentially along with light, they obtained an equation for the fraction
1667 of photosynthetically active radiation absorbed by the canopy, commonly abbreviated as FPAR.
1668 Importantly, the FPAR is related to the remotely sensed NDVI, which was mentioned in section
1669 6 d. Retrievals of NDVI from space allow global estimates of canopy-scale stomatal conductance
1670 and the rates of photosynthesis and transpiration based on leaf-level physiology and the FPAR
1671 relationship. Coupling of photosynthesis and transpiration with canopy integration from remote
1672 sensing was used to construct a new coupled GCM (Sellers et al. 1996a; Randall et al. 1996a), and
1673 a complete suite of satellite-derived parameters for land surface modeling (Sellers et al. 1996b; Los
1674 et al. 2000). Within a few years, many groups around the world also developed global land sur-
1675 face models based on integrated photosynthesis and transpiration, which were coupled to GCMs
1676 (Friend et al. 2007; Foley et al. 1996; Bonan 1996, 1998; Cox et al. 1998).

1677 Although Sellers et al. (1992) intended the FPAR to represent the continuous attenuation of
1678 light in vegetation canopies, Bonan (1996) showed that this quantity can also be interpreted as
1679 the sunlit (as opposed to shaded) leaf area index. In this interpretation, only sunlit leaves are
1680 integrated in the scheme of Sellers et al. (1992), meaning that photosynthesis and transpiration
1681 are likely underestimated due to the presence of shaded leaves illuminated by diffuse radiation

1682 from the sky. Pury and Farquhar (1997) developed a simple scheme to separate plant canopies
1683 into sunlit and shaded fractions with different temperatures, stomatal conductance, and rates of
1684 photosynthesis and transpiration. Although the photosynthesis rate of shaded leaves is less than
1685 that of sunlit leaves, they use light more efficiently because diffuse light penetrates more deeply
1686 into dense canopies. This “two-big-leaf” approach has since been adopted by most land models
1687 (Dai et al. 2004).

1688 *g. Sea ice advances during the 1990s*

1689 Eventually sea ice modelers tried to simplify the methods used to predict the motion of the sea
1690 ice, in order to make them practical for climate models. First Flato and Hibler III (1992) simplified
1691 the viscous-plastic dynamics by treating sea ice as a cavitating fluid, which lacks shear strength.
1692 Several modeling centers implemented cavitating-fluid dynamics and so became the first to simu-
1693 late sea ice with a constitutive law. But most of the centers abandoned cavitating-fluid dynamics
1694 when better options became available. Next, Los Alamos National Lab scientists Elizabeth Hunke
1695 and John Dukowicz developed a numerical approximation to the viscous-plastic dynamics to sim-
1696 ulate sea ice as an elastic-viscous-plastic material (Hunke and Dukowicz 1997), a method that
1697 asymptotes to the full viscous-plastic solution but is more efficient and highly parallelizable. In
1698 the same year, Zhang and Hibler III (1997) made the viscous-plastic numerics more efficient and
1699 parallelizable. The latter two dynamics schemes made possible major improvements in simulat-
1700 ing sea ice in climate models. The elastic-viscous-plastic approach is widely used among climate
1701 models today in part because the code was made readily available for sharing, with high-quality
1702 documentation and regular updates maintained by Hunke (1998) in a comprehensive model known
1703 as the Los Alamos sea ice model, or CICE.

1704 **8. Into the twenty-first century**

1705 Our story now approaches the present day, which means that much of the work is still ongoing,
1706 and we lack a historical perspective. Selected current issues are highlighted, but we do not attempt
1707 a comprehensive overview.

1708 *a. Current issues in atmospheric dynamical cores*

1709 1) HORIZONTAL GRIDS IN ATMOSPHERE AND OCEAN MODELS

1710 Evolving computer architectures are now having a significant effect on preferred numerical
1711 methods. From the mid 1990's onwards, the performance of computing machines has increased
1712 mainly through increased numbers of processors rather than faster processors. The communication
1713 of data between processors is relatively slow, and is becoming a significant bottleneck to compu-
1714 tational performance for both the spectral method, which requires global communication for the
1715 spectral transforms, and for grid-point methods on the longitude-latitude grid because of the polar
1716 resolution clustering. The trend towards massively parallel hardware has pushed the modeling
1717 world towards higher horizontal resolution. One consequence of these developments has been
1718 renewed interest in the use of quasi-uniform grids.

1719 It is now conventional to distinguish between “structured” and “unstructured” horizontal grids.
1720 A structured horizontal grid covers the sphere with quadrilateral cells, so that each cell in the grid
1721 can be identified by a pair of indices, such as (i, j) , and its neighbors can be specified by adding
1722 or subtracting 1 to i and/or j . Early structured grids made use of spherical latitude-longitude
1723 coordinates to tile the sphere. However, such grids suffer from singularities at the poles.

1724 Unstructured grids are more flexible. They cover the sphere with simple shapes, such as tri-
1725 angles, squares or hexagons. In contrast to structured methods, the unstructured approach does

1726 not rely on a fixed number of grid-cell neighbors, nor does it insist on local coordinate orthogo-
1727 nality. Although the spatial pattern of the cells may be very orderly, unstructured grids require a
1728 pre-stored list of the neighbors of each cell.

1729 Since the 1960's and 70's the importance of numerical properties such as conservation, mono-
1730 tonicity, accurate wave dispersion and balance, and avoidance of computational modes, has been
1731 much better appreciated, and a wide range of methods giving acceptable performance on unstruc-
1732 tured quasi-uniform grids has been developed (e.g., Masuda and Ohnishi 1986; Heikes and Randall
1733 1995). A related point is that the relative cost, in time and energy, of data movement in and out
1734 of memory as well as between processors, compared to computation, has greatly increased. Con-
1735 sequently, computationally intensive methods such as high-order Galerkin methods are no longer
1736 seen as prohibitively expensive.

1737 Starting with the German Weather Service's GME icosahedral grid model (Majewski et al.
1738 2002), this second wave of development on unstructured quasi-uniform grids has led to a number
1739 of production or production-capable models for both NWP and climate prediction (e.g., McGregor
1740 and Dix 2008; Satoh et al. 2008a; Putman and Lin 2007; Qaddouri and Lee 2011; Skamarock et al.
1741 2012a; Dennis et al. 2012; Zängl et al. 2015; Sun et al. 2018). This appears to be a trend.

1742 Today, most ocean models make use of structured grids in the horizontal according to either
1743 the Arakawa B-grid or C-grid (Arakawa and Lamb 1977; Griffies et al. 2000). With spherical
1744 coordinates, ocean models encounter a singularity at the North Pole, but not at the South Pole
1745 which lies in the middle of the Antarctic continent. To remove the north polar singularity while
1746 retaining a structured grid, ocean modelers today use alternative coordinates while retaining local
1747 orthogonality. A common approach for is the tripolar grid of Murray (1996) and Madec et al.
1748 (1997), whereby the North Pole singularity is split into two singularities safely "hidden" over
1749 land. An alternative is to displace the North Pole over land as in the displaced pole approach used

1750 by POP simulations (Smith et al. 1995). More specialized uses have also been considered, such as
1751 Marsland et al. (2007) who used the MPI ocean model to study ice shelves in a global model.

1752 Recent advances in the use of unstructured horizontal grids for ocean modeling have been based
1753 on both finite-volume (Ringler et al. 2013; Korn 2017) and finite-element (Danilov 2013) meth-
1754 ods. The MPAS-O has been developed at LANL (Ringler et al. 2013), and uses the ALE ver-
1755 tical discretization described earlier, as well as an unstructured horizontal grid based on finite-
1756 volume methods. This model is targeted towards global ocean circulation applications as well as
1757 coupled climate modeling. The Finite Element Sea-ice/Ocean Model (FESOM) was developed
1758 at the Alfred Wegener Institute, with particular applications focusing on high-latitude ocean do-
1759 mains and global ocean climate simulations (Danilov 2013). The greater flexibility of unstructured
1760 grids makes it possible to more faithfully represent the complex horizontal geometry of the World
1761 Ocean. It also offers an elegant means to nest fine resolution sub-domains within a coarser global
1762 grid. The drawback is that unstructured approaches can be more computationally expensive than
1763 structured approaches.

1764 2) COUPLERS

1765 As suggested in the discussion above, the atmosphere, ocean, and land-surface components of
1766 an ESM are often implemented on grids that have different shapes and different resolutions. For
1767 this reason, ESMs include “couplers” (e.g., Craig et al. 2012) that are designed to allow the
1768 components to exchange information via interpolation (particularly from coarser to finer grids)
1769 or averaging (from finer to coarser). These exchanges are formulated so as to respect important
1770 physical principles such as conservation of mass and energy. It is possible that future very high-
1771 resolution models will not need couplers.

1772 *b. Current issues in radiative transfer parameterization*

1773 With the widespread availability of accurate parameterizations of clear-sky radiative transfer,
1774 attention turned to clouds, and particularly problems introduced by subgrid-scale variability. A
1775 range of observations (Cahalan et al. 1994; Pincus et al. 1999; Rossow et al. 2002) had shown that
1776 clouds are substantially inhomogeneous on the 10-100 km scales of the day's global models, and
1777 Cahalan et al. (1994) had used simple calculations to argue that ignoring this variability inevitably
1778 biased reflectivity calculations, especially in the shortwave. Awareness that similar biases were
1779 likely influencing calculations of precipitation (Pincus and Klein 2000; Rotstayn 2000a) motivated
1780 the development of cloud schemes that explicitly predicted internal variability (e.g., Tompkins
1781 2002; Golaz et al. 2002a). Further discussion is given in section 8 c.

1782 Various solutions to the problem have been proposed. Barker (1996) and Oreopoulos and Barker
1783 (1999) developed a closed-form solution to the two-stream equations integrated over a specific
1784 distribution of optical depth. Cairns et al. (2000) and Petty (2002) proposed rescaling the optical
1785 properties of the clouds based on a measure of their variability, an idea related to methods for
1786 treating radiative transfer in random media. A more flexible solution was to do independent calcu-
1787 lations over optimally chosen elements of the cloud optical depth distribution (Collins 2001; Neu
1788 et al. 2007; Shonk and Hogan 2008).

1789 An intercomparison effort was key to identifying the intertwined roles of cloud overlap and
1790 internal variability in causing errors in cloudy-sky radiation calculations. ICRCCM-III (Barker
1791 et al. 2003) reported domain-averaged fluxes from a range of three- and one-dimensional radiative
1792 models applied to a high-resolution description of clouds obtained from fine-scale models.

1793 The intercomparison highlighted the weakness of the analytic treatments of cloud overlap that
1794 had been used since the 1960s, which introduce errors on par with those caused by neglecting

1795 variability. The paper describes errors as arising “mostly because of inappropriate cloud over-
1796 lap assumptions, incorrect application of overlap assumptions, neglect of horizontal variability of
1797 cloud, and inappropriate assumptions about horizontal variability.”

1798 ICRCM-III highlighted the need for flexibility in computing radiative transfer in cloudy skies:
1799 accuracy required that calculations be able to adapt to a wide range of overlap specifications as well
1800 as complicated descriptions of internal variability. Any practical new method had to meet these
1801 accuracy requirements without substantially increasing computational cost, which was already
1802 high enough that models typically computed radiation less frequently in time, and possibly at
1803 lower spatial resolution, than other physical processes.

1804 The Monte Carlo Independent Column Approximation (McICA; see Pincus et al. 2003) uses a
1805 different, randomly generated discrete sample from the distribution of all possible cloud states with
1806 each spectral quadrature point, essentially replacing a two-dimensional integral over wavelength
1807 and cloud state with a Monte Carlo estimate. The fluxes computed with McICA are unbiased
1808 but, if the states used in each calculation (location, time, etc.) are chosen independently, the error
1809 introduced is also random. Extensive experience (e.g., Barker et al. 2008) demonstrated that this
1810 random error does not impact the simulation, and the technique has been widely adopted.

1811 *c. New approaches to representing cloud processes in global atmospheric models*

1812 1) GLOBAL CLOUD-RESOLVING MODELS

1813 The continuing increase in computer power (Habata et al. 2003) has made possible the devel-
1814 opment of global atmospheric models with grid spacings of just a few kilometers, so that they
1815 can crudely but explicitly simulate individual large clouds (Tomita and Satoh 2004; Tomita et al.
1816 2005; Satoh et al. 2008b, 2014; Putman and Suarez 2011). For now, these “global cloud-resolving
1817 models” are too expensive for simulation of century-scale climate change, but at present they can

1818 be used for simulations of about one year. Global cloud-resolving models are qualitatively differ-
1819 ent from lower-resolution models because they do not need parameterizations of deep convection,
1820 but they still need parameterizations of radiation, microphysics, and turbulence including small
1821 clouds.

1822 2) SUPER-PARAMETERIZATION

1823 In 1999, NCAR scientists Wojciech Grabowski and Piotr Smolarkiewicz created a multiscale
1824 GCM in which the physical processes associated with clouds were represented by implement-
1825 ing a simple cloud-resolving model (CRM) within each grid column of a low-resolution global
1826 model (Grabowski and Smolarkiewicz 1999; Grabowski 2001, 2004). With the embedded CRM,
1827 parameterizations of radiation, cloud microphysics, and turbulence (including small clouds) are
1828 still needed, but larger clouds and some mesoscale processes are explicitly (though crudely) sim-
1829 ulated. The GCM simulates the large-scale weather, while the CRMs simulate the small-scale
1830 convective response, which is fed back to the GCM. Grabowski and Smolarkiewicz found that
1831 their model produced interesting simulations of organized tropical convection, including systems
1832 that resembled the Madden-Julian Oscillation (MJO; Madden and Julian 1971, 1972).

1833 Inspired by the results of Grabowski and Smolarkiewicz, Khairoutdinov and Randall (2001)
1834 created a multiscale version of the Community Atmosphere Model (CAM; Collins et al. 2006a).
1835 They replaced most of the parameterizations used by CAM with a simplified version of Khairout-
1836 dinov's CRM (Khairoutdinov and Randall 2003). Parameterizations of radiation, microphysics,
1837 and turbulence are included in the CRM. One copy of the CRM runs in each grid-column of the
1838 CAM. The CRM is two-dimensional (one horizontal dimension, plus the vertical), and uses peri-
1839 odic lateral boundary conditions. In the study of Khairoutdinov and Randall (2001), the CRM had
1840 a horizontal domain 64 grid columns wide, with a horizontal grid spacing of 4 km. Because the

1841 CRM is two-dimensional, it cannot produce realistic vertical fluxes of horizontal momentum. For
1842 this reason, the momentum feedback to the GCM was not included.

1843 Khairoutinov and Randall dubbed the embedded CRM a “super-parameterization.” The combi-
1844 nation of a GCM with a super-parameterization is now called a Multiscale Modeling Framework,
1845 or MMF, and the MMF based on the CAM is now called the SP-CAM. Several additional MMFs
1846 have since been created, each based on a different GCM. In a major step, Stan et al. (2010) cou-
1847 pled the SP-CAM to a low-resolution version of POP (the Parallel Ocean Program). As reported
1848 by Stan et al. (2010), the coupled model gives a more realistic simulation of the atmospheric cir-
1849 culation than the SP-CAM “right out of the box,” without any tuning, a somewhat surprising result
1850 in view of earlier experiences of others (e.g., Sausen et al. 1988). Super-parameterized GCMs are
1851 much less computationally expensive than global cloud-resolving models.

1852 SP-CAM and the other MMFs have produced interesting simulations of the MJO, the diurnal
1853 cycle of precipitation, the Asian and African monsoons, and other phenomena, including anthro-
1854 pogenic climate change. Further discussion is given by Randall et al. (2016).

1855 Super-parameterization has also been tested in an ocean model (Campin et al. 2011) to simulate
1856 the small but important regions where deep convection occurs. Though promising, the super-
1857 parameterization technique has up to now been used less for the ocean than for the atmosphere.

1858 3) CLOUD MICROPHYSICS AND AEROSOLS

1859 With increased computing power and the related trend toward finer model resolution, more
1860 detailed representations of microphysics, including two-moment schemes, have recently been
1861 adopted for operational numerical weather prediction. Examples include the two-moment
1862 Milbrandt-Yau scheme in the High Resolution Deterministic Prediction System in Canada (Mil-
1863 brandt et al. 2016), and the aerosol-aware Thompson scheme (Thompson and Eidhammer 2014) in

1864 the U.S. Rapid Refresh (RAP) and High Resolution Rapid Refresh (HRRR) models. A diagram of
1865 a typical two-moment, multi-ice class scheme is shown in Fig. 5b. The recent development and op-
1866 erational use of high-resolution, convection-permitting km-scale forecast models has in particular
1867 motivated the use of more sophisticated microphysics schemes, since convective and cloud scale
1868 motions are more directly coupled to the microphysics. Over the last decade schemes have also
1869 been developed that have moved away from the traditional paradigm of using fixed categories rep-
1870 resenting different types of ice (e.g., Hashino and Tripoli 2007; Harrington et al. 2013; Morrison
1871 and Milbrandt 2015). These schemes evolve ice properties smoothly by predicting characteristics
1872 such as particle aspect ratio and density, and avoid some of the difficulties that arise with fixed
1873 ice categories. Although bin schemes are still too computationally expensive for operational mod-
1874 eling, they have been used for process studies of topics such as cloud-aerosol interactions (e.g.,
1875 Feingold et al. 1996; Fridlind et al. 2004; Khain et al. 2005) and microphysical-dynamical interac-
1876 tions (e.g., Stevens et al. 1996; Ackerman et al. 2004). They have also been used to develop and
1877 test bulk-microphysics schemes for weather and climate models (e.g., Khairoutdinov and Kogan
1878 2000).

1879 Two-moment schemes have also been developed for climate models, but motivated more by
1880 a need to physically treat clouds and radiation by predicting cloud droplet number, and links to
1881 aerosols (e.g., Ghan et al. 1997; Lohmann et al. 1999; Ghan et al. 2001; Ming et al. 2007; Lohmann
1882 et al. 2007) which have important radiative as well as microphysical effects (Boucher et al. 2013).
1883 The models use parameterizations of cloud condensation nuclei activation, coupled with prognos-
1884 tic multi-species aerosol chemistry and transport schemes (e.g., Stier et al. 2005; Seland et al.
1885 2008; Liu et al. 2011). Over the last decade, some climate models have also incorporated the ef-
1886 fects on clouds of ice-nucleating aerosols (e.g., Lohmann and Hoose 2009; DeMott et al. 2010),
1887 and including mixed phase clouds (Hoose et al. 2010; Gettelman and Morrison 2015). Current

1888 state-of-the-art ice nucleation parameterizations (e.g., Hoose et al. 2010) can directly incorporate
1889 laboratory and field measurements of ice nucleating particles, but there are still large uncertainties
1890 in ice nucleation properties.

1891 With higher resolution and increased computational resources, the microphysics schemes used
1892 in climate models now incorporate many features previously used in mesoscale models, including
1893 prognostic two-moment precipitation (Posselt and Lohmann 2008; Gettelman and Morrison 2015).
1894 A critical issue when incorporating such schemes in larger-scale models is that the cloud-scale
1895 and mesoscale motions driving the microphysics are not resolved, and thus the microphysics must
1896 be coupled with “macrophysics” parameterizations of the driving dynamic and thermodynamic
1897 processes. A related issue is that subgrid-scale scale variability of cloud quantities, typically
1898 neglected in small-scale models, is critical in larger-scale models because microphysical process
1899 rates often depend non-linearly on predicted cloud quantities (e.g., Pincus and Klein 2000; Larson
1900 et al. 2001; Rotstajn 2000b). This has been dealt with in global climate models by ad-hoc tuning
1901 of process rates (e.g., Golaz et al. 2011), or by integrating them over an assumed subgrid scale
1902 distribution of cloud water amount in each grid cell (Morrison and Gettelman 2008).

1903 An important advance over the past decade has been the development of Lagrangian particle-
1904 based microphysics schemes in which the multitude of cloud and precipitation hydrometeors are
1905 represented by a collection of “super-particles” that evolve as they are transported by the mod-
1906 eled flow (e.g., Shima et al. 2009; Andrejczuk et al. 2010; Unterstrasser and Sölch 2010). Un-
1907 like bin (and bulk) schemes that employ continuous-medium, Eulerian microphysical variables,
1908 Lagrangian-based schemes do not suffer from numerical diffusion errors.

1909 Up to now, most of the work on microphysics parameterization has been focused on stratiform
1910 clouds. The treatment of microphysics in convection parameterizations has generally remained
1911 very simple and crude, despite the facts that cumulus clouds generate a large fraction of the Earth’s

1912 precipitation, and detrainment from cumulus updrafts produces many radiatively important strat-
1913 iform clouds. All of these important effects of cumulus clouds are influenced by microphysical
1914 processes at work within the cumuli. Kerry Emanuel (1991) forcefully argued that more realistic
1915 microphysics is needed in cumulus parameterizations. There has been some recent progress in
1916 this area (Song and Zhang 2011; Elsaesser et al. 2017; Zhao et al. 2016). In addition, attempts
1917 have been made to unify cloud microphysics across cloud schemes with unified closures in cli-
1918 mate models treating all clouds with the same microphysics (Bogenschutz et al. 2013). Overall,
1919 the ongoing convergence of models spanning scales from weather to climate requires detailed, yet
1920 efficient cloud microphysics schemes linked consistently to the parameterized turbulence, convec-
1921 tion, and radiation.

1922 *d. Current issues in ocean modeling*

1923 1) OCEAN MODEL INTERCOMPARISONS

1924 The integrity of climate models is directly related to the integrity of the physical parameteri-
1925 zations in the ocean component. Early coupled ocean-atmosphere models drifted away from an
1926 earth-like climate due to inaccuracies in the representation and parameterization of physical pro-
1927 cesses in the models. An important milestone was reached by Boville and Gent (1998) and Gordon
1928 et al. (2000), whereby their use of improved ocean physical parameterizations was shown to en-
1929 able a much more stable simulation without the use of “flux adjustments.” Gent (2013) offers
1930 an overview of climate modeling and the role of the ocean and ocean physical parameterizations.
1931 Such results lend support for the need to study the ocean and sea-ice components of climate models
1932 separately from the fully coupled AOGCMs. For that purpose, the community has developed the
1933 Ocean Model Intercomparison Project (OMIP) started in the late 1990s. It took nearly 20 years
1934 to develop a suitable protocol and to improve model integrity sufficiently to support the OMIP

1935 exercise (Griffies et al. 2016). Such comparison projects have been the foundation for ongoing
1936 model improvements throughout much of the history of ocean modeling, and will remain so into
1937 the future.

1938 2) MESOSCALE EDDIES AND PARAMETERIZATIONS OF ISOPYCNAL DIFFUSION

1939 Realizing the importance of mesoscale eddies for ocean dynamics and the transport of heat, car-
1940 bon, and other tracers, oceanographers became rather critical of numerical simulations that had
1941 no representation of these eddies. As with synoptic eddies in the atmosphere, ocean mesoscale
1942 eddies have scales largely determined by the first baroclinic Rossby radius due to their connection
1943 to baroclinic instability. Ocean mesoscale eddies range in size from 100 km in the tropics to less
1944 than 10 km near the poles and on continental shelves. One response to this situation was to focus
1945 on quasi-geostrophic models, whose simpler dynamical equations and lack of thermodynamics al-
1946 lowed for the explicit representation of transient eddy features (Holland 1978). Another response
1947 was to tackle the problem of eddy parameterization while continuing to improve primitive equa-
1948 tion models. Although much progress has been made since the 1970s, the eddy parameterization
1949 problem remains at the forefront of ocean theory and modeling to this day.

1950 A conceptual framework for how mesoscale eddies act on the large-scale tracer field arose during
1951 the 1970s to 1990s. This framework arose largely from field measurements of transient radioactive
1952 ocean tracers as well as through atmospheric insights into transport from synoptic atmospheric
1953 eddies. The two key pieces to the framework are eddy-induced diffusion along neutral surfaces
1954 and eddy-induced stirring of density in a manner that reduces available potential energy. See the
1955 book by Griffies (2004) for a pedagogical treatment.

1956 Neutral diffusion (more commonly known as isopycnal diffusion) was proposed by Solomon
1957 (1971) and Redi (1982). The neutral diffusion operator respected growing observational evidence

1958 (Veronis 1975) that tracers are stirred by mesoscale eddies along neutral directions rather than
1959 along constant geopotential surfaces (see McDougall 1987; McDougall et al. 2014, for discussion
1960 of neutral directions). Cox (1987) offered a numerical implementation of isopycnal diffusion, and
1961 Griffies et al. (1998) updated the Cox scheme to remove some pernicious numerical instabilities.

1962 The eddy-induced tracer transport was proposed by Gent and McWilliams (1990). As per the
1963 energetic impacts from mesoscale eddies, the eddy-induced velocity is designed to dissipate avail-
1964 able potential energy (Gent et al. 1995; Griffies 1998). Complementary ideas from Greatbatch
1965 and Lamb (1990) noted the equivalence, for geostrophic flows, of vertical momentum form drag
1966 realized through vertical viscosity.

1967 As shown by Danabasoglu et al. (1994), the combined use of neutral diffusion and eddy-induced
1968 stirring remedied a huge suite of model biases that had plagued the ocean GCMs of the time.
1969 Evolved versions of these two parameterizations are still in use today in all ocean GCMs that do
1970 not explicitly resolve transient mesoscale eddy features. Neutral diffusion is simpler to implement
1971 in isopycnal models than the rotated neutral diffusion of geopotential models, but precludes the
1972 representation of water mass transformation by thermobaricity.

1973 Models that use quasi-Lagrangian methods (see Section 7 c 2) to ensure that model coordinate
1974 surfaces are isopycnal surfaces can directly represent neutral diffusion without the need for special
1975 numerical methods.

1976 3) DIAPYCNAL MIXING WITHIN THE OCEAN INTERIOR AND BOUNDARY LAYERS

1977 Much of the ocean interior is a quasi-ideal fluid in that there is very little irreversible mixing
1978 between isopycnals. In contrast, mixing is vigorous in the mixed layer of the upper ocean, as well
1979 as in “benthic” boundary layers next to the ocean bottom. Mixing between interior ocean isopy-
1980 cnals (i.e., diapycnal mixing) affects stratification, ventilation, and the time scales for dynamical

1981 processes such as waves. Hence, this mixing has a very large impact on ocean circulation. The
1982 sensitivity of ocean circulation models to the levels of diapycnal mixing were emphasized by the
1983 watermass study of Bryan and Lewis (1979). They prescribed an enhanced diffusivity at depth
1984 to account for increased mixing in deep ocean regions of low stratification. This “Bryan-Lewis”
1985 diffusivity profile became the norm for ocean circulation models for the next 20 years, because it
1986 greatly improved the realism of the simulations, particularly those where deep flows appear such
1987 as in the Southern Ocean. This sensitivity of ocean circulation to diapycnal mixing has also been
1988 emphasized by the work of Walter Munk (1966) and Frank Bryan (1987)¹⁵.

1989 These two modeling studies pointed to the need for additional field measurements and process
1990 modeling to enable an understanding of the fundamental nature of interior ocean mixing. This
1991 work was recently reviewed by MacKinnon et al. (2013), who brought together ideas of interior
1992 mixing and summarized its connection to breaking internal gravity waves. Further, this study
1993 offers an example of how efforts at large-scale models, process-models, theory, and observations
1994 can be synergistically combined to render deeper understanding of how the ocean works.

1995 The ocean is strongly forced at its surface through air-sea and ice-sea interactions, and at the
1996 bottom through interactions with the solid earth. This forcing drives intense three-dimensional
1997 turbulent mixing with order unity vertical-to-horizontal aspect ratios (i.e., non-hydrostatic dynam-
1998 ics). It therefore must be parameterized in hydrostatic ocean models.

1999 In ocean circulation models of the 1980s, the surface boundary layer was “parameterized” by
2000 using a top layer of order 50 m thick. However, as modelers refined their vertical grid spacing,
2001 the needs for more physically based schemes became apparent. In response to this need, Large
2002 et al. (1994) provided a review of the extant methods (e.g., bulk boundary layers and 2nd-order
2003 turbulence closures). They proposed a new approach based on ideas that had been developed for

¹⁵Frank Bryan is not related to Kirk Bryan.

2004 atmospheric boundary layer parameterizations (Troen and Mahrt 1986; Holtslag et al. 1990; Holt-
2005 slag and Boville 1993). Their K-Profile Parameterization (KPP) has been incorporated into many
2006 ocean climate models. Alternative methods based on energetic approaches have also provided the
2007 framework for boundary layer closure (e.g., Gaspar et al. 1990), particularly those used by the
2008 NEMO community. Such energetic approaches have also been traditionally used by isopycnal
2009 models (Hallberg 2003).

2010 Much of the deep waters around Antarctica originate from overflows off the continental shelves.
2011 Similar processes occur in the Denmark Strait and Faroe Bank Channel regions of the North At-
2012 lantic. Faithfully incorporating such processes in ocean climate models is a combination of model
2013 frameworks (e.g., vertical coordinates) and parameterizations. The traditional geopotential verti-
2014 cal coordinate is ill-suited to representing these processes due to high levels of spurious mixing,
2015 whereas isopycnal and terrain following models are far better suited (Legg et al. 2006). Legg et al.
2016 (2009) summarized the results from a climate process team of global circulation modelers, theo-
2017 rists, process-physicists, and observationalists who focused on this overflow problem and offered
2018 recommendations for improving the climate scale models.

2019 *e. Current issues in sea ice modeling*

2020 With satisfactory methods to solve sea ice dynamics, attention turned to improving the ther-
2021 modynamics by implementing an ice-thickness distribution and brine-pocket physics, first in the
2022 University of Victoria Climate Model (Bitz and Lipscomb 1999; Bitz et al. 2001), soon after in
2023 Version 2 of the Community Earth System Model (CCSM2; Bitz et al. 2005; Holland et al. 2006)
2024 and in Version 2 of the GFDL Climate Model (CM2; Winton 2000; Gnanadesikan et al. 2006),
2025 and now in the majority of models. Detailed melt pond parameterizations and radiative transfer
2026 that includes scattering (important for sea ice due to brine inclusions and air bubbles) are in many

2027 models now too (e.g., Briegleb and Light 2007; Flocco and Feltham 2007; Holland et al. 2012). A
2028 desire to simulate brine pocket dynamics more faithfully, with prognostic salinity and sea ice bio-
2029 geochemistry, has motivated practical schemes to better approximate mushy-layer physics (e.g.,
2030 Vancoppenolle et al. 2009; Turner et al. 2013).

2031 Figure 11 is a schematic illustration of the grid cell of a state-of-the-art sea ice model with
2032 a thickness distribution. Each thickness category has a unique snow depth, melt pond depth and
2033 coverage, heat fluxes at the top and bottom, and vertical profile of temperature and salinity. A frac-
2034 tion of the grid cell may be open water. Models that do not parameterize the thickness distribution
2035 effectively have just one thickness category.

2036 In weather forecast systems, the initial sea ice concentration is usually specified based on pas-
2037 sive microwave satellite retrievals and held fixed throughout the forecast (e.g., Grumbine 2013).
2038 Other aspects of sea ice thermodynamics are usually rudimentary. Until recently, sea ice has
2039 been specified in medium-range and seasonal forecast models as well. However, with Version
2040 2 of the National Center for Environmental Prediction Climate Forecast System (CFSv2; Saha
2041 et al. 2010b), the GFDL sea ice component of CM2 was implemented. In 2017, the Euro-
2042 pean Centre for Medium Range Forecast (ECMWF) transitioned their sub-seasonal operational
2043 forecast model from fixed to active sea ice by adopting Version 2 of the Louvain-la-Neuve
2044 Sea Ice Model (LIM; Fichefet and Morales-Maqueda (1997), F. Vitart pers. comm., and see
2045 <https://www.ecmwf.int/en/research/modelling-and-prediction/marine>).

2046 *f. Current issues in land-surface modeling*

2047 Turbulent fluxes of latent and sensible heat and momentum can be estimated from high-
2048 frequency measurements of wind speed and scalars through a technique called eddy covariance,
2049 pioneered in the 1950s (Swinbank 1951). These fluxes are examples of the second moments con-

2050 sidered in boundary-layer parameterizations based on higher-order closure, as discussed in Section
2051 5 d 1. The development of relatively inexpensive sonic anemometers and fast-response sensors led
2052 to rapid expansion in the use of eddy covariance in the 1990s. The application of the technique
2053 to measure the carbon balance of ecosystems has led to the creation of a worldwide network of
2054 many hundreds of semi-permanent eddy covariance towers which monitor turbulent fluxes over
2055 land surfaces (Baldocchi et al. 2001; Baldocchi 2003). The availability of hourly estimates of tur-
2056 bulent fluxes of heat, moisture, and CO₂ over all kinds of surfaces in all kinds of weather has been
2057 incredibly valuable for the development and maturation of land surface modeling (Friend et al.
2058 2007; Stöckli et al. 2008b).

2059 The use of satellite imagery to prescribe vegetation and soil parameters made land models more
2060 realistic in the 1990s, but also limited their usefulness for prediction, since satellite imagery will
2061 never be available for the future. Two major developments in the 2000s intended to address this
2062 were prognostic phenology and dynamic global vegetation models (DGVMs). Rather than using
2063 satellite vegetation data as model input, land models seek to predict both seasonal and longer-term
2064 changes in vegetation properties. Observations of vegetation properties from satellites and other
2065 sources are then used to evaluate model output.

2066 “Phenology” refers to the seasonal growth and shedding of leaves in response to changing envi-
2067 ronmental conditions. Models with prognostic phenology “grow their own leaves.” These models
2068 are based on empirical relationships between the timing of leaf activity and day length, tempera-
2069 ture, and moisture (White et al. 1997; Lawrence and Slingo 2004; Arora and Boer 2005; Gienapp
2070 et al. 2005; Jolly et al. 2005; Stöckli et al. 2008a; Dickinson et al. 2008). The availability of global
2071 satellite coverage and hundreds of hourly flux tower records greatly accelerated the development
2072 of skillful parameterizations of phenology (Zhang et al. 2003; Reed et al. 1994; Gibelin et al. 2006;
2073 Bradley et al. 2007; Kathuroju et al. 2007; Stöckli et al. 2011).

2074 Dynamic global vegetation models seek to predict not just the seasonal greening and browning
2075 of the land surface, but changes in long term distribution of vegetation in response to climate.
2076 These models are important for century and longer scale climate simulation, allowing for feedback
2077 between the physical climate and the geographic patterns of surface properties (Cramer et al. 2001;
2078 Sitch et al. 2008). These models incorporate well-established physical and biological algorithms
2079 of earlier land surface parameterizations, but add algorithms for plant establishment, mortality, and
2080 competition for light and water (Cox 2001; Bonan et al. 2003; Woodward and Lomas 2004; Gerten
2081 et al. 2004; Krinner et al. 2005; Sitch et al. 2005; Lucht et al. 2006). Introduction of a new feedback
2082 process such as vegetation-climate interaction can result in large perturbations which may not be
2083 realistic. An early DGVM result was catastrophic dieback of the Amazon rainforest in one such
2084 coupled model (Cox et al. 2000, 2004), which released large amounts of CO₂ to the atmosphere
2085 and accelerated global warming. This result may reflect excessive drought stress in the hydrologic
2086 model component (Baker et al. 2008; Harper et al. 2014) than with a realistic assessment of carbon
2087 cycle instability (Cox et al. 2013).

2088 Having linked land-atmosphere exchanges of energy and water with photosynthesis in the 1990s
2089 and then incorporated prognostic phenology and dynamic vegetation in the 2000s, the coupled
2090 models were then used to analyze sources and sinks of atmospheric CO₂. It has long been known
2091 that terrestrial ecosystems currently sequester about half of global fossil fuel emissions due to an
2092 excess of photosynthesis over decomposition (Tans et al. 1990; Le Quéré et al. 2009). Increased
2093 atmospheric CO₂ directly induces enhanced rates of photosynthesis (Norby et al. 2005; Luo et al.
2094 2006), but nutrient limitation typically restricts growth (Oren et al. 2001; LeBauer and Treseder
2095 2008; Thornton et al. 2007, 2009). Land carbon sinks also result from changes in land management
2096 and the age structure of forests (Shevliakova et al. 2009; Pan et al. 2011). Each of these carbon

2097 sink processes is likely to change in the future: some (e.g., CO₂ fertilization) are likely to get
2098 stronger while others (e.g., regrowing forests) are likely to get weaker.

2099 A systematic intercomparison of coupled carbon-climate models was undertaken by Friedling-
2100 stein et al. (2006). They ran eleven Earth system models from 1850 to 2100, prescribing fossil fuel
2101 emissions, allowed ocean and land sinks to interact, and predicted both CO₂ and climate change.
2102 Their results showed a striking divergence in CO₂ and climate in the 21st Century. Most simu-
2103 lations developed stronger and stronger land carbon sinks driven primarily by CO₂ fertilization,
2104 but the effect was highly variable across participating models. But several simulations showed
2105 sharply decreased land carbon uptake or even the release of hundreds of gigaton of land carbon
2106 as atmospheric CO₂ as death and decomposition overtook photosynthesis. This highly uncertain
2107 carbon-climate feedback (Dufresne et al. 2002; Friedlingstein et al. 2003) was shown to produce
2108 uncertainty of over 250 ppm in simulated CO₂ at the end of the runs (Friedlingstein et al. 2006),
2109 given identical fossil fuel emissions, with a resulting spread of about 1.5 K of global warming.
2110 A quantitative analysis of Earth system climate feedback showed that carbon-climate feedback is
2111 among the most uncertain, rivaling uncertainty in cloud feedbacks (Gregory et al. 2009).

2112 **9. The future**

2113 *a. Increasing resolution*

2114 GCMs have always used the fastest computers available. Up to about the year 2000, the “clock
2115 speeds” of computer processors steadily increased. A faster clock means that a given arithmetic
2116 operation (e.g., addition or multiplication) can be performed in a shorter time. Faster clocks thus
2117 allowed longer simulations with the same model, or simulations of a given length with more “ex-

2118 pensive” models, i.e., models that use higher spatial resolution or more computationally demand-
2119 ing physical parameterizations.

2120 The increase in clock speeds came to an end in large part because faster clocks demand in-
2121 creasing amounts of expensive electrical power; the cost has simply become unsupportable. Since
2122 about 2000, the supercomputers used to run ESMs have increased in performance largely through
2123 the use of increasing numbers of processors running in parallel. The most straightforward way
2124 for a modeling center to use more processors is to increase the horizontal resolution of the model.
2125 Unfortunately, however, having four times as many processors does not enable simulations of a
2126 given length with four times as many grid points, because the time step of the model will have to
2127 decrease at higher resolution. There are various practical difficulties of this type.

2128 Increasing resolution brings a different issue. As a model’s grid cells become smaller, the char-
2129 acter of the unresolved physical processes changes. For example, with grid cells 100 km across,
2130 an atmospheric model needs a parameterization that represents the grid-cell-averaged heating and
2131 drying (and other processes) associated with deep cumulus convection, including vertical trans-
2132 ports by strong but unresolved convective updrafts and downdrafts. This is because multiple deep
2133 cumulus clouds can fit in a grid cell 100 km wide. In stark contrast, a grid cell 1 km across can
2134 actually fit inside a deep cumulus cloud; a model with a horizontal grid spacing of 1 km can explic-
2135 itly (if crudely) simulate the deep convective clouds, so that parameterizing them is inappropriate
2136 (and unnecessary), although of course parameterizations of microphysical processes, radiation,
2137 and small-scale turbulence are still needed.

2138 There is an intermediate range of grid spacings, on the order of 10 km, that is too coarse to
2139 allow explicit simulation of deep cumulus clouds, but too fine to permit an accurate *statistical*
2140 representation of such clouds. This troublesome range of grid spacings, used today in some global
2141 models, is often called the “grey zone.” An analogous grey zone can be defined with respect to

2142 the turbulent eddies of the boundary layer, which are an order of magnitude smaller than deep
2143 cumulus clouds. In fact, because the atmosphere and ocean contain eddies on all scales larger than
2144 a millimeter or so, a grey zone can be defined for any practical choice of horizontal resolution.

2145 The grey zone for deep cumulus convection is thought to be particularly important, however.
2146 Many of today’s models have grid spacings that are in or approaching the grey zone for deep
2147 convection. Ongoing research aims to create *resolution-independent* parameterizations that can
2148 work for a wide range of horizontal grid spacings, including those that fall within the grey zone
2149 (e.g., Arakawa and Wu 2013). This will allow a single code, based on a single set of equations, to
2150 be used with a wide range of horizontal grid spacings – a very practical and convenient modeling
2151 system.

2152 *b. The future of atmospheric dynamical cores*

2153 The ongoing increase in horizontal resolution, mentioned in the preceding section, has motivated
2154 the development of “non-hydrostatic” dynamical cores for global models, which do not use the
2155 quasi-static approximation. Some current research is aimed at evaluating the relative merits of
2156 using the “fully compressible” system of equations, which allows vertically propagating sound
2157 waves, versus alternative systems that filter such waves (e.g., Arakawa and Konor 2009)

2158 Because its cost grows faster than the number of degrees of freedom, and because of issues
2159 such as “spectral ringing” in the presence of sharp gradients, the imminent demise of the spec-
2160 tral method has been predicted for several decades! The communication burden of the spectral
2161 transforms on massively parallel machines may be the final nail in the coffin.

2162 Semi-Lagrangian advection schemes are complex both algorithmically and in terms of their
2163 communication patterns. At the same time, their advantage in being able to take large time steps is

2164 less important on quasi-uniform grids. We may see a move away from semi-Lagrangian schemes
2165 in the future.

2166 Finally, semi-implicit integration schemes require the solution of global elliptic problems, which
2167 are perceived to be difficult to solve efficiently on massively parallel machines. Consequently, new
2168 nonhydrostatic model developments aimed at massively parallel machines have tended to time
2169 splitting or vertically implicit integration schemes (Satoh et al. 2008a; Skamarock et al. 2012b;
2170 Zängl et al. 2015), though some attempts have been made to demonstrate the feasibility and com-
2171 petitiveness of parallel elliptic solvers (Heikes et al. 2013; Sandbach et al. 2015).

2172 There is now a vast number and variety of numerical methods for atmospheric modeling under
2173 consideration by the research community. A range of quasi-uniform grids is being explored, the
2174 most popular being cubed spheres, triangular and hexagonal icosahedra, and the overset Yin-Yang
2175 grid (Figure 12). Spatial discretizations include finite-difference methods, finite-volume methods,
2176 and a variety of finite-element methods, which are analogous to spectral methods but use local
2177 (rather than global) basis functions. These are coupled with a range of explicit, implicit, subcy-
2178 cling, and Riemann-solver-based time integration schemes.

2179 Current work is exploring some approaches that have the potential for a major impact on the
2180 field, if they can be made to work well enough. Grids with geographically variable (but temporally
2181 fixed) resolution are being tested (e.g., Rauscher and Ringler 2014; Zarzycki and Jablonowski
2182 2015). An idea that has great potential to improve the computational efficiency of weather and
2183 climate simulations is to use a grid that dynamically adapts to the solution, placing the highest
2184 resolution where it is most needed. Alternative approaches are moving the grid while retaining
2185 the grid topology, or inserting and removing grid points where needed. Experiments with both
2186 approaches appeared in the 1990s (e.g., Dietachmayer and Droegemeier 1992; Skamarock and
2187 Klemp 1993). Adaptive vertical grids are also being investigated (Marchand and Ackerman 2011;

2188 Yamaguchi et al. 2017). However, there are significant challenges both in defining suitable criteria
2189 for where to refine the grid and in maintaining conservation and balance and avoiding noise as
2190 the grid adapts. The only operational adaptive grid forecast model to date appears to be that of
2191 Bacon et al. (2000). Some of the challenges mentioned above are being addressed (e.g., St-Cyr
2192 et al. (2008), Dubos et al. (2013), Bauer et al. (2014); see also the 28 November 2009 issue
2193 of *Phil. Trans. Roy. Soc.*). Also, with the evolution of supercomputers towards ever greater
2194 numbers of processors, a significant challenge is to devise algorithms with sufficient parallelism
2195 to take advantage. This has led to some exploration of parallel-in-time algorithms (e.g., Haut and
2196 Wingate 2014).

2197 The evolution of computer architecture (which itself is uncertain) is likely to continue to influ-
2198 ence the development of numerical methods into the future. Efforts are currently under way to test
2199 the feasibility of running global atmospheric models on machines that include GPUs (i.e., graphics
2200 processing units) to achieve greater speed (e.g., Leutwyler et al. 2016; Abdi et al. 2017).

2201 *c. The future of radiation parameterizations*

2202 Radiation is unique as a parameterization problem for atmospheric modeling because funda-
2203 mental understanding of the problem is so complete. The parameterization of radiative processes,
2204 therefore, focuses on how to use incomplete information from the model to compute fluxes of
2205 sufficient accuracy with acceptable computational cost. Future efforts will likely be focused on
2206 strategies for mitigating computational cost and increasing accuracy and accounting for the hori-
2207 zontal transport of radiation.

2208 As described in Section 6 c, the high computational cost of spectrally-integrated calculations
2209 means that radiative fluxes are typically computed more sparsely in time than any other subgrid-
2210 scale diabatic processes, potentially degrading simulations by blurring the coupling between fast-

2211 changing clouds and radiative fluxes. One promising approach is to devote specific computational
2212 resources to computing radiative fluxes (e.g., Balaji et al. 2016), allowing more frequent radiation
2213 computations and speeding time to solution at the cost of using more resources overall. Because
2214 radiation calculations integrate over a spectral dimension the problem is well suited to exploit
2215 heterogenous computing environments. Highly-parallel processors such as GPUs in particular
2216 offer tantalizing hints of very high efficiency (e.g., Price et al. 2013; Clement et al. 2018).

2217 New frontiers for accuracy include better coupling of radiation among the atmospheric, oceanic,
2218 cryospheric, and terrestrial components of earth system models and steps to relax the strong one-
2219 dimensional plane-parallel assumption. In all ESMs of which we are aware radiative fluxes are
2220 computed independently in each domain, i.e. in the atmosphere, ocean, and sea-ice, using inde-
2221 pendent models that are nonetheless based on the same underlying equations (e.g., Yuan et al.
2222 2017). Results from each domain serve as boundary conditions for the other domains; the cost
2223 of coupling components often requires that spectral resolution is degraded at the potential cost of
2224 accuracy. A more natural and potentially more accurate approach would be to compute radiative
2225 fluxes in the atmosphere and ocean simultaneously (e.g., Lee and Liou 2007); extending this ap-
2226 proach to sea-ice, whose albedo can vary dramatically, might improve prediction in the Arctic.
2227 Problems arising in the computation of radiation in heterogenous vegetation canopies (e.g., Yuan
2228 et al. 2017) have much in common with similar efforts in clouds, suggesting that progress might
2229 come from the two communities working more closely together (Hogan et al. 2018).

2230 Despite ample evidence to the contrary, essentially all parameterizations of radiative transfer
2231 used in global models adopt plane-parallel geometry and make use of the assumption that all
2232 radiation travels straight up and down. New techniques are now emerging (Schäfer et al. 2016;
2233 Hogan et al. 2016), which relax the one-dimensional assumption, accounting parametrically for
2234 effects such as the casting of cloud shadows, the illumination of cloud sides, and the increased

2235 cooling from cloud edges (Hogan et al. 2016) within each column. These effects are small but
2236 systematic: finite clouds uniformly increase surface and top-of-atmosphere fluxes relative to their
2237 plane-parallel counterparts while impacts of solar illumination vary with solar zenith angle, and
2238 hence latitudinally and seasonally. As parametric treatments are evaluated more rigorously efforts
2239 to include these effects in coarse-resolution models may become more common.

2240 *d. The future of cloud and microphysics parameterizations*

2241 Parameterizing microphysics remains highly challenging due to the complexity of the underlying
2242 physics and a lack of fundamental knowledge on these processes, especially for ice microphysics.
2243 This is a critical challenge for weather and climate modeling because simulations are often quite
2244 sensitive to microphysical parameter settings, and the increasing complexity of schemes has not
2245 changed this picture. Overall, continued advancement of parameterizations will require greater
2246 knowledge of the underlying physical processes in order to reduce parameter uncertainty, including
2247 from laboratory studies, cloud observations, and detailed process modeling. Representing sub-grid
2248 scale cloud processes consistently across all model scales continues to be another major challenge
2249 despite increasing model resolution. Efforts have been made to develop sub-grid representations
2250 of clouds and dynamics to consistently drive cloud microphysics across a range of scales and cloud
2251 types (e.g., Thayer-Calder et al. (2015)). These “unified” cloud parameterization efforts will likely
2252 be an important part of weather and climate model development in the coming years.

2253 New approaches to super-parameterization are also under development. For example, (Parishani
2254 et al. 2017) report encouraging results with an “ultra-parameterization” in which the horizon-
2255 tal grid spacing of the embedded cloud-resolving models is reduced to 250 m, and the vertical
2256 resolution is also increased, so that the eddies associated with shallow clouds can be explicitly
2257 simulated. Jung and Arakawa (2014) have developed a “Quasi-three-dimensional” (Q3D) super-

2258 parameterization, in which the CRMs take the form of narrow channels that form closed loops on
2259 the global model's grid, e.g., around meridians or latitude circles. The channels cross but do not
2260 intersect; they communicate only through the host GCM. With the Q3D approach, it is possible to
2261 include realistic topography (Jung 2016) including orographically enhanced precipitation, as well as
2262 vertical momentum transport by both convection and gravity waves, as explicitly simulated on the
2263 CRM grids.

2264 Meanwhile, efforts are under way to use machine learning to create accurate and computation-
2265 ally efficient parameterizations (Chevallier et al. 1998; Brenowitz and Bretherton 2018; Gentine
2266 et al. 2018; Schneider et al. 2017). It seems likely that this approach can lead to improved sim-
2267 ulations with tolerable computational cost, at least for the current climate. Can it also be used to
2268 simulate different climate states? Can it be used to learn more about the actual physical mech-
2269 anisms through which the cloud systems interact with larger-scale motions? Work is needed to
2270 address these questions.

2271 *e. The future of ocean models*

2272 Since the 1970s, much of the focus of global ocean circulation modeling has been at understand-
2273 ing, representing, and parameterizing the impacts from mesoscale eddies. This focus remains a
2274 large part of today's efforts. For example, prototype centennial-scale climate simulations have
2275 been run with a vigorous eddy field. In particular, Griffies et al. (2015) emphasize the role of
2276 mesoscale eddies in the vertical transport of heat in the ocean, thus directly impacting on the
2277 rate of transient climate change. Small et al. (2014) emphasize the role of small-scale ocean fea-
2278 tures in forcing the atmosphere circulation through the surface fluxes. However, new avenues
2279 of research are focused on the submesoscales, which are intermediate between the balanced mo-
2280 tions at the mesoscale and unbalanced motions at the gravity-wave scale (Fox-Kemper et al. 2008;

2281 McWilliams 2016). Submesoscale processes impact the vertical transfer of properties in the upper
2282 ocean, and mediate the downscale cascade of energy and tracer variance to the small scales. In
2283 parallel, modelers are increasingly pushing the frontiers of coastal and shelf processes within the
2284 global climate models by grid refinement or nesting approaches. It is here that impacts from the
2285 changing climate will have their largest footprint on civilization due to changes in ecosystems and
2286 sea level.

2287 We expect that numerical models of the ocean will continue to improve through advances in
2288 numerical methods and physical parameterizations, including many of the approaches outlined
2289 here (e.g., ALE for the vertical and unstructured meshes for the horizontal). Improvements to
2290 observational datasets will also be necessary to evaluate the simulations. The history of ocean
2291 modeling has not been linear, with examples of advances in one sub-field spawning new under-
2292 standing and development in unexpected areas. Nonetheless, ongoing advances in ocean models
2293 and modeling practices, along with new theoretical insights, will ensure that numerical models
2294 remain a fundamental component of oceanography and climate science into the future.

2295 *f. The future of sea ice models*

2296 The next developments for sea ice are likely to be more realistic sea ice dynamics that replicate
2297 the effects of anisotropy on lead formation (e.g., Sulsky et al. 2007; Tsamados et al. 2013) and
2298 joint thickness-floe distribution models (Horvat and Tziperman 2015; Roach et al. 2018) - the
2299 latter permitting better representation of the region near the sea ice edge where ocean surface waves
2300 interact with floes and floe size influences ice-albedo feedback.

2301 *g. The future of land surface models*

2302 As more processes are added to Earth system models, there is more room for unexpected inter-
2303 actions. Just as the coupling of ocean and atmosphere GCMs produced nonphysical climate drift
2304 that required flux corrections (e.g., Cubasch et al. 1992), fully coupled land-atmosphere models
2305 produced highly uncertain carbon-climate feedback (Friedlingstein et al. 2006). In response to the
2306 large spread in Earth system model outcomes, the land modeling community has embarked on
2307 a series of systematic model intercomparisons, evaluations, and benchmarking exercises using a
2308 wide range of global data sets (Luo et al. 2012; Huntzinger et al. 2012).

2309 Land-atmosphere coupling in the CMIP5 ensemble of Earth System Models produced an even
2310 wider spread of outcomes (Arora et al. 2013) than had been documented a decade earlier as
2311 more model complexity was added. An important approach to improving predictability of land-
2312 atmosphere climate futures is the application of emergent constraints on carbon-climate feedbacks
2313 (Wenzel et al. 2014). A subset of CMIP5 models forced with identical emissions and allowed
2314 to predict the behavior of land and ocean sinks and atmospheric CO₂ found a spread of almost
2315 350 ppm in CO₂ concentration in 2100 (Hoffman et al. 2014). Uncertain carbon-climate feedback
2316 resulted in a spread in radiative forcing of more than 2 W m⁻², comparable to emission scenario
2317 uncertainty. Hoffman et al. (2014) compared the models predicted CO₂ concentrations in 2100
2318 to observations and found that their biases in the present day were good linear predictors of the
2319 spread in 2100. Using integral constraints on anthropogenic carbon inventories in the ocean and
2320 atmosphere, they adjusted carbon sinks to match. This reduced the spread of CO₂ in 2100 by a
2321 factor of seven relative to the control (CMIP) simulations, showing the potential for leveraging
2322 emergent constraints to solve the carbon-climate feedback problem.

2323 The International Land Model Benchmarking Project (ILAMB; Hoffman et al. 2016) provides
2324 a comprehensive suite of observational data sets from flux towers, field experiments, satellite
2325 imagery, and atmospheric sampling in a transparent framework for model evaluation and inter-
2326 comparison. Dozens of land modeling groups from around the world have participated in the
2327 development of the benchmarks, and in model intercomparison and evaluation studies. As of late
2328 2017, model evaluation and improvement is among the highest priorities for predictive modeling
2329 of land-atmosphere futures in the Earth system (Huntzinger et al. 2017).

2330 **10. The road goes ever on**

2331 Developments in atmospheric dynamics and physics, instrumentation and observing practice,
2332 and digital computing have made the utopian visions of Abbe, Bjerknes and Richardson an ev-
2333 eryday reality. Global numerical weather prediction models are now at the center of operational
2334 forecasting, and enable us to predict the weather for several days in advance with a high degree
2335 of confidence. Progress has been rapid; the useful range of deterministic prediction has been in-
2336 creasing by about one day per decade (Bauer et al. 2015). In addition, Earth System Models are
2337 now being used to simulate future climate changes that will have enormous societal consequences.
2338 Using Earth System Models, we are gaining great insight into the factors causing changes in our
2339 climate, and the likely timing and severity of those changes.

2340 As a result of these spectacular achievements, meteorology and oceanography are now firmly
2341 established as quantitative sciences, and their value and validity are demonstrated daily by the
2342 acid test of any science: its ability to predict the results of measurements. The advances in Earth
2343 System Modeling over the past century have been truly revolutionary. The development of com-
2344 prehensive Earth System Models is a major and insufficiently appreciated scientific achievement
2345 of the twentieth century. Today's most advanced models simulate not only the physics of the at-

2346 mosphere, oceans and land surface, but also a wide range of chemical and biological processes
2347 and the associated couplings and feedbacks. The conceptual breadth of the models has rapidly
2348 increased over the last few decades, and is now rather breathtaking.

2349 It is also essential, however, to maintain a focus on the conceptual *depth* of the models. The
2350 ever-expanding range of parameterized processes must be tied back to fundamental physics, as
2351 securely as possible. Although it is exciting and important to add new processes to a model, it is at
2352 least equally important (and, for some of us, equally exciting) to strengthen the conceptual foun-
2353 dations of a model’s “legacy” components, including such things as parameterizations of clouds
2354 and turbulence, and the numerical methods used to solve the equations that govern fluid motion,
2355 over a wide range of scales, on a great big rotating sphere.

2356 A comprehensive ESM can simulate many of the emergent phenomena that we see in nature,
2357 but the output of such a simulation is just a pile of numbers; it is not an *explanation* of the natural
2358 world. To claim that we understand the results of a highly detailed and successful simulation,
2359 and by extension that we understand the real world, we must work to create much simpler models
2360 that can semi-quantitatively reproduce the key results of the comprehensive models. Meeting this
2361 inspiring challenge is the highest goal of our science.

2362 *Acknowledgments.* We gratefully acknowledge valuable input provided by our friend Albert J.
2363 Semtner, Jr., who passed away in December 2018. Bert was a pioneer of ocean modeling.

2364 Paul Edwards of Stanford University and Wayne Schubert of Colorado State University helped
2365 us to locate some of the early references. Additional input came from Richard Somerville of the
2366 Scripps Institution for Oceanography, and Milton Halem of the University of Maryland.

2367 We are grateful to the three reviewers for very helpful comments on the manuscript. Bjorn
2368 Stevens, in particular, liberally annotated the 186-page-long first version of the manuscript.

2369 David Randall acknowledges support from NSF grant AGS-1538532. Cecilia M. Bitz is grate-
2370 ful for support from NSF PLR-1643431. Stephen Griffies thanks his longstanding support from
2371 GFDL for vigorous ocean and climate modeling activities. The National Center for Atmospheric
2372 Research is sponsored by the National Science Foundation.

2373 **References**

2374 Abbe, C., 1901: The physical basis of long-range weather forecasts. *Monthly Weather Re-*
2375 *view*, **29 (12)**, 551–561, doi:10.1175/1520-0493(1901)29[551c:TPBOLW]2.0.CO;2, URL
2376 [https://doi.org/10.1175/](https://doi.org/10.1175/1520-0493(1901)29[551c:TPBOLW]2.0.CO;2)
2377 [1520-0493\(1901\)29\[551c:TPBOLW\]2.0.CO;2](https://doi.org/10.1175/1520-0493(1901)29[551c:TPBOLW]2.0.CO;2).

2378 Abdi, D. S., L. C. Wilcox, T. C. Warburton, and F. X. Giraldo, 2017: A gpu-accelerated continuous
2379 and discontinuous galerkin non-hydrostatic atmospheric model. *The International Journal of*
2380 *High Performance Computing Applications*, 1094342017694427.

2381 Ackerman, A. S., M. P. Kirkpatrick, D. E. Stevens, and O. B. Toon, 2004: The impact of humidity
2382 above stratiform clouds on indirect aerosol climate forcing. *Nature*, **432 (7020)**, 1014.

2383 Adcroft, A., and J.-M. Campin, 2004: Rescaled height coordinates for accurate representation of
2384 free-surface flows in ocean circulation models. *Ocean Modelling*, **7 (3-4)**, 269–284.

2385 Adcroft, A., and R. Hallberg, 2006: On methods for solving the oceanic equations of motion in
2386 generalized vertical coordinates. *Ocean Modelling*, **11 (1-2)**, 224–233.

2387 Ambartsumian, V., 1936: The effect of absorption lines on the radiative equilibrium of the outer
2388 layers of stars. *Publ. Astron. Obser. Leningrad*, **6**, 7–18.

2389 André, J., G. De Moor, P. Lacarrere, and R. Du Vachat, 1976: Turbulence approximation for
2390 inhomogeneous flows: Part ii. the numerical simulation of a penetrative convection experiment.
2391 *Journal of the Atmospheric Sciences*, **33** (3), 482–491.

2392 Andrejczuk, M., W. Grabowski, J. Reisner, and A. Gadian, 2010: Cloud-aerosol interactions for
2393 boundary layer stratocumulus in the lagrangian cloud model. *Journal of Geophysical Research:*
2394 *Atmospheres*, **115** (D22).

2395 Anthes, R. A., 1977: A cumulus parameterization scheme utilizing a one-dimensional cloud
2396 model. *Monthly Weather Review*, **105** (3), 270–286.

2397 Anthes, R. A., 1984: Enhancement of convective precipitation by mesoscale variations in vegeta-
2398 tive covering in semiarid regions. *Journal of Climate and Applied Meteorology*, **23** (4), 541–554.

2399 Arakawa, A., 1966: Computational design for long-term numerical integration of the equations of
2400 fluid motion: Two-dimensional incompressible flow. Part I. *Journal of Computational Physics*,
2401 **1** (1), 119–143.

2402 Arakawa, A., 1969: Parameterization of cumulus convection. *Proceedings of the WMO/IUGG*
2403 *Symposium on Numerical Weather Prediction, Tokyo, 26 November to 4 December, 1968*, Japan
2404 Meteorological Agency, Vol. IV, 1–6.

2405 Arakawa, A., 1972: *Design of the UCLA general circulation model*, Vol. 7. Department of Mete-
2406 orology, University of California, Los Angeles, 1–116 pp.

2407 Arakawa, A., 2000: A personal perspective on the early years of general circulation modeling.
2408 *General Circulation Model Development, Randall DA (ed.)*. Academic Press: New York, 1–65.

2409 Arakawa, A., 2004: The cumulus parameterization problem: Past, present, and future. *Journal of*
2410 *Climate*, **17** (13), 2493–2525.

- 2411 Arakawa, A., and C. S. Konor, 2009: Unification of the anelastic and quasi-hydrostatic systems of
2412 equations. *Monthly Weather Review*, **137** (2), 710–726.
- 2413 Arakawa, A., and V. R. Lamb, 1977: Computational design of the basic dynamical processes of
2414 the UCLA general circulation model. *General Circulation Models of the Atmosphere*, J. Chang,
2415 Ed., Academic Press, Methods in Computational Physics, Vol. 17, 173–265.
- 2416 Arakawa, A., and V. R. Lamb, 1981: A potential enstrophy and energy conserving scheme for the
2417 shallow water equations. *Monthly Weather Review*, **109** (1), 18–36.
- 2418 Arakawa, A., Y. Mintz, and A. Katayama, 1968: *Numerical simulation of the general circulation*
2419 *of the atmosphere*. Department of Meteorology, University of California.
- 2420 Arakawa, A., and S. Moorthi, 1988: Baroclinic instability in vertically discrete systems. *Journal*
2421 *of the atmospheric sciences*, **45** (11), 1688–1708.
- 2422 Arakawa, A., and W. H. Schubert, 1974: Interaction of a cumulus cloud ensemble with the large-
2423 scale environment, Part I. *J. Atmos. Sci.*, **31**, 674–701.
- 2424 Arakawa, A., and C.-M. Wu, 2013: A unified representation of deep moist convection in numerical
2425 modeling of the atmosphere. part i. *Journal of the Atmospheric Sciences*, **70** (7), 1977–1992,
2426 doi:10.1175/JAS-D-12-0330.1, URL <https://doi.org/10.1175/JAS-D-12-0330.1>, [https://doi.org/](https://doi.org/10.1175/JAS-D-12-0330.1)
2427 [10.1175/JAS-D-12-0330.1](https://doi.org/10.1175/JAS-D-12-0330.1).
- 2428 Arora, V. K., and G. J. Boer, 2005: A parameterization of leaf phenology for the terrestrial ecosys-
2429 tem component of climate models. *Global Change Biology*, **11** (1), 39–59.
- 2430 Arora, V. K., and Coauthors, 2013: Carbon–concentration and carbon–climate feedbacks in cmip5
2431 earth system models. *Journal of Climate*, **26** (15), 5289–5314.

- 2432 Ashford, O. M., 1985: *Prophet—or professor?: The life and work of Lewis Fry Richardson*. Taylor
2433 & Francis.
- 2434 Avissar, R., and R. A. Pielke, 1989: A parameterization of heterogeneous land surfaces for at-
2435 mospheric numerical models and its impact on regional meteorology. *Monthly Weather Review*,
2436 **117 (10)**, 2113–2136.
- 2437 Bacon, D. P., and Coauthors, 2000: A dynamically adapting weather and dispersion model: the op-
2438 erational multiscale environment model with grid adaptivity (omega). *Monthly Weather Review*,
2439 **128 (7)**, 2044–2076.
- 2440 Baer, F., 1972: An alternate scale representation of atmospheric energy spectra. *Journal of the*
2441 *Atmospheric Sciences*, **29 (4)**, 649–664.
- 2442 Baker, I., L. Prihodko, A. Denning, M. Goulden, S. Miller, and H. Da Rocha, 2008: Seasonal
2443 drought stress in the amazon: Reconciling models and observations. *Journal of Geophysical*
2444 *Research: Biogeosciences*, **113 (G1)**.
- 2445 Balaji, V., R. Benson, B. Wyman, and I. Held, 2016: Coarse-grained component concurrency in
2446 earth system modeling: parallelizing atmospheric radiative transfer in the gfdl am3 model using
2447 the flexible modeling system coupling framework. *Geoscientific Model Development*, **9 (10)**,
2448 3605.
- 2449 Baldocchi, D., and Coauthors, 2001: Fluxnet: A new tool to study the temporal and spatial vari-
2450 ability of ecosystem–scale carbon dioxide, water vapor, and energy flux densities. *Bulletin of*
2451 *the American Meteorological Society*, **82 (11)**, 2415–2434.
- 2452 Baldocchi, D. D., 2003: Assessing the eddy covariance technique for evaluating carbon dioxide
2453 exchange rates of ecosystems: past, present and future. *Global change biology*, **9 (4)**, 479–492.

- 2454 Ball, J. T., 1988: An analysis of stomatal conductance. Ph.D. thesis, Stanford University Stanford.
- 2455 Balmaseda, M. A., K. Mogensen, and A. T. Weaver, 2013: Evaluation of the ecmwf ocean reanaly-
2456 sis system oras4. *Quarterly Journal of the Royal Meteorological Society*, **139 (674)**, 1132–1161.
- 2457 Barker, H. W., 1996: A parameterization for computing grid-averaged solar fluxes for inhomoge-
2458 neous marine boundary layer clouds. 1. Methodology and homogeneous biases. *J. Atmos. Sci.*,
2459 **53 (16)**, 2289–2303.
- 2460 Barker, H. W., J. N. S. Cole, J.-J. Morcrette, R. Pincus, P. Ræisaenen, K. von Salzen, and P. A.
2461 Vaillancourt, 2008: The Monte Carlo Independent Column Approximation: An assessment
2462 using several global atmospheric models. *Quart. J. Royal Met. Soc.*, **134 (635, Part B)**, 1463–
2463 1478.
- 2464 Barker, H. W., and Coauthors, 2003: Assessing 1D atmospheric solar radiative transfer models:
2465 Interpretation and handling of unresolved clouds. *J. Climate*, **16 (16)**, 2676–2699.
- 2466 Barkstrom, B. R., 1984: The earth radiation budget experiment (erbe). *Bulletin of the American*
2467 *Meteorological Society*, **65 (11)**, 1170–1185.
- 2468 Bates, J., F. Semazzi, R. Higgins, and S. R. Barros, 1990: Integration of the shallow water equa-
2469 tions on the sphere using a vector semi-lagrangian scheme with a multigrid solver. *Monthly*
2470 *Weather Review*, **118 (8)**, 1615–1627.
- 2471 Bauer, P., A. Thorpe, and G. Brunet, 2015: The quiet revolution of numerical weather prediction.
2472 *Nature*, **525 (7567)**, 47.
- 2473 Bauer, W., M. Baumann, L. Scheck, A. Gassmann, V. Heuveline, and S. C. Jones, 2014:
2474 Simulation of tropical-cyclone-like vortices in shallow-water icon-hex using goal-oriented r-

2475 adaptivity. *Theoretical and Computational Fluid Dynamics*, **28 (1)**, 107–128, doi:10.1007/
2476 s00162-013-0303-4, URL <https://doi.org/10.1007/s00162-013-0303-4>.

2477 Beckwith, I. E., and D. M. Bushnell, 1968: Detailed description and results of a method for
2478 computing mean and fluctuating quantities in turbulent boundary layers.

2479 Beljaars, A. C., P. Viterbo, M. J. Miller, and A. K. Betts, 1996: The anomalous rainfall over the
2480 united states during july 1993: Sensitivity to land surface parameterization and soil moisture
2481 anomalies. *Monthly Weather Review*, **124 (3)**, 362–383.

2482 Bengtsson, L., M. Kanamitsu, P. Kållberg, and S. Uppala, 1982: Fgge research activities at ecmwf.
2483 *Bulletin of the American Meteorological Society*, **63 (3)**, 277–303.

2484 Benjamin, S. G., G. A. Grell, J. M. Brown, T. G. Smirnova, and R. Bleck, 2004: Mesoscale
2485 weather prediction with the ruc hybrid isentropic–terrain-following coordinate model. *Monthly*
2486 *Weather Review*, **132 (2)**, 473–494.

2487 Bentsen, M., and Coauthors, 2013: The norwegian earth system model, noresm1-m—part 1: De-
2488 scription and basic evaluation of the physical climate. *Geosci. Model Dev*, **6 (3)**, 687–720.

2489 Berry, E. X., and R. L. Reinhardt, 1974: An analysis of cloud drop growth by collection: Part i.
2490 double distributions. *Journal of the Atmospheric Sciences*, **31 (7)**, 1814–1824.

2491 Betts, A., and M. Miller, 1986: A new convective adjustment scheme. part ii: Single column
2492 tests using gate wave, bomex, atex and arctic air-mass data sets. *Quarterly Journal of the Royal*
2493 *Meteorological Society*, **112 (473)**, 693–709.

2494 Betts, A. K., 1986: A new convective adjustment scheme. part i: Observational and theoretical
2495 basis. *Quarterly Journal of the Royal Meteorological Society*, **112 (473)**, 677–691.

- 2496 Betts, A. K., J. H. Ball, A. Beljaars, M. J. Miller, and P. A. Viterbo, 1996: The land surface-
2497 atmosphere interaction: A review based on observational and global modeling perspectives.
2498 *Journal of Geophysical Research: Atmospheres*, **101 (D3)**, 7209–7225.
- 2499 Bitz, C. M., M. M. Holland, E. C. Hunke, and R. E. Moritz, 2005: Maintenance of the sea-ice
2500 edge. *Journal of Climate*, **18 (15)**, 2903–2921.
- 2501 Bitz, C. M., M. M. Holland, A. J. Weaver, and M. Eby, 2001: Simulating the ice-thickness distri-
2502 bution in a coupled climate model. *J. Geophys. Res.*, **106**, 2441–2464.
- 2503 Bitz, C. M., and W. H. Lipscomb, 1999: An energy-conserving thermodynamic model of sea ice.
2504 *J. Geophys. Res.*, **104**, 15,669–15,677.
- 2505 Bjerknes, J., 1955: *Investigations of the general circulation of the atmosphere*. Department of
2506 Meteorology, University of California, Los Angeles.
- 2507 Bjerknes, V., 1904: Das problem der wettervorhersage, betrachtet vom standpunkte der mechanik
2508 und der physik. *METZEIT*, **21**, 1–7.
- 2509 Bleck, R., 1970: A fast, approximative method for integrating the stochastic coalescence equation.
2510 *Journal of Geophysical Research*, **75 (27)**, 5165–5171.
- 2511 Bleck, R., 1973: Numerical forecasting experiments based on the conservation of potential vortic-
2512 ity on isentropic surfaces. *Journal of Applied Meteorology*, **12 (5)**, 737–752.
- 2513 Bleck, R., 2002: An oceanic general circulation model framed in hybrid isopycnic-cartesian coor-
2514 dinates. *Ocean modelling*, **4 (1)**, 55–88.
- 2515 Bleck, R., S. Benjamin, J. Lee, and A. E. MacDonald, 2010a: On the use of an adaptive,
2516 hybrid-isentropic vertical coordinate in global atmospheric modeling. *Monthly Weather Review*,
2517 **138 (6)**, 2188–2210.

2518 Bleck, R., S. Benjamin, J. Lee, and A. E. MacDonald, 2010b: On the use of an adaptive,
2519 hybrid-isentropic vertical coordinate in global atmospheric modeling. *Monthly Weather Review*,
2520 **138 (6)**, 2188–2210, doi:10.1175/2009MWR3103.1.

2521 Bleck, R., and S. G. Benjamin, 1993: Regional weather prediction with a model combining
2522 terrain-following and isentropic coordinates. part i: Model description. *Monthly Weather Re-*
2523 *view*, **121 (6)**, 1770–1785.

2524 Bleck, R., and D. Boudra, 1986: Wind-driven spin-up in eddy-resolving ocean models formu-
2525 lated in isopycnic and isobaric coordinates. *Journal of Geophysical Research: Oceans*, **91 (C6)**,
2526 7611–7621.

2527 Bleck, R., and Coauthors, 2015: A vertically flow-following icosahedral grid model for medium-
2528 range and seasonal prediction. part i: Model description. *Monthly Weather Review*, **143 (6)**,
2529 2386–2403.

2530 Bogenschutz, P. A., A. Gettelman, C. Hannay, V. E. Larson, R. B. Neale, C. Craig, and C.-C.
2531 Chen, 2018: The path to cam6: coupled simulations with cam5. 4 and cam5. 5. *Geoscientific*
2532 *Model Development*, **11 (1)**, 235.

2533 Bogenschutz, P. A., A. Gettelman, H. Morrison, V. E. Larson, C. Craig, and D. P. Schanen, 2013:
2534 Higher-order turbulence closure and its impact on climate simulations in the community atmo-
2535 sphere model. *Journal of Climate*, **26 (23)**, 9655–9676.

2536 Bogenschutz, P. A., and S. K. Krueger, 2013: A simplified pdf parameterization of subgrid-scale
2537 clouds and turbulence for cloud-resolving models. *Journal of Advances in Modeling Earth Sys-*
2538 *tems*, **5 (2)**, 195–211.

2539 Bolin, B., 1955: Numerical forecasting with the barotropic model 1. *Tellus*, **7 (1)**, 27–49.

- 2540 Bonan, B., 1996: A land surface model (lsm version 1.0) for ecological, hydrological, and atmo-
2541 spheric studies: Technical description and user's guide.
- 2542 Bonan, G., 2015: *Ecological climatology: concepts and applications*. Cambridge University
2543 Press.
- 2544 Bonan, G. B., 1998: The land surface climatology of the near land surface model coupled to the
2545 near community climate model. *Journal of Climate*, **11** (6), 1307–1326.
- 2546 Bonan, G. B., S. Levis, S. Sitch, M. Vertenstein, and K. W. Oleson, 2003: A dynamic global
2547 vegetation model for use with climate models: concepts and description of simulated vegetation
2548 dynamics. *Global Change Biology*, **9** (11), 1543–1566.
- 2549 Boucher, O., and U. Lohmann, 1995: The sulfate-ccn-cloud albedo effect. *Tellus B: Chemical and*
2550 *Physical Meteorology*, **47** (3), 281–300.
- 2551 Boucher, O., and Coauthors, 2013: Clouds and aerosols. *Climate change 2013: the physical sci-*
2552 *ence basis. Contribution of Working Group I to the Fifth Assessment Report of the Intergovern-*
2553 *mental Panel on Climate Change*, Cambridge University Press, 571–657.
- 2554 Bourke, W., 1974: A multi-level spectral model. I. Formulation and hemispheric integrations.
2555 *Mon. Wea. Rev.*, **102**, 687–701.
- 2556 Boville, B. A., and P. R. Gent, 1998: The near climate system model, version one. *Journal of*
2557 *Climate*, **11** (6), 1115–1130.
- 2558 Bradley, B. A., R. W. Jacob, J. F. Hermance, and J. F. Mustard, 2007: A curve fitting procedure to
2559 derive inter-annual phenologies from time series of noisy satellite ndvi data. *Remote sensing of*
2560 *environment*, **106** (2), 137–145.

- 2561 Bradshaw, P., D. Ferriss, and N. Atwell, 1967: Calculation of boundary-layer development using
2562 the turbulent energy equation. *Journal of Fluid Mechanics*, **28 (3)**, 593–616.
- 2563 Brenowitz, N. D., and C. S. Bretherton, 2018: Prognostic validation of a neural network unified
2564 physics parameterization. *Geophysical Research Letters*.
- 2565 Briegleb, B. P., and B. Light, 2007: *A Delta-Eddington multiple scattering parameterization for*
2566 *solar radiation in the sea ice component of the Community Climate System Model*. NCAR Tech.
2567 Note 472+STR, pp. 100.
- 2568 Brubaker, K. L., and D. Entekhabi, 1996: Analysis of feedback mechanisms in land-atmosphere
2569 interaction. *Water Resources Research*, **32 (5)**, 1343–1357.
- 2570 Bryan, F., 1987: Parameter sensitivity of primitive equation ocean general circulation models.
2571 *Journal of Physical Oceanography*, **17 (7)**, 970–985.
- 2572 Bryan, K., 1966: A scheme for numerical integration of the equations of motion on an irregular
2573 grid free of nonlinear instability. *Mon. Wea. Rev.*, **94**, 39–40.
- 2574 Bryan, K., 1969a: Climate and the ocean circulation iii. the ocean model. *Mon. Wea. Rev.*, **97**,
2575 806–827.
- 2576 Bryan, K., 1969b: A numerical method for the study of the circulation of the world ocean. *Journal*
2577 *of computational physics*, **4 (3)**, 347–376.
- 2578 Bryan, K., 1991: Michael Cox (1941–1989): His pioneering contributions to ocean circulation
2579 modeling. *Journal of physical oceanography*, **21 (9)**, 1259–1270.
- 2580 Bryan, K., and M. D. Cox, 1967: A numerical investigation of the oceanic general circulation.
2581 *Tellus*, **19 (1)**, 54–80.

- 2582 Bryan, K., and L. Lewis, 1979: A water mass model of the world ocean. *Journal of Geophysical*
2583 *Research: Oceans*, **84 (C5)**, 2503–2517.
- 2584 Budyko, M., and L. Zubenok, 1961: The determination of evaporation from the land surface. *Izv.*
2585 *Akad. Nauk SSSR Ser. Geogr.*, **6 (3)**, 3–17.
- 2586 Budyko, M. I., 1969: The effect of solar radiatin variations on the climate of the earth. *Tellus*, **21**,
2587 611–619.
- 2588 Bunker, A. F., B. Haurwitz, J. S. Malkus, and H. M. Stommel, 1949: *Vertical distribution of*
2589 *temperature and humidity over the Caribbean Sea*. Massachusetts Institute of Technology and
2590 Woods Hole Oceanographic Institution.
- 2591 Burridge, D. M., and J. Haseler, 1977: *A Model for Medium Range Weather Forecasts: Adiabatic*
2592 *Formation*. European Centre for Medium Range Weather Forecasts.
- 2593 Bushby, F., and M. S. Timpson, 1967: A 10-level atmospheric model and frontal rain. *Quarterly*
2594 *Journal of the Royal Meteorological Society*, **93 (395)**, 1–17.
- 2595 Businger, J. A., J. C. Wyngaard, Y. Izumi, and E. F. Bradley, 1971: Flux-profile relationships in
2596 the atmospheric surface layer. *Journal of the atmospheric Sciences*, **28 (2)**, 181–189.
- 2597 Cahalan, R. F., W. Ridgway, W. J. Wiscombe, T. L. Bell, and J. B. Snider, 1994: The Albedo of
2598 Fractal Stratocumulus Clouds. *J. Atmos. Sci.*, **51 (16)**, 2434–2455.
- 2599 Cairns, B., A. A. Lacis, and B. E. Carlson, 2000: Absorption within Inhomogeneous Clouds and
2600 Its Parameterization in General Circulation Models. *J. Atmos. Sci.*, **57 (5)**, 700–714.
- 2601 Callendar, G. S., 1938: The artificial production of carbon dioxide and its influence on tempera-
2602 ture. *Quarterly Journal of the Royal Meteorological Society*, **64 (275)**, 223–240.

- 2603 Campin, J.-M., C. Hill, H. Jones, and J. Marshall, 2011: Super-parameterization in ocean model-
2604 ing: Application to deep convection. *Ocean Modelling*, **36 (1-2)**, 90–101.
- 2605 Cess, R. D., and Coauthors, 1989: Interpretation of cloud-climate feedback as produced by 14
2606 atmospheric general circulation models. *Science*, **245 (4917)**, 513–516.
- 2607 Charney, J., M. Halem, and R. Jastrow, 1969: Use of incomplete historical data to infer the present
2608 state of the atmosphere. *Journal of the Atmospheric Sciences*, **26 (5)**, 1160–1163.
- 2609 Charney, J. G., 1962: Integration of the primitive and balance equations, proc. international sympo-
2610 sium on numerical weather prediction in tokyo. *Meteor. Soc. Japan*, 131–152.
- 2611 Charney, J. G., 1966: The feasibility of a global observation and analysis experiment. *Bull. Amer.*
2612 *Meteor. Soc.*, **47**, 200–230.
- 2613 Charney, J. G., 1975: Dynamics of deserts and drought in the sahel. *Quarterly Journal of the Royal*
2614 *Meteorological Society*, **101 (428)**, 193–202.
- 2615 Charney, J. G., R. Fjørtoft, and J. v. Neumann, 1950: Numerical integration of the barotropic
2616 vorticity equation. *Tellus*, **2 (4)**, 237–254.
- 2617 Charney, J. G., and N. A. Phillips, 1953: Numerical integration of the quasi-geostrophic equations
2618 for barotropic and simple baroclinic flow. *J. Meteorol.*, **10**, 71–99.
- 2619 Charney, J. G., and Coauthors, 1979: *Carbon dioxide and climate: a scientific assessment*. Na-
2620 tional Academy of Sciences, Washington, DC.
- 2621 Chen, J.-M., 1991: Turbulence-scale condensation parameterization. *Journal of the atmospheric*
2622 *sciences*, **48 (12)**, 1510–1512.

- 2623 Cheng, M.-D., and A. Arakawa, 1997: Inclusion of rainwater budget and convective downdrafts in
2624 the arakawa–schubert cumulus parameterization. *Journal of the atmospheric sciences*, **54 (10)**,
2625 1359–1378.
- 2626 Chevallier, F., F. Chéruy, N. Scott, and A. Chédin, 1998: A neural network approach for a fast and
2627 accurate computation of a longwave radiative budget. *Journal of Applied Meteorology*, **37 (11)**,
2628 1385–1397.
- 2629 Clement, V., S. Ferrachat, O. Fuhrer, X. Lapillonne, C. E. Osuna, R. Pincus, J. Rood, and
2630 W. Sawyer, 2018: The claw dsl: Abstractions for performance portable weather and cli-
2631 mate models. *Proceedings of the Platform for Advanced Scientific Computing Conference*,
2632 ACM, New York, NY, USA, 2:1–2:10, PASC '18, doi:10.1145/3218176.3218226, URL <http://doi.acm.org/10.1145/3218176.3218226>.
2633
- 2634 Clough, S. A., M. J. Iacono, and J.-L. Moncet, 1992: Line-by-line calculations of atmospheric
2635 fluxes and cooling rates: Application to water vapor. *J. Geophys. Res.*, **97 (D14)**, 15 761–15 785.
- 2636 Cohard, J.-M., and J.-P. Pinty, 2000: A comprehensive two-moment warm microphysical bulk
2637 scheme. i: Description and tests. *Quarterly Journal of the Royal Meteorological Society*,
2638 **126 (566)**, 1815–1842.
- 2639 Collatz, G. J., J. T. Ball, C. Grivet, and J. A. Berry, 1991: Physiological and environmental regula-
2640 tion of stomatal conductance, photosynthesis and transpiration: a model that includes a laminar
2641 boundary layer. *Agricultural and Forest meteorology*, **54 (2-4)**, 107–136.
- 2642 Collins, W. D., 2001: Parameterization of Generalized Cloud Overlap for Radiative Calculations
2643 in General Circulation Models. *J. Atmos. Sci.*, **58 (21)**, 3224–3242.

2644 Collins, W. D., and Coauthors, 2006a: The Community Climate System Model Version 3, CCSM3.
2645 **19**, 2122–2143.

2646 Collins, W. D., and Coauthors, 2006b: Radiative forcing by well-mixed greenhouse gases: Esti-
2647 mates from climate models in the Intergovernmental Panel on Climate Change (IPCC) Fourth
2648 Assessment Report (AR4). *J. Geophys. Res.*, **111 (D14)**, D14 317.

2649 Coon, M. D., G. A. Maykut, R. S. Pritchard, D. A. Rothrock, and A. S. Thorndike, 1974: Modeling
2650 the pack ice as an elastic-plastic material. *AIDJEX Bull.*, **24**, 1–105.

2651 Corby, G., A. Gilchrist, and P. Rowntree, 1977: United kingdom meteorological office five-level
2652 general circulation model. *Methods in Computational Physics: Advances in Research and Ap-
2653 plications*, Vol. 17, Elsevier, 67–110.

2654 Côté, J., and A. Staniforth, 1988: A two-time-level semi-lagrangian semi-implicit scheme for
2655 spectral models. *Monthly weather review*, **116 (10)**, 2003–2012.

2656 Courant, R., K. Friedrichs, and H. Lewy, 1928: Über die partiellen differenzgleichungen der
2657 mathematischen physik. *Mathematische annalen*, **100 (1)**, 32–74.

2658 Courant, R., K. Friedrichs, and H. Lewy, 1967: On the partial difference equations of mathematical
2659 physics. *IBM journal of Research and Development*, **11 (2)**, 215–234.

2660 Courtier, P., and M. Naughton, 1994: A pole problem in the reduced gaussian grid. *Quarterly
2661 Journal of the Royal Meteorological Society*, **120 (519)**, 1389–1407.

2662 Covey, C., K. M. AchutaRao, U. Cubasch, P. Jones, S. J. Lambert, M. E. Mann, T. J. Phillips, and
2663 K. E. Taylor, 2003: An overview of results from the coupled model intercomparison project.
2664 *Global and Planetary Change*, **37 (1-2)**, 103–133.

- 2665 Cox, M., 1987: Isopycnal diffusion in a z-coordinate ocean model. *Ocean modelling*, **74**, 1–5.
- 2666 Cox, M. D., 1984: A primitive equation, 3-dimensional model of the ocean. *GFDL Ocean Group*
2667 *Technical Report No 1, GFDL, Princeton University.*
- 2668 Cox, P., C. Huntingford, and R. Harding, 1998: A canopy conductance and photosynthesis model
2669 for use in a gcm land surface scheme. *Journal of Hydrology*, **212**, 79–94.
- 2670 Cox, P. M., 2001: Description of the triffid dynamic global vegetation model. *Hadley Centre*
2671 *technical note*, **24**, 1–16.
- 2672 Cox, P. M., R. Betts, M. Collins, P. P. Harris, C. Huntingford, and C. Jones, 2004: Amazonian for-
2673 est dieback under climate-carbon cycle projections for the 21st century. *Theoretical and applied*
2674 *climatology*, **78 (1-3)**, 137–156.
- 2675 Cox, P. M., R. A. Betts, C. D. Jones, S. A. Spall, and I. J. Totterdell, 2000: Acceleration of global
2676 warming due to carbon-cycle feedbacks in a coupled climate model. *Nature*, **408 (6809)**, 184.
- 2677 Cox, P. M., D. Pearson, B. B. Booth, P. Friedlingstein, C. Huntingford, C. D. Jones, and C. M.
2678 Luke, 2013: Sensitivity of tropical carbon to climate change constrained by carbon dioxide
2679 variability. *Nature*, **494 (7437)**, 341.
- 2680 Cox, S. K., D. S. McDougal, D. A. Randall, and R. A. Schiffer, 1987: Fire—the first isccp regional
2681 experiment. *Bulletin of the American Meteorological Society*, **68 (2)**, 114–118.
- 2682 Craig, A. P., M. Vertenstein, and R. Jacob, 2012: A new flexible coupler for earth system modeling
2683 developed for ccsm4 and cesm1. *The International Journal of High Performance Computing*
2684 *Applications*, **26 (1)**, 31–42.

2685 Cramer, W., and Coauthors, 2001: Global response of terrestrial ecosystem structure and function
2686 to co2 and climate change: results from six dynamic global vegetation models. *Global change*
2687 *biology*, **7 (4)**, 357–373.

2688 Cubasch, U., K. Hasselmann, H. Höck, E. Maier-Reimer, U. Mikolajewicz, B. D. Santer, and
2689 R. Sausen, 1992: Time-dependent greenhouse warming computations with a coupled ocean-
2690 atmosphere model. *Climate Dynamics*, **8 (2)**, 55–69.

2691 Cullen, M., 1993a: The Unified forecast climate model. *Mat. Mag.*, **122 (1449)**, 81–94.

2692 Cullen, M., 1993b: The unified forecast/climate model. *Meteorological Magazine*, **122 (1449)**,
2693 81–94.

2694 Cullen, M., T. Davies, M. Mawson, J. James, S. Coulter, and A. Malcolm, 1997: An overview
2695 of numerical methods for the next generation uk nwp and climate model. *atmosphere-ocean*,
2696 **35 (sup1)**, 425–444.

2697 Curtis, A. R., 1956: The Computation of Radiative Heating Rates in the Atmosphere. *Proc. Royal*
2698 *Soc. A*, **236 (1205)**, 156–159.

2699 Curtis, A. R., and R. M. Goody, 1954: Spectral line shape and its effect on atmospheric transmis-
2700 sions. *Quart. J. Royal Met. Soc.*, **80 (343)**, 58–67.

2701 Dai, Y., R. E. Dickinson, and Y.-P. Wang, 2004: A two-big-leaf model for canopy temperature,
2702 photosynthesis, and stomatal conductance. *Journal of Climate*, **17 (12)**, 2281–2299.

2703 Danabasoglu, G., S. C. Bates, B. P. Briegleb, S. R. Jayne, M. Jochum, W. G. Large, S. Peacock,
2704 and S. G. Yeager, 2012: The ccsm4 ocean component. *Journal of Climate*, **25 (5)**, 1361–1389.

2705 Danabasoglu, G., W. G. Large, J. J. Tribbia, P. R. Gent, B. P. Briegleb, and J. C. McWilliams, 2006:
2706 Diurnal coupling in the tropical oceans of ccsm3. *Journal of climate*, **19 (11)**, 2347–2365.

2707 Danabasoglu, G., J. C. McWilliams, and P. R. Gent, 1994: The role of mesoscale tracer transports
2708 in the global ocean circulation. *Science*, **264 (5162)**, 1123–1126.

2709 Danilov, S., 2013: Ocean modeling on unstructured meshes. *Ocean Modelling*, **69**, 195–210.

2710 Davies, T., M. Cullen, M. Mawson, and A. Malcolm, 1998: A new dynamical formulation for
2711 the uk meteorological office unified model. *Proceedings of ECMWF seminar on recent devel-*
2712 *opments in numerical methods for atmospheric modelling*, 7–11.

2713 Deardorff, J., 1972a: Parameterization of the planetary boundary layer for use in general circula-
2714 tion models. *Mon. Wea. Rev.*, **100**, 93–106.

2715 Deardorff, J. W., 1964: A numerical study of two-dimensional parallel-plate convection. *Journal*
2716 *of the Atmospheric Sciences*, **21 (4)**, 419–438.

2717 Deardorff, J. W., 1972b: Numerical investigation of neutral and unstable planetary boundary lay-
2718 ers. *Journal of the Atmospheric Sciences*, **29 (1)**, 91–115.

2719 Deardorff, J. W., 1974: Three-dimensional numerical study of the height and mean structure of a
2720 heated planetary boundary layer. *Boundary-Layer Meteorology*, **7 (1)**, 81–106.

2721 Deardorff, J. W., 1978: Efficient prediction of ground surface temperature and moisture, with
2722 inclusion of a layer of vegetation. *J. Geophys. Res.*, **83**, 1889–1903.

2723 Deardorff, J. W., 1980: Stratocumulus-capped mixed layers derived from a three-dimensional
2724 model. *Boundary-Layer Meteorology*, **18 (4)**, 495–527.

2725 Dee, D. P., and Coauthors, 2011: The era-interim reanalysis: Configuration and performance of
2726 the data assimilation system. *Quarterly Journal of the royal meteorological society*, **137 (656)**,
2727 553–597.

- 2728 DeMott, P. J., and Coauthors, 2010: Predicting global atmospheric ice nuclei distributions and
2729 their impacts on climate. *Proceedings of the National Academy of Sciences*.
- 2730 Dennis, J. M., and Coauthors, 2012: Cam-se: A scalable spectral element dynamical core for
2731 the community atmosphere model. *The International Journal of High Performance Computing*
2732 *Applications*, **26 (1)**, 74–89.
- 2733 Dickinson, R. E., and A. Henderson-Sellers, 1988: Modelling tropical deforestation: A study
2734 of gcm land-surface parametrizations. *Quarterly Journal of the Royal Meteorological Society*,
2735 **114 (480)**, 439–462.
- 2736 Dickinson, R. E., A. Henderson-Sellers, P. Kennedy, and M. Wilson, 1986: Biosphere-atmosphere
2737 transfer schemes (bats) for the ncar community climate model. *Tech. Note NCAR/TN-275+ STR*,
2738 **69**.
- 2739 Dickinson, R. E., Y. Tian, Q. Liu, and L. Zhou, 2008: Dynamics of leaf area for climate and
2740 weather models. *Journal of Geophysical Research: Atmospheres*, **113 (D16)**.
- 2741 Diedhiou, A., and J.-F. Mahfouf, 1996: Comparative influence of land and sea surfaces on the
2742 sahelian drought: a numerical study. *Annales Geophysicae*, Springer, Vol. 14, 115–130.
- 2743 Dietachmayer, G. S., and K. K. Droegemeier, 1992: Application of continuous dynamic grid adap-
2744 tion techniques to meteorological modeling. part i: Basic formulation and accuracy. *Monthly*
2745 *weather review*, **120 (8)**, 1675–1706.
- 2746 Dirmeyer, P. A., 1994: Vegetation stress as a feedback mechanism in midlatitude drought. *Journal*
2747 *of climate*, **7 (10)**, 1463–1483.

2748 Donaldson, C. d. P., 1973: Construction of a dynamic model of the production of atmospheric
2749 turbulence and the dispersal of atmospheric pollutants. *Workshop on Micrometeorology*, Amer.
2750 Meteor. Soc, 313–392.

2751 Donaldson, C. d. P., and H. Rosenbaum, 1969: Calculation of turbulent, shear flows through
2752 closure of the reynolds equations by invariant modeling. *NASA Special Publication*, **216**, 231.

2753 Donea, J., A. Huerta, J.-P. Ponthot, and A. Rodriguez-Ferran, 2004: Encyclopedia of computa-
2754 tional mechanics vol. 1: Fundamentals., chapter 14: Arbitrary lagrangian-eulerian methods.
2755 Wiley & Sons.

2756 Donner, L., W. Schubert, and R. Somerville, 2011: *The Development of Atmospheric General*
2757 *Circulation Models: Complexity, Synthesis and Computation*. Cambridge University Press.

2758 Douville, H., F. Chauvin, and H. Broqua, 2001: Influence of soil moisture on the asian and african
2759 monsoons. part i: Mean monsoon and daily precipitation. *Journal of Climate*, **14 (11)**, 2381–
2760 2403.

2761 Dubos, T., N. Kevlahan, and Coauthors, 2013: A conservative adaptive wavelet method for the
2762 shallow-water equations on staggered grids. *Quarterly Journal of the Royal Meteorological*
2763 *Society*, **139 (677)**, 1997–2020.

2764 Dufresne, J.-L., L. Fairhead, H. Le Treut, M. Berthelot, L. Bopp, P. Ciais, P. Friedlingstein, and
2765 P. Monfray, 2002: On the magnitude of positive feedback between future climate change and
2766 the carbon cycle. *Geophysical Research Letters*, **29 (10)**, 43–1.

2767 Dukowicz, J. K., and R. D. Smith, 1994: Implicit free-surface method for the bryan-cox-semtner
2768 ocean model. *Journal of Geophysical Research: Oceans*, **99 (C4)**, 7991–8014.

2769 Dunne, J. P., and Coauthors, 2012: Gfdl’s esm2 global coupled climate–carbon earth system mod-
2770 els. part i: Physical formulation and baseline simulation characteristics. *Journal of Climate*,
2771 **25 (19)**, 6646–6665.

2772 Eddington, A. S., 1916: On the Radiative Equilibrium of the Stars. *Mon. Notices Royal Astron.*
2773 *Soc*, **77 (1)**, 16–35.

2774 Edwards, J. M., and A. Slingo, 1996: Studies with a flexible new radiation code. I: Choosing a
2775 configuration for a large-scale model. *Quart. J. Royal Met. Soc.*, **122 (531)**, 689–719.

2776 Edwards, P., 2010: A vast machine: Computer models, climate data, and the politics of global
2777 warming, 528 pp. MIT Press, Cambridge, Mass.

2778 Edwards, P. N., 2011: History of climate modeling. *Wiley Interdisciplinary Reviews: Climate*
2779 *Change*, **2 (1)**, 128–139.

2780 Eliassen, A., 1960: On the transfer of energy in stationary mountain waves. *Geophys. Publ.*, **22**,
2781 1–23.

2782 Eliassen, A., and E. Raustein, 1968: A numerical integration experiment with a model atmosphere
2783 based on isentropic surfaces. *Meteorologiske Annaler*, **5**, 45–63.

2784 Eliassen, E., B. Machenhauer, and E. Rasmussen, 1970: *On a numerical method for integration*
2785 *of the hydrodynamical equations with a spectral representation of the horizontal fields*. Koben-
2786 havns Universitet, Institut for Teoretisk Meteorologi.

2787 Ellingson, R. G., J. Ellis, and S. Fels, 1991: The intercomparison of radiation codes used in climate
2788 models: Long wave results. *J. Geophys. Res.*, **96 (D5)**, 8929–8953.

2789 Ellingson, R. G., and Y. Fouquart, 1991: The intercomparison of radiation codes in climate mod-
2790 els: An overview. *J. Geophys. Res.*, **96 (D5)**, 8925–8927.

- 2791 Elsaesser, G. S., A. D. Del Genio, J. H. Jiang, and M. van Lier-Walqui, 2017: An improved
2792 convective ice parameterization for the nasa giss global climate model and impacts on cloud ice
2793 simulation. *Journal of Climate*, **30** (1), 317–336.
- 2794 Elsasser, W. M., and M. F. Culbertson, 1960: Atmospheric Radiation Tables. *Meteorol. Monogr.*,
2795 **4**, 1–43.
- 2796 Eltahir, E. A., 1998: A soil moisture–rainfall feedback mechanism: 1. theory and observations.
2797 *Water Resources Research*, **34** (4), 765–776.
- 2798 Emanuel, K. A., 1981: A similarity theory for unsaturated downdrafts within clouds. *Journal of*
2799 *the Atmospheric Sciences*, **38** (8), 1541–1557.
- 2800 Emanuel, K. A., 1991: A scheme for representing cumulus convection in large-scale models.
2801 *Journal of the Atmospheric Sciences*, **48** (21), 2313–2329.
- 2802 Eyring, V., S. Bony, G. A. Meehl, C. A. Senior, B. Stevens, R. J. Stouffer, and K. E. Taylor, 2016:
2803 Overview of the coupled model intercomparison project phase 6 (cmip6) experimental design
2804 and organization. *Geoscientific Model Development*, **9** (5), 1937–1958.
- 2805 Farquhar, G. v., S. v. von Caemmerer, and J. Berry, 1980: A biochemical model of photosynthetic
2806 co2 assimilation in leaves of c3 species. *Planta*, **149** (1), 78–90.
- 2807 Feingold, G., S. M. Kreidenweis, B. Stevens, and W. Cotton, 1996: Numerical simulations of
2808 stratocumulus processing of cloud condensation nuclei through collision-coalescence. *Journal*
2809 *of Geophysical Research: Atmospheres*, **101** (D16), 21 391–21 402.
- 2810 Fels, S. B., and M. D. Schwarzkopf, 1975: The Simplified Exchange Approximation: A New
2811 Method for Radiative Transfer Calculations. *J. Atmos. Sci.*, **32** (7), 1475–1488.

- 2812 Fennessy, M. J., and J. Shukla, 1999: Impact of initial soil wetness on seasonal atmospheric
2813 prediction. *Journal of Climate*, **12** (11), 3167–3180.
- 2814 Fichet, T., and M. A. Morales-Maqueda, 1997: Sensitivity of a global sea ice model to the
2815 treatment of ice thermodynamics and dynamics. *J. Geophys. Res.*, **102**, 12,609–12,646.
- 2816 Fiedler, F., and H. A. Panofsky, 1970: Atmospheric scales and spectral gaps. *Bulletin of the Amer-*
2817 *ican Meteorological Society*, **51** (12), 1114–1120.
- 2818 Flato, G., G. Boer, W. Lee, N. McFarlane, D. Ramsden, M. Reader, and A. Weaver, 2000: The
2819 canadian centre for climate modelling and analysis global coupled model and its climate. *Cli-*
2820 *mate Dynamics*, **16** (6), 451–467.
- 2821 Flato, G. M., and W. D. Hibler III, 1992: Modeling pack ice as a cavitating fluid. *J. Phys.*
2822 *Oceanogr.*, **22**, 626–651.
- 2823 Fleming, J. R., 2016: *Inventing atmospheric science: Bjerknes, Rossby, Wexler, and the founda-*
2824 *tions of modern meteorology*. MIT Press.
- 2825 Flocco, D., and D. L. Feltham, 2007: A continuum model of melt pond evolution on Arctic sea
2826 ice. *J. Geophys. Res.*, **112**, doi:10.1029/2006JC003 836.
- 2827 Foken, T., 2006: 50 years of the monin–obukhov similarity theory. *Boundary-Layer Meteorology*,
2828 **119** (3), 431–447.
- 2829 Foley, J. A., I. C. Prentice, N. Ramankutty, S. Levis, D. Pollard, S. Sitch, and A. Haxeltine,
2830 1996: An integrated biosphere model of land surface processes, terrestrial carbon balance, and
2831 vegetation dynamics. *Global Biogeochemical Cycles*, **10** (4), 603–628.
- 2832 Folland, C. K., D. J. Griggs, and J. T. Houghton, 2004: History of the hadley centre for climate
2833 prediction and research. *Weather*, **59** (11), 317–323.

2834 Fouquart, Y., B. Bonnel, and V. Ramaswamy, 1991: Intercomparing shortwave radiation codes for
2835 climate studies. *J. Geophys. Res.*, **96 (D5)**, 8955–8968.

2836 Fovell, R., D. Durran, and J. Holton, 1992: Numerical simulations of convectively generated
2837 stratospheric gravity waves. *Journal of the atmospheric sciences*, **49 (16)**, 1427–1442.

2838 Fowler, L. D., D. A. Randall, and S. A. Rutledge, 1996: Liquid and ice cloud microphysics in the
2839 csu general circulation model. part 1: Model description and simulated microphysical processes.
2840 *Journal of climate*, **9 (3)**, 489–529.

2841 Fox-Kemper, B., R. Ferrari, and R. Hallberg, 2008: Parameterization of mixed layer eddies. part
2842 i: Theory and diagnosis. *Journal of Physical Oceanography*, **38 (6)**, 1145–1165.

2843 Fridlind, A. M., and Coauthors, 2004: Evidence for the predominance of mid-tropospheric
2844 aerosols as subtropical anvil cloud nuclei. *Science*, **304 (5671)**, 718–722.

2845 Friedlingstein, P., J.-L. Dufresne, P. Cox, and P. Rayner, 2003: How positive is the feedback
2846 between climate change and the carbon cycle? *Tellus B: Chemical and Physical Meteorology*,
2847 **55 (2)**, 692–700.

2848 Friedlingstein, P., and Coauthors, 2006: Climate–carbon cycle feedback analysis: results from the
2849 c4mip model intercomparison. *Journal of climate*, **19 (14)**, 3337–3353.

2850 Friend, A. D., and Coauthors, 2007: Fluxnet and modelling the global carbon cycle. *Global
2851 Change Biology*, **13 (3)**, 610–633.

2852 Fu, Q., and K. N. Liou, 1992: On the correlated k -distribution method for radiative transfer in
2853 nonhomogeneous atmospheres. *J. Atmos. Sci.*, **49 (22)**, 2139–2156.

2854 Fultz, D., R. R. Long, G. V. Owens, W. Bohan, R. Kaylor, and J. Weil, 1959: Studies of thermal
2855 convection in a rotating cylinder with some implications for large-scale atmospheric motions.

- 2856 *Studies of Thermal Convection in a Rotating Cylinder with Some Implications for Large-Scale*
2857 *Atmospheric Motions*, Springer, 1–104.
- 2858 Fung, I., C. Tucker, and K. Prentice, 1987: Application of advanced very high resolution radiome-
2859 ter vegetation index to study atmosphere-biosphere exchange of co₂. *Journal of Geophysical*
2860 *Research: Atmospheres*, **92 (D3)**, 2999–3015.
- 2861 Gaspar, P., Y. Grégoris, and J.-M. Lefevre, 1990: A simple eddy kinetic energy model for simula-
2862 tions of the oceanic vertical mixing: Tests at station papa and long-term upper ocean study site.
2863 *Journal of Geophysical Research: Oceans*, **95 (C9)**, 16 179–16 193.
- 2864 Gates, W. L., 1992: AMIP: The Atmospheric Model Intercomparison Project. *Bull. Amer. Meteor.*
2865 *Soc.*, **73**, 1962–1970.
- 2866 Geleyn, J. F., and A. Hollingsworth, 1979: An economical analytical method for the computa-
2867 tion of the interaction between scattering and line absorption of radiation. *Beiträge zur Physik*
2868 *Atmosphäre*, **52**, 1–16.
- 2869 Gent, P. R., 2013: Coupled models and climate projections. *International Geophysics*, Vol. 103,
2870 Elsevier, 609–623.
- 2871 Gent, P. R., F. O. Bryan, G. Danabasoglu, S. C. Doney, W. R. Holland, W. G. Large, and J. C.
2872 McWilliams, 1998: The near climate system model global ocean component. *Journal of Cli-*
2873 *mate*, **11 (6)**, 1287–1306.
- 2874 Gent, P. R., and J. C. McWilliams, 1990: Isopycnal mixing in ocean circulation models. *Journal*
2875 *of Physical Oceanography*, **20 (1)**, 150–155.

- 2876 Gent, P. R., J. Willebrand, T. J. McDougall, and J. C. McWilliams, 1995: Parameterizing eddy-
2877 induced tracer transports in ocean circulation models. *Journal of Physical Oceanography*,
2878 **25 (4)**, 463–474.
- 2879 Gentine, P., M. Pritchard, S. Rasp, G. Reinaudi, and G. Yacalis, 2018: Could machine learning
2880 break the convection parameterization deadlock? *Geophysical Research Letters*.
- 2881 Gerten, D., S. Schaphoff, U. Haberlandt, W. Lucht, and S. Sitch, 2004: Terrestrial vegetation
2882 and water balance—hydrological evaluation of a dynamic global vegetation model. *Journal of*
2883 *Hydrology*, **286 (1-4)**, 249–270.
- 2884 Gettelman, A., and H. Morrison, 2015: Advanced two-moment bulk microphysics for global mod-
2885 els. part i: Off-line tests and comparison with other schemes. *Journal of Climate*, **28 (3)**, 1268–
2886 1287.
- 2887 GEWEX Cloud System Science Team, 1993: The gewex cloud system study (gcss). *Bulletin of*
2888 *the American Meteorological Society*, **74 (3)**, 387–400.
- 2889 Ghan, S. J., and R. C. Easter, 1992: Computationally efficient approximations to stratiform cloud
2890 microphysics parameterization. *Monthly weather review*, **120 (8)**, 1572–1582.
- 2891 Ghan, S. J., L. R. Leung, R. C. Easter, and H. Abdul-Razzak, 1997: Prediction of cloud
2892 droplet number in a general circulation model. *Journal of Geophysical Research: Atmospheres*,
2893 **102 (D18)**, 21 777–21 794.
- 2894 Ghan, S. J., and Coauthors, 2001: A physically based estimate of radiative forcing by anthro-
2895 pogenic sulfate aerosol. *Journal of Geophysical Research: Atmospheres*, **106 (D6)**, 5279–5293.

- 2896 Gibelin, A.-L., J.-C. Calvet, J.-L. Roujean, L. Jarlan, and S. O. Los, 2006: Ability of the land sur-
2897 face model isba-a-gs to simulate leaf area index at the global scale: Comparison with satellites
2898 products. *Journal of Geophysical Research: Atmospheres*, **111** (D18).
- 2899 Gibson, J., 1997: Era description. *ECMWF re-analysis project report series*, **1**.
- 2900 Gienapp, P., L. Hemerik, and M. E. Visser, 2005: A new statistical tool to predict phenology under
2901 climate change scenarios. *Global Change Biology*, **11** (4), 600–606.
- 2902 Gilchrist, A., G. A. Corby, and R. L. Newson, 1973: A numerical experiment using a general
2903 circulation model of the atmosphere. *Quarterly Journal of the Royal Meteorological Society*,
2904 **99** (419), 2–34.
- 2905 Giorgetta, M. A., and Coauthors, 2018: Icon-a, the atmosphere component of the icon earth system
2906 model. part i: Model description. *Journal of Advances in Modeling Earth Systems*.
- 2907 Girard, C., and Coauthors, 2014: Staggered vertical discretization of the canadian environmen-
2908 tal multiscale (gem) model using a coordinate of the log-hydrostatic-pressure type. *Monthly*
2909 *Weather Review*, **142** (3), 1183–1196.
- 2910 Glushko, G., 1966: Turbulent boundary layer on a flat plate in an incompressible fluid. Tech.
2911 rep., TECHNICAL INFORMATION AND LIBRARY SERVICES MINISTRY OF AVIATION
2912 LONDON (ENGLAND).
- 2913 Gnanadesikan, A., and Coauthors, 2006: Gfdl's cm2 global coupled climate models. part ii: The
2914 baseline ocean simulation. *Journal of Climate*, **19** (5), 675–697, doi:10.1175/JCLI3630.1, URL
2915 <https://doi.org/10.1175/JCLI3630.1>, <https://doi.org/10.1175/JCLI3630.1>.
- 2916 Golaz, J.-C., V. E. Larson, and W. R. Cotton, 2002a: A PDF-based model for boundary layer
2917 clouds. Part I: Method and model description. *J. Atmos. Sci.*, **59** (24), 3540–3551.

2918 Golaz, J.-C., V. E. Larson, and W. R. Cotton, 2002b: A pdf-based model for boundary layer clouds.
2919 part i: Method and model description. *Journal of the atmospheric sciences*, **59 (24)**, 3540–3551.

2920 Golaz, J.-C., M. Salzmann, L. J. Donner, L. W. Horowitz, Y. Ming, and M. Zhao, 2011: Sensitivity
2921 of the aerosol indirect effect to subgrid variability in the cloud parameterization of the gfdl
2922 atmosphere general circulation model am3. *Journal of Climate*, **24 (13)**, 3145–3160.

2923 Goldberg, D., C. Little, O. Sergienko, A. Gnanadesikan, R. Hallberg, and M. Oppenheimer, 2012:
2924 Investigation of land ice-ocean interaction with a fully coupled ice-ocean model: 2. sensitivity
2925 to external forcings. *Journal of Geophysical Research: Earth Surface*, **117 (F2)**.

2926 Goody, R., R. West, L. Chen, and D. Crisp, 1989: The correlated-k method for radiation calcula-
2927 tions in nonhomogeneous atmospheres. *J. Quant. Spectrosc. Radiat. Transfer*, **42 (6)**, 539–550.

2928 Gordon, C., C. Cooper, C. A. Senior, H. Banks, J. M. Gregory, T. C. Johns, J. F. Mitchell, and R. A.
2929 Wood, 2000: The simulation of sst, sea ice extents and ocean heat transports in a version of the
2930 hadley centre coupled model without flux adjustments. *Climate dynamics*, **16 (2-3)**, 147–168.

2931 Grabowski, W. W., 2001: Coupling cloud processes with the large-scale dynamics using the cloud-
2932 resolving convection parameterization (crcp). *Journal of the Atmospheric Sciences*, **58 (9)**, 978–
2933 997.

2934 Grabowski, W. W., 2004: An improved framework for superparameterization. *Journal of the at-
2935 mospheric sciences*, **61 (15)**, 1940–1952.

2936 Grabowski, W. W., and P. K. Smolarkiewicz, 1999: Crcp: A cloud resolving convection parame-
2937 terization for modeling the tropical convecting atmosphere. *Physica D: Nonlinear Phenomena*,
2938 **133 (1-4)**, 171–178.

2939 Greatbatch, R. J., and K. G. Lamb, 1990: On parameterizing vertical mixing of momentum in
2940 non-eddy resolving ocean models. *Journal of Physical Oceanography*, **20** (10), 1634–1637.

2941 Green, J. S. A., 1967: Division of radiative streams into internal transfer and cooling to space.
2942 *Quart. J. Royal Met. Soc.*, **93** (397), 371–372.

2943 Gregory, J. M., C. Jones, P. Cadule, and P. Friedlingstein, 2009: Quantifying carbon cycle feed-
2944 backs. *Journal of Climate*, **22** (19), 5232–5250.

2945 Griffies, S., and Coauthors, 2005: Formulation of an ocean model for global climate simulations.
2946 *Ocean Science*, **1** (1), 45–79.

2947 Griffies, S. M., 1998: The gent–mcwilliams skew flux. *Journal of Physical Oceanography*, **28** (5),
2948 831–841.

2949 Griffies, S. M., 2004: *Fundamentals of ocean climate models*, Vol. 518. Citeseer.

2950 Griffies, S. M., A. Gnanadesikan, R. C. Pacanowski, V. D. Larichev, J. K. Dukowicz, and R. D.
2951 Smith, 1998: Isonutral diffusion in az-coordinate ocean model. *Journal of Physical Oceanog-*
2952 *raphy*, **28** (5), 805–830.

2953 Griffies, S. M., and R. J. Greatbatch, 2012: Physical processes that impact the evolution of global
2954 mean sea level in ocean climate models. *Ocean Modelling*, **51**, 37–72.

2955 Griffies, S. M., and Coauthors, 2000: Developments in ocean climate modelling. *Ocean Mod-*
2956 *elling*, **2** (3-4), 123–192.

2957 Griffies, S. M., and Coauthors, 2015: Impacts on ocean heat from transient mesoscale eddies in a
2958 hierarchy of climate models. *Journal of Climate*, **28** (3), 952–977.

2959 Griffies, S. M., and Coauthors, 2016: Omip contribution to cmip6: experimental and diagnostic
2960 protocol for the physical component of the ocean model intercomparison project. *Geoscientific*
2961 *Model Development*, **9 (9)**, 3231.

2962 Grobecker, A., S. C. Coroniti, and R. Cannon Jr, 1974: Report of findings. the effects of strato-
2963 spheric pollution by aircraft. Tech. rep., DEPARTMENT OF TRANSPORTATION WASHING-
2964 TON DC SYSTEMS DEVELOPMENT AND TECHNOLOGY.

2965 Grumbine, R. W., 2013: Keeping Ice’S Simplicity — A modeling start. Tech. Rep. MMAB Contri-
2966 bution No. 314, 30pp, http://polar.ncep.noaa.gov/mmab/papers/tn314/MMAB_314.pdf, NOAA
2967 National Weather Service National Center for Environmental Prediction, 30 pp.

2968 Habata, S., M. Yokokawa, S. Kitawaki, and Coauthors, 2003: The earth simulator system. *NEC*
2969 *Research and Development*, **44 (1)**, 21–26.

2970 Hall, F., and P. Sellers, 1995: First international satellite land surface climatology project (islscp)
2971 field experiment (fife) in 1995. *Journal of Geophysical Research: Atmospheres*, **100 (D12)**,
2972 25 383–25 395.

2973 Hallberg, R., 2003: The ability of large-scale ocean models to accept parameterizations of bound-
2974 ary mixing, and a description of a refined bulk mixed-layer model. *Proceedings of the 2003 Aha*
2975 *Hulikoa Hawaiian Winter Workshop*, 187–203.

2976 Hansen, J., D. Johnson, A. Lacis, S. Lebedeff, P. Lee, D. Rind, and G. Russell, 1981: Climate
2977 impact of increasing atmospheric carbon dioxide. *Science*, **213 (4511)**, 957–966.

2978 Hansen, J., A. Lacis, D. Rind, G. Russell, P. Stone, I. Fung, R. Ruedy, and J. Lerner, 1984: Climate
2979 sensitivity: Analysis of feedback mechanisms. *Climate processes and climate sensitivity*, 130–
2980 163.

2981 Hansen, J., G. Russell, D. Rind, P. Stone, A. Lacis, S. Lebedeff, R. Ruedy, and L. Travis, 1983:
2982 Efficient Three-Dimensional Global Models for Climate Studies: Models I and II. *Mon. Wea.*
2983 *Rev.*, **111 (4)**, 609–662.

2984 Hansen, J. E., and L. D. Travis, 1974: Light scattering in planetary atmospheres. *Space Sci. Rev.*,
2985 **16 (4)**, 527–610.

2986 Harper, A., I. T. Baker, A. S. Denning, D. A. Randall, D. Dazlich, and M. Branson, 2014: Impact
2987 of evapotranspiration on dry season climate in the amazon forest. *Journal of Climate*, **27 (2)**,
2988 574–591.

2989 Harper, K. C., 2012: *Weather by the numbers: the genesis of modern meteorology*. MIT Press.

2990 Harrington, J. Y., K. Sulia, and H. Morrison, 2013: A method for adaptive habit prediction in bulk
2991 microphysical models. part i: Theoretical development. *Journal of the Atmospheric Sciences*,
2992 **70 (2)**, 349–364.

2993 Harris, L. M., P. H. Lauritzen, and R. Mittal, 2011: A flux-form version of the conservative semi-
2994 lagrangian multi-tracer transport scheme (cslam) on the cubed sphere grid. *Journal of Compu-*
2995 *tational Physics*, **230 (4)**, 1215–1237.

2996 Harshvardhan, R. Davies, D. A. Randall, and T. G. Corsetti, 1987: A fast radiation parameteriza-
2997 tion for atmospheric circulation models. *J. Geophys. Res.*, **92 (D1)**, 1009–1016.

2998 Harshvardhan, D. A. Randall, T. G. Corsetti, and D. A. Dazlich, 1989: Earth Radiation Budget and
2999 Cloudiness Simulations with a General Circulation Model. *J. Atmos. Sci.*, **46 (13)**, 1922–1942.

3000 Hashino, T., and G. Tripoli, 2007: The spectral ice habit prediction system (ships). part i: Model
3001 description and simulation of the vapor deposition process. *Journal of the atmospheric sciences*,
3002 **64 (7)**, 2210–2237.

3003 Haugen, D., J. Kaimal, and E. Bradley, 1971: An experimental study of reynolds stress and heat
3004 flux in the atmospheric surface layer. *Quarterly Journal of the Royal Meteorological Society*,
3005 **97 (412)**, 168–180.

3006 Haut, T., and B. Wingate, 2014: An asymptotic parallel-in-time method for highly oscillatory
3007 pdes. *SIAM Journal on Scientific Computing*, **36 (2)**, A693–A713, doi:10.1137/130914577.

3008 Haywood, J., D. Roberts, A. Slingo, J. Edwards, and K. Shine, 1997: General circulation model
3009 calculations of the direct radiative forcing by anthropogenic sulfate and fossil-fuel soot aerosol.
3010 *Journal of climate*, **10 (7)**, 1562–1577.

3011 Heikes, R., and D. A. Randall, 1995: Numerical integration of the shallow-water equa-
3012 tions on a twisted icosahedral grid. part i: Basic design and results of tests. *Monthly*
3013 *Weather Review*, **123 (6)**, 1862–1880, doi:10.1175/1520-0493(1995)123<1862:NIOTSW>2.
3014 0.CO;2, URL [https://doi.org/10.1175/1520-0493\(1995\)123<1862:NIOTSW>2.0.CO;2](https://doi.org/10.1175/1520-0493(1995)123<1862:NIOTSW>2.0.CO;2), [https://doi.org/10.1175/1520-0493\(1995\)123<1862:NIOTSW>2.0.CO;2](https://doi.org/10.1175/1520-0493(1995)123<1862:NIOTSW>2.0.CO;2).

3016 Heikes, R. P., D. A. Randall, and C. S. Konor, 2013: Optimized icosahedral grids: Performance of
3017 finite-difference operators and multigrid solver. *Monthly Weather Review*, **141 (12)**, 4450–4469.

3018 Hibler, W. D., 1979: A dynamic thermodynamic sea ice model. *J. Phys. Oceanogr.*, **9**, 815–846.

3019 Hibler, W. D., 1980: Modeling a variable thickness ice cover. *Mon. Wea. Rev.*, **108**, 1943–1973.

3020 Hinkelmann, K., 1951: Der mechanismus des meteorologischen lärmes. *Tellus*, **3 (4)**, 285–296.

3021 Hoffman, F. M., W. J. Riley, J. T. Randerson, G. Keppel-Aleks, D. M. Lawrence, and C. D. Koven,
3022 2016: 2016 international land model benchmarking (ilamb) workshop report. Tech. rep., US-
3023 DOE Office of Science, Washington, DC (United States).

- 3024 Hoffman, F. M., and Coauthors, 2014: Causes and implications of persistent atmospheric car-
3025 bon dioxide biases in earth system models. *Journal of Geophysical Research: Biogeosciences*,
3026 **119** (2), 141–162.
- 3027 Hogan, R. J., T. Quaife, and R. Braghieri, 2018: Fast matrix treatment of 3-d radiative transfer in
3028 vegetation canopies: Spartacus-vegetation 1.1. *Geoscientific Model Development*, **11** (1), 339.
- 3029 Hogan, R. J., S. A. Schäfer, C. Klinger, J. C. Chiu, and B. Mayer, 2016: Representing 3-d cloud ra-
3030 diation effects in two-stream schemes: 2. matrix formulation and broadband evaluation. *Journal*
3031 *of Geophysical Research: Atmospheres*, **121** (14), 8583–8599.
- 3032 Holland, M. M., D. A. Bailey, B. P. Briegleb, B. Light, and E. Hunke, 2012: Improved sea ice
3033 shortwave radiation physics in ccsm4: The impact of melt ponds and aerosols on arctic sea ice.
3034 *Journal of Climate*, **25** (5), 1413–1430.
- 3035 Holland, M. M., C. M. Bitz, E. C. Hunke, W. H. Lipscomb, and J. L. Schramm, 2006: Influence
3036 of the Sea Ice Thickness Distribution on Polar Climate in CCSM3. *Journal of Climate*, **19** (11),
3037 2398–2414.
- 3038 Holland, W. R., 1978: The role of mesoscale eddies in the general circulation of the
3039 ocean—numerical experiments using a wind-driven quasi-geostrophic model. *Journal of Phys-*
3040 *ical Oceanography*, **8** (3), 363–392.
- 3041 Holloway, J. L., Jr., and S. Manabe, 1971: Simulation of climate by a global general circulation
3042 model: I. hydrologic cycle and heat balance. *Monthly Weather Review*, **99** (5), 335–370.
- 3043 Holtslag, A., and B. Boville, 1993: Local versus nonlocal boundary-layer diffusion in a global
3044 climate model. *Journal of Climate*, **6** (10), 1825–1842.

- 3045 Holtslag, A., E. De Bruijn, and H. Pan, 1990: A high resolution air mass transformation model for
3046 short-range weather forecasting. *Monthly Weather Review*, **118 (8)**, 1561–1575.
- 3047 Hoose, C., J. E. Kristjánsson, J.-P. Chen, and A. Hazra, 2010: A classical-theory-based param-
3048 eterization of heterogeneous ice nucleation by mineral dust, soot, and biological particles in a
3049 global climate model. *Journal of the Atmospheric Sciences*, **67 (8)**, 2483–2503.
- 3050 Hortal, M., and A. Simmons, 1991: Use of reduced gaussian grids in spectral models. *Monthly*
3051 *Weather Review*, **119 (4)**, 1057–1074.
- 3052 Horvat, C., and E. Tziperman, 2015: A prognostic model of the sea-ice floe size and thickness
3053 distribution. *The Cryosphere*, **9**, 2119–2134.
- 3054 Hoskins, B. J., M. E. McIntyre, and A. W. Robertson, 1985: On the use and significance of
3055 isentropic potential vorticity maps. *Quart. J. Roy. Meteor. Soc.*, **111**, 877–946.
- 3056 Hoskins, B. J., and A. J. Simmons, 1975: A multi-layer spectral model and the semi-implicit
3057 method. *Quart. J. Roy. Meteor. Soc.*, **101**, 637–655.
- 3058 Houze, R. A., Jr., 1977: Structure and dynamics of a tropical squall–line system. *Monthly Weather*
3059 *Review*, **105 (12)**, 1540–1567.
- 3060 Hsie, E.-Y., R. A. Anthes, and D. Keyser, 1984: Numerical simulation of frontogenesis in a moist
3061 atmosphere. *Journal of the Atmospheric Sciences*, **41 (17)**, 2581–2594.
- 3062 Hsu, Y.-J. G., and A. Arakawa, 1990: Numerical modeling of the atmosphere with an isentropic
3063 vertical coordinate. *Monthly Weather Review*, **118 (10)**, 1933–1959.
- 3064 Hunke, E. C., 1998: CICE: The Los Alamos sea ice model, documentation and software. Tech.
3065 Rep. LA-CC-98-16, Los Alamos National Laboratory, Los Alamos.

- 3066 Hunke, E. C., and J. K. Dukowicz, 1997: An elastic-viscous-plastic model for sea ice dynamics.
3067 *J. Phys. Oceanogr.*, **27**, 1849–1867.
- 3068 Huntzinger, D., and Coauthors, 2017: Uncertainty in the response of terrestrial carbon sink to en-
3069 vironmental drivers undermines carbon-climate feedback predictions. *Scientific Reports*, **7** (1),
3070 4765.
- 3071 Huntzinger, D. N., and Coauthors, 2012: North american carbon program (nacp) regional interim
3072 synthesis: Terrestrial biospheric model intercomparison. *Ecological Modelling*, **232**, 144–157.
- 3073 Hurrell, J. W., and Coauthors, 2013: The community earth system model: a framework for collab-
3074 orative research. *Bulletin of the American Meteorological Society*, **94** (9), 1339–1360.
- 3075 Hyman, J. M., and M. Shashkov, 1997: Natural discretizations for the divergence, gradient, and
3076 curl on logically rectangular grids. *Computers & Mathematics with Applications*, **33** (4), 81–
3077 104.
- 3078 IPCC, 1990: Climate Change: The IPCC Scientific Assessment. Cambridge University Press,
3079 Cambridge, UK, 365pp, 365pp.
- 3080 Izumi, Y., and J. S. Caughey, 1976: Minnesota 1973 atmospheric boundary layer experiment data
3081 report. Tech. rep., AIR FORCE CAMBRIDGE RESEARCH LABS HANSCOM AFB MASS.
- 3082 Janjić, Z. I., 1994: The step-mountain eta coordinate model: Further developments of the con-
3083 vection, viscous sublayer, and turbulence closure schemes. *Monthly Weather Review*, **122** (5),
3084 927–945.
- 3085 Jarraud, M., and A. J. Simmons, 1983: The spectral technique. *Seminar on Numerical Methods*
3086 *for Weather Prediction*, European Centre for Medium Range Weather Prediction, Vol. 2, 15–19.

- 3087 Jarvis, P., 1976: The interpretation of the variations in leaf water potential and stomatal conduc-
3088 tance found in canopies in the field. *Phil. Trans. R. Soc. Lond. B*, **273 (927)**, 593–610.
- 3089 Jarvis, P. G., and K. McNaughton, 1986: Stomatal control of transpiration: scaling up from leaf to
3090 region. *Advances in ecological research*, Vol. 15, Elsevier, 1–49.
- 3091 Johnson, D. R., 1989: The forcing and maintenance of global monsoonal circulations: An isen-
3092 tropic analysis. *Advances in Geophysics*, Vol. 31, Elsevier, 43–316.
- 3093 Johnson, D. R., 1997: “general coldness of climate models” and the second law: implications for
3094 modeling the earth system. *Journal of climate*, **10 (11)**, 2826–2846.
- 3095 Johnson, D. R., and L. W. Uccellini, 1983: A comparison of methods for computing the sigma-
3096 coordinate pressure gradient force for flow over sloped terrain in a hybrid theta-sigma model.
3097 *Monthly Weather Review*, **111 (4)**, 870–886.
- 3098 Johnson, R. H., 1976: The role of convective-scale precipitation downdrafts in cumulus and
3099 synoptic-scale interactions. *Journal of the Atmospheric Sciences*, **33 (10)**, 1890–1910.
- 3100 Johnston, H., 1971: Reduction of stratospheric ozone by nitrogen oxide catalysts from supersonic
3101 transport exhaust. *Science*, **173 (3996)**, 517–522.
- 3102 Jolly, W. M., R. Nemani, and S. W. Running, 2005: A generalized, bioclimatic index to predict
3103 foliar phenology in response to climate. *Global Change Biology*, **11 (4)**, 619–632.
- 3104 Joseph, J. H., W. J. Wiscombe, and J. A. Weinman, 1976: The Delta-Eddington Approximation
3105 for Radiative Flux Transfer. *J. Atmos. Sci.*, **33 (12)**, 2452–2459.
- 3106 Jung, J.-H., 2016: Simulation of orographic effects with a quasi-3-d multiscale modeling frame-
3107 work: Basic algorithm and preliminary results. *Journal of Advances in Modeling Earth Systems*,
3108 **8 (4)**, 1657–1673.

3109 Jung, J.-H., and A. Arakawa, 2014: Modeling the moist-convective atmosphere with a quasi-3-d
3110 multiscale modeling framework (q3d mmf). *Journal of Advances in Modeling Earth Systems*,
3111 **6 (1)**, 185–205.

3112 Kalnay, E., and Coauthors, 1996: The ncep/ncar 40-year reanalysis project. *Bulletin of the Ameri-*
3113 *can meteorological Society*, **77 (3)**, 437–471.

3114 Kanamitsu, M., and Coauthors, 2002: Ncep dynamical seasonal forecast system 2000. *Bulletin of*
3115 *the American Meteorological Society*, **83 (7)**, 1019–1037.

3116 Kasahara, A., 1974: Various vertical coordinate systems used for numerical weather prediction.
3117 *Monthly Weather Review*, **102 (7)**, 509–522.

3118 Kasahara, A., and W. M. Washington, 1967: Ncar global general circulation model of the at-
3119 mosphere. *Monthly Weather Review*, **95 (7)**, 389–402, doi:10.1175/1520-0493(1967)095<0389:
3120 NGGCMO>2.3.CO;2, URL [http://dx.doi.org/10.1175/1520-0493\(1967\)095<0389:NGGCMO>](http://dx.doi.org/10.1175/1520-0493(1967)095<0389:NGGCMO>2.3.CO;2)
3121 [2.3.CO;2](http://dx.doi.org/10.1175/1520-0493(1967)095<0389:NGGCMO>2.3.CO;2).

3122 Kasahara, A., and W. M. Washington, 1969: Thermal and dynamical effects of orography on the
3123 general circulation of the atmosphere. *Proc. WMO/IUGG Symp. Numer. Wea. Pred.*

3124 Kasahara, A., and W. M. Washington, 1971: General circulation experiments with a six-layer near
3125 model, including orography, cloudiness and surface temperature calculations. *Journal of the*
3126 *Atmospheric Sciences*, **28 (5)**, 657–701.

3127 Katayama, A., 1967: On the radiation budget of the troposphere over the northern hemisphere (ii).
3128 *Journal of the Meteorological Society of Japan. Ser. II*, **45 (1)**, 1–25.

3129 Katayama, A., 1972: A simplified scheme for computing radiation transfer in the troposphere.,
3130 numerical simulation of weather and climate. *Tech. Rep. No. 6, Dept. Met., UCLA*, **77**.

3131 Kathuroju, N., M. A. White, J. Symanzik, M. D. Schwartz, J. A. Powell, and R. R. Nemani, 2007:
3132 On the use of the advanced very high resolution radiometer for development of prognostic land
3133 surface phenology models. *ecological modelling*, **201 (2)**, 144–156.

3134 Keller, M., M. A. Silva-Dias, D. C. Nepstad, and M. O. Silva-Andrae, 2004: The large-scale
3135 biosphere-atmosphere experiment in amazonia: Analyzing regional land use change effects.
3136 *Ecosystems and Land Use Change*, 321–334.

3137 Kessler, E., 1969: On the distribution and continuity of water substance in atmospheric cir-
3138 culations. *On the distribution and continuity of water substance in atmospheric circulations*,
3139 Springer, 1–84.

3140 Kessler, E., 1995: On the continuity and distribution of water substance in atmospheric circula-
3141 tions. *Atmospheric research*, **38 (1-4)**, 109–145.

3142 Khain, A., D. Rosenfeld, and A. Pokrovsky, 2005: Aerosol impact on the dynamics and mi-
3143 crophysics of deep convective clouds. *Quarterly Journal of the Royal Meteorological Soci-
3144 ety: A journal of the atmospheric sciences, applied meteorology and physical oceanography*,
3145 **131 (611)**, 2639–2663.

3146 Khairoutdinov, M., and Y. Kogan, 2000: A new cloud physics parameterization in a large-eddy
3147 simulation model of marine stratocumulus. *Monthly weather review*, **128 (1)**, 229–243.

3148 Khairoutdinov, M. F., and D. A. Randall, 2001: A cloud resolving model as a cloud parameteriza-
3149 tion in the near community climate system model: Preliminary results. *Geophysical Research
3150 Letters*, **28 (18)**, 3617–3620.

3151 Khairoutdinov, M. F., and D. a. Randall, 2003: Cloud Resolving Modeling of the ARM Summer
3152 1997 IOP: Model Formulation, Results, Uncertainties, and Sensitivities. *J. Atmos. Sci.*, **60** (4),
3153 607–625.

3154 Kiehl, J., and B. Briegleb, 1993: The relative roles of sulfate aerosols and greenhouse gases in
3155 climate forcing. *Science*, **260** (5106), 311–314.

3156 Kiehl, J., J. Hack, G. Bonan, B. Boville, D. Williamson, and P. Rasch, 1998: The national center
3157 for atmospheric research community climate model: Ccm3. *Journal of Climate*, **11** (6), 1131–
3158 1149.

3159 Killworth, P. D., D. J. Webb, D. Stainforth, and S. M. Paterson, 1991: The development of a free-
3160 surface Bryan–Cox–Semtner ocean model. *Journal of Physical Oceanography*, **21** (9), 1333–
3161 1348.

3162 Kirtman, B., and A. Pirani, 2009: The state of the art of seasonal prediction: Outcomes and rec-
3163 ommendations from the first world climate research program workshop on seasonal prediction.
3164 *Bulletin of the American Meteorological Society*, **90** (4), 455–458.

3165 Klemp, J. B., and R. B. Wilhelmson, 1978: The simulation of three-dimensional convective storm
3166 dynamics. *Journal of the Atmospheric Sciences*, **35** (6), 1070–1096.

3167 Koenig, L. R., and F. W. Murray, 1976: Ice-bearing cumulus cloud evolution: Numerical sim-
3168 ulation and general comparison against observations. *Journal of Applied Meteorology*, **15** (7),
3169 747–762.

3170 Konor, C. S., and A. Arakawa, 1997: Design of an atmospheric model based on a generalized
3171 vertical coordinate. *Monthly weather review*, **125** (7), 1649–1673.

- 3172 Korn, P., 2017: Formulation of an unstructured grid model for global ocean dynamics. *Journal of*
3173 *Computational Physics*, **339**, 525–552.
- 3174 Koster, R. D., and M. J. Suarez, 1992: Modeling the land surface boundary in climate models as
3175 a composite of independent vegetation stands. *Journal of Geophysical Research: Atmospheres*,
3176 **97 (D3)**, 2697–2715.
- 3177 Krinner, G., and Coauthors, 2005: A dynamic global vegetation model for studies of the coupled
3178 atmosphere-biosphere system. *Global Biogeochemical Cycles*, **19 (1)**.
- 3179 Krueger, S. K., 1988: Numerical simulation of tropical cumulus clouds and their interaction with
3180 the subcloud layer. *Journal of the atmospheric sciences*, **45 (16)**, 2221–2250.
- 3181 Kuo, H.-L., 1965: On formation and intensification of tropical cyclones through latent heat release
3182 by cumulus convection. *Journal of the Atmospheric Sciences*, **22 (1)**, 40–63.
- 3183 Kuo, H.-L., 1974: Further studies of the parameterization of the influence of cumulus convection
3184 on large-scale flow. *Journal of the Atmospheric Sciences*, **31 (5)**, 1232–1240.
- 3185 Kurihara, Y., 1965: Numerical integration of the primitive equations on a spherical grid. *Monthly*
3186 *Weather Review*, **93 (7)**, 399–415, doi:10.1175/1520-0493(1965)093<0399:NIOTPE>2.3.CO;2,
3187 URL [https://doi.org/10.1175/1520-0493\(1965\)093<0399:NIOTPE>2.3.CO;2](https://doi.org/10.1175/1520-0493(1965)093<0399:NIOTPE>2.3.CO;2), [https://doi.org/10.](https://doi.org/10.1175/1520-0493(1965)093<0399:NIOTPE>2.3.CO;2)
3188 [1175/1520-0493\(1965\)093<0399:NIOTPE>2.3.CO;2](https://doi.org/10.1175/1520-0493(1965)093<0399:NIOTPE>2.3.CO;2).
- 3189 Kurihara, Y., 1968: Note on finite difference expressions for the hydrostatic relation and pressure
3190 gradient force. *Mon. Wea. Rev.*, **96**, 654–656.
- 3191 Kwizak, M., and A. J. Robert, 1971: A semi-implicit scheme for grid point atmospheric models of
3192 the primitive equations. *Monthly Weather Review*, **99 (1)**, 32–36, doi:10.1175/1520-0493(1971)

3193 099<0032:ASSFGP>2.3.CO;2, URL [https://doi.org/10.1175/1520-0493\(1971\)099<0032:](https://doi.org/10.1175/1520-0493(1971)099<0032:)
3194 [ASSFGP>2.3.CO;2](https://doi.org/10.1175/1520-0493(1971)099<0032:ASSFGP>2.3.CO;2), [https://doi.org/10.1175/1520-0493\(1971\)099<0032:ASSFGP>2.3.CO;2](https://doi.org/10.1175/1520-0493(1971)099<0032:ASSFGP>2.3.CO;2).

3195 Lacis, A. A., and J. Hansen, 1974: A Parameterization for the Absorption of Solar Radiation in
3196 the Earth's Atmosphere. *J. Atmos. Sci.*, **31 (1)**, 118–133.

3197 Lacis, A. A., and V. Oinas, 1991: A description of the correlated *k*-distribution method for mod-
3198 eling non-grey gaseous absorption, thermal emission, and multiple scattering in vertically inho-
3199 mogeneous atmospheres. *J. Geophys. Res.*, **96 (D5)**, 9027–9063.

3200 Laloyaux, P., and Coauthors, 2018: Cera-20c: A coupled reanalysis of the twentieth century.
3201 *Journal of Advances in Modeling Earth Systems*.

3202 Langlois, W., and H. Kwok, 1969: *Description of the Mintz-Arakawa numerical general circula-*
3203 *tion model*. Department of Meteorology, University of California.

3204 Lappen, C.-L., and D. A. Randall, 2001: Toward a unified parameterization of the boundary layer
3205 and moist convection. part i: A new type of mass-flux model. *Journal of the atmospheric sci-*
3206 *ences*, **58 (15)**, 2021–2036.

3207 Large, W. G., J. C. McWilliams, and S. C. Doney, 1994: Oceanic vertical mixing: A review
3208 and a model with a nonlocal boundary layer parameterization. *Reviews of Geophysics*, **32 (4)**,
3209 363–403.

3210 Larson, V. E., R. Wood, P. R. Field, J.-C. Golaz, T. H. Vonder Haar, and W. R. Cotton, 2001:
3211 Systematic biases in the microphysics and thermodynamics of numerical models that ignore
3212 subgrid-scale variability. *Journal of the atmospheric sciences*, **58 (9)**, 1117–1128.

3213 Lau, N.-C., 1985: Modeling the seasonal dependence of the atmospheric response to observed el
3214 ninos in 1962–76. *Monthly Weather Review*, **113 (11)**, 1970–1996.

- 3215 Lauritzen, P. H., and R. D. Nair, 2008: Monotone and conservative cascade remapping between
3216 spherical grids (cars): Regular latitude–longitude and cubed-sphere grids. *Monthly Weather*
3217 *Review*, **136 (4)**, 1416–1432.
- 3218 Laval, K., and R. Sadourny, 1979: Expériences de simulation de la circulation générale de
3219 l’atmosphère avec le modèle du lmd. *Evolution of Planetary Atmospheres and Climatology of*
3220 *the Earth*, 493.
- 3221 Laval, K., R. Sadourny, and Y. Serafini, 1981a: Land surface processes in a simplified gen-
3222 eral circulation model. *Geophysical & Astrophysical Fluid Dynamics*, **17 (1)**, 129–150, doi:
3223 10.1080/03091928108243677, URL <https://doi.org/10.1080/03091928108243677>, <https://doi.org/10.1080/03091928108243677>.
- 3224
- 3225 Laval, K., H. L. Treut, and R. Sadourny, 1981b: Effect of cumulus parameterization on
3226 the dynamics of a general circulation model. *Geophysical & Astrophysical Fluid Dy-*
3227 *namics*, **17 (1)**, 113–127, doi:10.1080/03091928108243676, URL [https://doi.org/10.1080/](https://doi.org/10.1080/03091928108243676)
3228 [03091928108243676](https://doi.org/10.1080/03091928108243676), <https://doi.org/10.1080/03091928108243676>.
- 3229 Lawrence, D. M., and J. M. Slingo, 2004: An annual cycle of vegetation in a gcm. part i: imple-
3230 mentation and impact on evaporation. *Climate Dynamics*, **22 (2-3)**, 87–105.
- 3231 Le Quéré, C., and Coauthors, 2009: Trends in the sources and sinks of carbon dioxide. *Nature*
3232 *geoscience*, **2 (12)**, 831.
- 3233 Lean, J., and P. Rowntree, 1993: A gcm simulation of the impact of amazonian deforestation on
3234 climate using an improved canopy representation. *Quarterly Journal of the Royal Meteorologi-*
3235 *cal Society*, **119 (511)**, 509–530.

- 3236 LeBauer, D. S., and K. K. Treseder, 2008: Nitrogen limitation of net primary productivity in
3237 terrestrial ecosystems is globally distributed. *Ecology*, **89** (2), 371–379.
- 3238 Lee, W.-L., and K. Liou, 2007: A coupled atmosphere–ocean radiative transfer system using the
3239 analytic four-stream approximation. *Journal of the Atmospheric Sciences*, **64** (10), 3681–3694.
- 3240 Legg, S., R. W. Hallberg, and J. B. Girton, 2006: Comparison of entrainment in overflows simu-
3241 lated by z-coordinate, isopycnal and non-hydrostatic models. *Ocean Modelling*, **11** (1-2), 69–97.
- 3242 Legg, S., and Coauthors, 2009: Improving oceanic overflow representation in climate models:
3243 the gravity current entrainment climate process team. *Bulletin of the American Meteorological*
3244 *Society*, **90** (5), 657–670.
- 3245 Leith, C., 1965a: Numerical simulation of the earth’s atmosphere. *Methods of Computational*
3246 *Physics*, **4**, 1–28.
- 3247 Leith, C., 1988: The computational physics of the global atmosphere. *Energy in Physics, War and*
3248 *Peace*, Springer, 161–173.
- 3249 Leith, C. E., 1965b: Convection in a six-level model atmosphere. Tech. rep., Lawrence Radiation
3250 Lab., Univ. of California, Livermore.
- 3251 Lemarié, F., J. Kurian, A. F. Shchepetkin, M. J. Molemaker, F. Colas, and J. C. McWilliams,
3252 2012: Are there inescapable issues prohibiting the use of terrain-following coordinates in cli-
3253 mate models? *Ocean Modelling*, **42**, 57–79.
- 3254 Lettau, H., 1954: Improved models of thermal diffusion in the soil. *Eos, Transactions American*
3255 *Geophysical Union*, **35** (1), 121–132.

- 3256 Leutwyler, D., O. Fuhrer, X. Lapillonne, D. Lüthi, and C. Schär, 2016: Towards european-scale
3257 convection-resolving climate simulations with gpus: a study with cosmo 4.19. *Geoscientific*
3258 *Model Development*, **9** (9), 3393–3412.
- 3259 Lewellen, W., and S. Yoh, 1993: Binormal model of ensemble partial cloudiness. *Journal of the*
3260 *atmospheric sciences*, **50** (9), 1228–1237.
- 3261 Lewis, J. M., 1998: Clarifying the dynamics of the general circulation: Phillips’s 1956 experiment.
3262 *Bulletin of the American Meteorological Society*, **79** (1), 39–60.
- 3263 Lewis, J. M., 2005: Roots of ensemble forecasting. *Monthly weather review*, **133** (7), 1865–1885.
- 3264 Lewis, J. M., 2008: Smagorinsky’s gfdl: Building the team. *Bulletin of the American Meteorolog-*
3265 *ical Society*, **89** (9), 1339–1353.
- 3266 Lilly, D. K., 1962: On the numerical simulation of buoyant convection. *Tellus*, **14** (2), 148–172.
- 3267 Lilly, D. K., 1968: Models of cloud-topped mixed layers under a strong inversion. *Quarterly*
3268 *Journal of the Royal Meteorological Society*, **94** (401), 292–309.
- 3269 Lilly, D. K., 1997: Introduction to “computational design for long-term numerical integration
3270 of the equations of fluid motion: Two-dimensional incompressible flow. part i”. *Journal of*
3271 *Computational Physics*, **135** (2), 101–102.
- 3272 Lin, C., R. Laprise, and H. Ritchie, Eds., 1997: *Numerical methods in atmosphere and ocean*
3273 *modelling. The Andre Robert memorial volume*. Canadian Meteorological and Oceanographic
3274 Society, Ottawa, Canada, 581 pp.
- 3275 Lin, S.-J., 2004: A “vertically lagrangian” finite-volume dynamical core for global models.
3276 *Monthly Weather Review*, **132** (10), 2293–2307.

- 3277 Lin, Y.-L., R. D. Farley, and H. D. Orville, 1983: Bulk parameterization of the snow field in a
3278 cloud model. *Journal of Climate and Applied Meteorology*, **22 (6)**, 1065–1092.
- 3279 Lindzen, R. S., 1981: Turbulence and stress owing to gravity wave and tidal breakdown. *Journal*
3280 *of Geophysical Research: Oceans*, **86 (C10)**, 9707–9714.
- 3281 Liu, X., and Coauthors, 2011: Toward a minimal representation of aerosol direct and indirect
3282 effects: Model description and evaluation. *Geoscientific Model Development Discussions*, **4**,
3283 3485–3598.
- 3284 Lohmann, U., J. Feichter, C. C. Chuang, and J. E. Penner, 1999: Prediction of the number of
3285 cloud droplets in the echam gcm. *Journal of Geophysical Research: Atmospheres*, **104 (D8)**,
3286 9169–9198.
- 3287 Lohmann, U., and C. Hoose, 2009: Sensitivity studies of different aerosol indirect effects in mixed-
3288 phase clouds. *Atmospheric Chemistry and Physics*, **9 (22)**, 8917–8934.
- 3289 Lohmann, U., and E. Roeckner, 1996: Design and performance of a new cloud microphysics
3290 scheme developed for the ECHAM general circulation model. *Climate Dynamics*, **12 (8)**, 557–
3291 572.
- 3292 Lohmann, U., P. Stier, C. Hoose, S. Ferrachat, S. Kloster, E. Roeckner, and J. Zhang, 2007: Cloud
3293 microphysics and aerosol indirect effects in the global climate model echam5-ham. *Atmospheric*
3294 *Chemistry and Physics*, **7 (13)**, 3425–3446.
- 3295 Lorenz, E. N., 1955: Available potential energy and the maintenance of the general circulation.
3296 *Tellus*, **7 (2)**, 157–167.
- 3297 Lorenz, E. N., 1960: Energy and numerical weather prediction. *Tellus*, **12 (4)**, 364–373.

- 3298 Lorenz, E. N., 1963: Deterministic nonperiodic flow. *Journal of the Atmospheric Sciences*, **20** (2),
3299 130–141.
- 3300 Los, S., and Coauthors, 2000: A global 9-yr biophysical land surface dataset from noaa avhrr data.
3301 *Journal of Hydrometeorology*, **1** (2), 183–199.
- 3302 Louis, J.-F., 1979: A parametric model of vertical eddy fluxes in the atmosphere. *Boundary-Layer*
3303 *Meteorology*, **17** (2), 187–202.
- 3304 Lucht, W., S. Schaphoff, T. Erbrecht, U. Heyder, and W. Cramer, 2006: Terrestrial vegetation
3305 redistribution and carbon balance under climate change. *Carbon Balance and Management*,
3306 **1** (1), 6.
- 3307 Luo, W.-g., S. Wang, J. Huang, L. Yan, and J. Huang, 2006: Influence of plant photosynthesis and
3308 transpiration character on nitrogen removal effect in wetland. *China Environmental Science*,
3309 **26** (1), 30–33.
- 3310 Luo, Y., and Coauthors, 2012: A framework for benchmarking land models.
- 3311 Lynch, P., 2006: *The emergence of numerical weather prediction: Richardson’s dream*. Cambridge
3312 University Press.
- 3313 Lynch, P., and O. Lynch, 2008: Forecasts by phoniatic. *Weather*, **63** (11), 324–326.
- 3314 Lynch, P., and Coauthors, 1993: Richardson’s forecast factory: The \$64 000 question. *Meteoro-*
3315 *logical Magazine*, **122**, 69–69.
- 3316 MacKinnon, J., L. St Laurent, and A. C. N. Garabato, 2013: Diapycnal mixing processes in the
3317 ocean interior. *International Geophysics*, Vol. 103, Elsevier, 159–183.

- 3318 Madden, R. A., and P. R. Julian, 1971: Detection of a 40-50 day oscillation in the zonal wind in
3319 the tropical Pacific. *J. Atmos. Sci.*, **28**, 702–708.
- 3320 Madden, R. A., and P. R. Julian, 1972: Description of global-scale circulation cells in the tropics
3321 with a 40–50 day period. *J. Atmos. Sci.*, **29**, 1109–1123.
- 3322 Madec, G., P. Delecluse, M. Imbard, and C. Levy, 1997: Ocean general circulation model refer-
3323 ence manual. *LODYC, Paris*, **91**.
- 3324 Majewski, D., and Coauthors, 2002: The operational global icosahedral–hexagonal gridpoint
3325 model gme: description and high-resolution tests. *Monthly Weather Review*, **130** (2), 319–338.
- 3326 Malkus, J. S., 1952: Recent advances in the study of convective clouds and their interaction with
3327 the environment. *Tellus*, **4** (2), 71–87.
- 3328 Malkus, J. S., and G. Witt, 1959: The evolution of a convective element: A numerical calculation.
3329 *The atmosphere and sea in motion*, 425–439.
- 3330 Manabe, S., 1969a: Climate and the ocean circulation i. the atmospheric circulation and the hy-
3331 drology of the earth’s surface. *Mon. Wea. Rev.*, **97**, 739–774.
- 3332 Manabe, S., 1969b: Climate and the ocean circulation ii. the atmospheric circulation and the effect
3333 of heat transport by ocean currents. *Mon. Wea. Rev.*, **97**, 775–805.
- 3334 Manabe, S., and K. Bryan, 1969: Climate calculations with a combined ocean-atmosphere model.
3335 *Journal of the Atmospheric Sciences*, **26** (4), 786–789.
- 3336 Manabe, S., and B. G. Hunt, 1968: Experiments with a stratospheric general circulation model.
3337 *Monthly Weather Review*, **96** (8).

- 3338 Manabe, S., and J. Mahlman, 1976: Simulation of seasonal and interhemispheric variations in the
3339 stratospheric circulation. *Journal of the Atmospheric Sciences*, **33** (11), 2185–2217.
- 3340 Manabe, S., and F. Möller, 1961a: On the radiative equilibrium and heat balance of the atmo-
3341 sphere. *Monthly Weather Review*, **89** (12), 503–532, doi:10.1175/1520-0493(1961)089<0503:
3342 OTREAH>2.0.CO;2, URL [https://doi.org/10.1175/1520-0493\(1961\)089<0503:OTREAH>2.0.](https://doi.org/10.1175/1520-0493(1961)089<0503:OTREAH>2.0.CO;2)
3343 [CO;2, https://doi.org/10.1175/1520-0493\(1961\)089<0503:OTREAH>2.0.CO;2.](https://doi.org/10.1175/1520-0493(1961)089<0503:OTREAH>2.0.CO;2)
- 3344 Manabe, S., and F. Möller, 1961b: On the Radiative Equilibrium and Heat Balance of the Atmo-
3345 sphere. *Mon. Wea. Rev.*, **89** (12), 503–532.
- 3346 Manabe, S., and J. Smagorinsky, 1967: Simulated climatology of a general circulation model
3347 with a hydrologic cycle ii. analysis of the tropical atmosphere. *Monthly Weather Review*, **95** (4),
3348 155–169.
- 3349 Manabe, S., J. Smagorinsky, and R. F. Strickler, 1965: Simulated climatology of a general circu-
3350 lation model with a hydrologic cycle. *Mon. Wea. Rev.*, **93** (12), 769–798.
- 3351 Manabe, S., and R. J. Stouffer, 1980: Sensitivity of a global climate model to an increase of CO₂
3352 concentration in the atmosphere. *J. Geophys. Res.*, **85**, 5529–5554.
- 3353 Manabe, S., and R. F. Strickler, 1964a: Thermal equilibrium of the atmosphere with a convective
3354 adjustment. *Journal of the Atmospheric Sciences*, **21** (4), 361–385.
- 3355 Manabe, S., and R. F. Strickler, 1964b: Thermal Equilibrium of the Atmosphere with a Convective
3356 Adjustment. *J. Atmos. Sci.*, **21** (4), 361–385.
- 3357 Manabe, S., and R. Wetherald, 1975: The effects of doubling the CO₂ concentration on the climate
3358 of a general circulation model. *J. Atmos. Sci.*, **32**, 3–15.

- 3359 Manabe, S., and R. Wetherald, 1980: On the distribution of climate change resulting from an
3360 increase of CO₂ content in the atmosphere. *J. Atmos. Sci.*, **37**, 99–118.
- 3361 Manabe, S., and R. T. Wetherald, 1967: Thermal Equilibrium of the Atmosphere with a Given
3362 Distribution of Relative Humidity. *J. Atmos. Sci.*, **24** (3), 241–259.
- 3363 Manton, M. J., and W. R. Cotton, 1977: Formulation of approximate equations for modeling moist
3364 deep convection on the mesoscale. *Atmospheric science paper; no. 266*.
- 3365 Marchand, R., and T. Ackerman, 2011: A cloud-resolving model with an adaptive vertical grid for
3366 boundary layer clouds. *Journal of the Atmospheric Sciences*, **68** (5), 1058–1074.
- 3367 Marshall, J., A. Adcroft, J.-M. Campin, C. Hill, and A. White, 2004: Atmosphere–ocean modeling
3368 exploiting fluid isomorphisms. *Monthly Weather Review*, **132** (12), 2882–2894.
- 3369 Marsland, S., J. Church, N. Bindoff, and G. Williams, 2007: Antarctic coastal polynya response
3370 to climate change. *Journal of Geophysical Research: Oceans*, **112** (C7).
- 3371 Marsland, S. J., H. Haak, J. H. Jungclaus, M. Latif, and F. Röske, 2003: The max-planck-institute
3372 global ocean/sea ice model with orthogonal curvilinear coordinates. *Ocean modelling*, **5** (2),
3373 91–127.
- 3374 Masuda, Y., and H. Ohnishi, 1986: An integration scheme of the primitive equation model with an
3375 icosahedral-hexagonal grid system and its application to the shallow water equations. *Journal*
3376 *of the Meteorological Society of Japan. Ser. II*, **64**, 317–326.
- 3377 Matsuno, T., 2016: Prologue: Tropical meteorology 1960–2010—personal recollections. *Meteo-*
3378 *rological Monographs*, **56**, vii–xv.
- 3379 Maykut, G. A., and N. Untersteiner, 1971: Some results from a time-dependent thermodynamic
3380 model of sea ice. *J. Geophys. Res.*, **76**, 1550–1575.

- 3381 McCartney, S., 1999: *ENIAC: The triumphs and tragedies of the world's first computer*. Walker &
3382 Company.
- 3383 McDonald, A., and J. Bates, 1987: Improving the estimate of the departure point position in a
3384 two-time level semi-lagrangian and semi-implicit scheme. *Monthly Weather Review*, **115** (3),
3385 737–739.
- 3386 McDougall, T. J., 1987: Neutral surfaces. *Journal of Physical Oceanography*, **17** (11), 1950–1964.
- 3387 McDougall, T. J., S. Groeskamp, and S. M. Griffies, 2014: On geometrical aspects of interior
3388 ocean mixing. *Journal of Physical Oceanography*, **44** (8), 2164–2175.
- 3389 McFarlane, N., 1987: The effect of orographically excited gravity wave drag on the general circu-
3390 lation of the lower stratosphere and troposphere. *Journal of the atmospheric sciences*, **44** (14),
3391 1775–1800.
- 3392 McGregor, J. L., and M. R. Dix, 2008: An updated description of the conformal-cubic atmospheric
3393 model. *High resolution numerical modelling of the atmosphere and ocean*, Springer, 51–75.
- 3394 McWilliams, J. C., 2016: Submesoscale currents in the ocean. *Proc. R. Soc. A*, **472** (2189),
3395 20160117.
- 3396 Meador, W. E., and W. R. Weaver, 1980: Two-Stream Approximations to Radiative Transfer in
3397 Planetary Atmospheres: A Unified Description of Existing Methods and a New Improvement.
3398 *J. Atmos. Sci.*, **37** (3), 630–643.
- 3399 Meehl, G. A., G. J. Boer, C. Covey, M. Latif, and R. J. Stouffer, 2000: The coupled model inter-
3400 comparison project (cmip). *Bulletin of the American Meteorological Society*, **81** (2), 313–318.

3401 Meehl, G. A., W. M. Washington, T. Wigley, J. M. Arblaster, and A. Dai, 2003: Solar and green-
3402 house gas forcing and climate response in the twentieth century. *Journal of Climate*, **16 (3)**,
3403 426–444.

3404 Mellor, G. L., 1977: The gaussian cloud model relations. *Journal of the Atmospheric Sciences*,
3405 **34 (2)**, 356–358.

3406 Mellor, G. L., and T. Yamada, 1974: A hierarchy of turbulence closure models for planetary
3407 boundary layers. *Journal of the Atmospheric Sciences*, **31 (7)**, 1791–1806.

3408 Mesinger, F., 1982: On the convergence and error problems of the calculation of the pressure
3409 gradient force in sigma coordinate models. *Geophysical & Astrophysical Fluid Dynamics*,
3410 **19 (1-2)**, 105–117.

3411 Mesinger, F., and Z. I. Janjić, 1985: Problems and numerical methods of the incorporation of
3412 mountains in atmospheric models. *Lectures in Applied Mathematics*, **22**, 81–120.

3413 Michael, G. A., 1996: URL <http://www.computer-history.info/Page1.dir/pages/Leith.html>.

3414 Mie, G., 1908: Beiträge zur Optik trüber Medien, speziell kolloidaler Metallösungen. *Ann. Phys.*,
3415 **330 (3)**, 377–445.

3416 Milbrandt, J. A., S. Bélair, M. Faucher, M. Vallée, M. L. Carrera, and A. Glazer, 2016: The pan-
3417 canadian high resolution (2.5 km) deterministic prediction system. *Weather and Forecasting*,
3418 **31 (6)**, 1791–1816.

3419 Milly, P., and K. Dunne, 1994: Sensitivity of the global water cycle to the water-holding capacity
3420 of land. *Journal of Climate*, **7 (4)**, 506–526.

3421 Ming, Y., V. Ramaswamy, L. J. Donner, V. T. Phillips, S. A. Klein, P. A. Ginoux, and L. W.
3422 Horowitz, 2007: Modeling the interactions between aerosols and liquid water clouds with a self-

3423 consistent cloud scheme in a general circulation model. *Journal of the atmospheric sciences*,
3424 **64 (4)**, 1189–1209.

3425 Mintz, Y., 1968: Very long-term global integration of the primitive equations of atmospheric mo-
3426 tion: An experiment in climate simulation. *Causes of Climatic Change*, Springer, 20–36.

3427 Mintz, Y., and J. Bjerknes, 1951: *Progress Report: Investigation of the General Circulation of the*
3428 *Atmosphere*. University of California, Los Angeles.

3429 Mitchell, J., R. Davis, W. a. Ingram, and C. Senior, 1995a: On surface temperature, greenhouse
3430 gases, and aerosols: Models and observations. *Journal of Climate*, **8 (10)**, 2364–2386.

3431 Mitchell, J. F., T. Johns, J. M. Gregory, and S. Tett, 1995b: Climate response to increasing levels
3432 of greenhouse gases and sulphate aerosols. *Nature*, **376 (6540)**, 501.

3433 Miyakoda, K., and J. Sirutis, 1977: Comparative integrations of global models with various
3434 parameterized processes of subgrid-scale vertical transports- description of the parameteriza-
3435 tions(atmospheric circulation). *Beitraege zur Physik der Atmosphaere*, **50 (4)**, 445–487.

3436 Miyakoda, K., J. Smagorinsky, R. F. Strickler, and G. Hembree, 1969: Experimental extended
3437 predictions with a nine-level hemispheric model. *Mon. Wea. Rev.*, **97**, 1–76.

3438 Mlawer, E. J., M. J. Iacono, R. Pincus, H. W. Barker, L. Oreopoulos, and D. L. Mitchell, 2016:
3439 Contributions of the ARM Program to Radiative Transfer Modeling for Climate and Weather
3440 Applications. *Meteorol. Monogr.*, **57**, 15.1–15.19.

3441 Mlawer, E. J., S. J. Taubman, P. D. Brown, M. J. Iacono, and S. A. Clough, 1997: Radiative transfer
3442 for inhomogeneous atmospheres: RRTM, a validated correlated-k model for the longwave. *J.*
3443 *Geophys. Res.*, **102 (D14)**, 16 663–16 682.

- 3444 Moeng, C.-H., 1984: A large-eddy-simulation model for the study of planetary boundary-layer
3445 turbulence. *Journal of the Atmospheric Sciences*, **41 (13)**, 2052–2062.
- 3446 Monin, A. S., and A. M. Obukhov, 1954: Osnovnye zakonomernosti turbulentnogo peremesivaniya
3447 v prizemnom sloe atmosfery. *Trudy geofiz. inst. AN SSSR*, **24**, 163–187.
- 3448 Monteith, J., 1965: Evaporation and the environment, the state and movement of water in living
3449 organisms. xixth symposium. Cambridge University Press, Swansea.
- 3450 Morcrette, J.-J., 1990: Impact of changes to the radiation transfer parameterizations plus cloud
3451 optical properties in the ECMWF model. *Mon. Wea. Rev.*, **118 (4)**, 847–873.
- 3452 Morcrette, J.-J., 1991: Radiation and cloud radiative properties in the European Centre for Medium
3453 Range Weather Forecasts forecasting system. *J. Geophys. Res.*, **96 (D5)**, 9121–9132.
- 3454 Morrisette, P. M., 1989: The evolution of policy responses to stratospheric ozone depletion. *Natu-
3455 ral Resources Journal*, 793–820.
- 3456 Morrison, H., and A. Gettelman, 2008: A new two-moment bulk stratiform cloud microphysics
3457 scheme in the Community Atmosphere Model, version 3 (CAM3). part I: Description and nu-
3458 merical tests. *J. Climate*, **21 (15)**, 3642–3659.
- 3459 Morrison, H., and J. A. Milbrandt, 2015: Parameterization of cloud microphysics based on the
3460 prediction of bulk ice particle properties. part i: Scheme description and idealized tests. *Journal
3461 of the Atmospheric Sciences*, **72 (1)**, 287–311.
- 3462 Munk, W. H., 1966: Abyssal recipes. *Deep Sea Research and Oceanographic Abstracts*, Elsevier,
3463 Vol. 13, 707–730.

- 3464 Murphy, J., 1995: Transient response of the hadley centre coupled ocean-atmosphere model to
3465 increasing carbon dioxide. part 1: control climate and flux adjustment. *Journal of Climate*,
3466 **8 (1)**, 36–56.
- 3467 Murray, R. J., 1996: Explicit generation of orthogonal grids for ocean models. *Journal of Compu-*
3468 *tational Physics*, **126 (2)**, 251–273.
- 3469 Nastrom, G., K. Gage, and W. Jasperson, 1984: Kinetic energy spectrum of large-and mesoscale
3470 atmospheric processes. *Nature*, **310 (5972)**, 36.
- 3471 National Research Council Climatic Impact Committee, 1975: *Environmental impact of strato-*
3472 *spheric flight: Biological and climatic effects of aircraft emissions in the stratosphere*. National
3473 Academies.
- 3474 Neu, J. L., M. J. Prather, and J. E. Penner, 2007: Global atmospheric chemistry: Integrating over
3475 fractional cloud cover. *J. Geophys. Res.*, **112 (D11)**, D11 306.
- 3476 Noilhan, J., and S. Planton, 1989: A simple parameterization of land surface processes for meteo-
3477 rological models. *Monthly weather review*, **117 (3)**, 536–549.
- 3478 Norby, R. J., and Coauthors, 2005: Forest response to elevated co2 is conserved across a broad
3479 range of productivity. *Proceedings of the National Academy of Sciences of the United States of*
3480 *America*, **102 (50)**, 18 052–18 056.
- 3481 Nordeng, T. E., 1994: Extended versions of the convective parametrization scheme at ecmwf and
3482 their impact on the mean and transient activity of the model in the tropics. *Research Department*
3483 *Technical Memorandum*, **206**, 1–41.
- 3484 Notz, D., and C. M. Bitz, 2017: Sea ice in earth system models. *Sea Ice*, **3**, 304–25.

3485 Oglesby, R. J., and D. J. Erickson III, 1989: Soil moisture and the persistence of north american
3486 drought. *Journal of Climate*, **2** (11), 1362–1380.

3487 Ogura, Y., 1962: Convection of isolated masses of a buoyant fluid: A numerical calculation.
3488 *Journal of the Atmospheric Sciences*, **19** (6), 492–502.

3489 Oliger, E., E. Welck, A. Kasahara, and M. Washington, 1970: Description of near global circula-
3490 tion model.

3491 Onogi, K., and Coauthors, 2007: The jra-25 reanalysis. *Journal of the Meteorological Society of*
3492 *Japan. Ser. II*, **85** (3), 369–432.

3493 Oren, R., and Coauthors, 2001: Soil fertility limits carbon sequestration by forest ecosystems in a
3494 co 2-enriched atmosphere. *Nature*, **411** (6836), 469.

3495 Oreopoulos, L., and H. W. Barker, 1999: Accounting for subgrid-scale cloud variability in a multi-
3496 layer 1D solar radiative transfer algorithm. *Quart. J. Royal Met. Soc.*, **125** (553, Part A), 301–
3497 330.

3498 Oreopoulos, L., and Coauthors, 2012: The Continual Intercomparison of Radiation Codes: Results
3499 from Phase I. *J. Geophys. Res.*, **117** (D6), n/a–n/a.

3500 Orszag, S. A., 1970: Transform method for the calculation of vector-coupled sums: Application
3501 to the spectral form of the vorticity equation. *Journal of the Atmospheric Sciences*, **27** (6), 890–
3502 895.

3503 Ose, T., 1993: An examination of the effects of explicit cloud water in the UCLA GCM. *Journal*
3504 *of the Meteorological Society of Japan. Ser. II*, **71** (1), 93–109.

3505 Palmén, E., 1948: On the distribution of temperature and wind in the upper westerlies. *Journal of*
3506 *Meteorology*, **5** (1), 20–27.

- 3507 Palmén, E., and H. Riehl, 1957: Budget of angular momentum and energy in tropical cyclones.
3508 *Journal of Meteorology*, **14** (2), 150–159.
- 3509 Palmer, T., Č. Branković, and D. Richardson, 2000: A probability and decision-model analysis of
3510 provost seasonal multi-model ensemble integrations. *Quarterly Journal of the Royal Meteorological Society*, **126** (567), 2013–2033.
3511
- 3512 Palmer, T., F. Doblas-Reyes, A. Weisheimer, and M. Rodwell, 2008: Toward seamless prediction:
3513 Calibration of climate change projections using seasonal forecasts. *Bulletin of the American Meteorological Society*, **89** (4), 459–470.
3514
- 3515 Palmer, T., G. Shutts, and R. Swinbank, 1986: Alleviation of a systematic westerly bias in general
3516 circulation and numerical weather prediction models through an orographic gravity wave drag
3517 parametrization. *Quarterly Journal of the Royal Meteorological Society*, **112** (474), 1001–1039.
- 3518 Pan, Y., and Coauthors, 2011: A large and persistent carbon sink in the world’s forests. *Science*,
3519 1201609.
- 3520 Parishani, H., M. S. Pritchard, C. S. Bretherton, M. C. Wyant, and M. Khairoutdinov, 2017: To-
3521 ward low cloud-permitting cloud superparameterization with explicit boundary layer turbulence.
3522 *Journal of Advances in Modeling Earth Systems*.
- 3523 Penman, H. L., 1948: Natural evaporation from open water, bare soil and grass. *Proc. R. Soc. Lond. A*, The Royal Society, Vol. 193, 120–145.
3524
- 3525 Persson, A., 2005a: Early operational numerical weather prediction outside the usa: an historical
3526 introduction. part 1: Internationalism and engineering nwp in sweden, 1952–69. *Meteorological Applications*, **12** (2), 135–159.
3527

- 3528 Persson, A., 2005b: Early operational numerical weather prediction outside the usa: an historical
3529 introduction: Part ii: Twenty countries around the world. *Meteorological Applications*, **12** (3),
3530 269–289.
- 3531 Persson, A., 2005c: Early operational numerical weather prediction outside the usa: an historical
3532 introduction: Part ii: Twenty countries around the world. *Meteorological Applications*, **12** (3),
3533 269–289.
- 3534 Petty, G. W., 2002: Area-Average Solar Radiative Transfer in Three-Dimensionally Inhomoge-
3535 neous Clouds: The Independently Scattering Cloudlet Model. *J. Atmos. Sci.*, **59** (20), 2910–
3536 2929.
- 3537 Phillips, N. A., 1956: The general circulation of the atmosphere: A numerical experiment. *Quar-*
3538 *terly Journal of the Royal Meteorological Society*, **82** (352), 123–164.
- 3539 Phillips, N. A., 1957a: A coordinate system having some special advantages for numerical fore-
3540 casting. *Journal of Meteorology*, **14** (2), 184–185.
- 3541 Phillips, N. A., 1957b: A map projection system suitable for large-scale numerical weather pre-
3542 diction. *Journal of the Meteorological Society of Japan. Ser. II*, **35**, 262–267.
- 3543 Phillips, N. A., 1959: An example of non-linear computational instability. *The Atmosphere and*
3544 *the Sea in motion*, **501**.
- 3545 Pielke, R. A., G. Dalu, J. Snook, T. Lee, and T. Kittel, 1991: Nonlinear influence of mesoscale
3546 land use on weather and climate. *Journal of climate*, **4** (11), 1053–1069.
- 3547 Pincus, R., H. W. Barker, and J.-J. Morcrette, 2003: A fast, flexible, approximate technique for
3548 computing radiative transfer in inhomogeneous cloud fields. *J. Geophys. Res.*, **108** (D13), 4376–
3549 n/a.

- 3550 Pincus, R., and S. A. Klein, 2000: Unresolved spatial variability and microphysical process rates
3551 in large-scale models. *J. Geophys. Res.*, **105 (D22)**, 27 059–27 065.
- 3552 Pincus, R., S. A. McFarlane, and S. A. Klein, 1999: Albedo bias and the horizontal variabil-
3553 ity of clouds in subtropical marine boundary layers: Observations from ships and satellites. *J.*
3554 *Geophys. Res.*, **104 (D6)**, 6183–6191.
- 3555 Pincus, R., and Coauthors, 2015: Radiative flux and forcing parameterization error in aerosol-free
3556 clear skies. *Geophys. Res. Lett.*, **42 (13)**, 5485–5492.
- 3557 Pinty, J.-P., P. Mascart, E. Richard, and R. Rosset, 1989: An investigation of mesoscale flows
3558 induced by vegetation inhomogeneities using an evapotranspiration model calibrated against
3559 hapex-mobilhy data. *Journal of Applied Meteorology*, **28 (9)**, 976–992.
- 3560 Pitcher, E. J., R. C. Malone, V. Ramanathan, M. L. Blackmon, K. Puri, and W. Bourke, 1983: Jan-
3561 uary and july simulations with a spectral general circulation model. *Journal of the Atmospheric*
3562 *Sciences*, **40 (3)**, 580–604.
- 3563 Posselt, R., and U. Lohmann, 2008: Introduction of prognostic rain in echam5: design and single
3564 column model simulations. *Atmospheric Chemistry and Physics*, **8 (11)**, 2949–2963.
- 3565 Potter, J. F., 1970: The Delta Function Approximation in Radiative Transfer Theory. *J. Atmos.*
3566 *Sci.*, **27 (6)**, 943–949.
- 3567 Price, E., J. Mielikainen, B. Huang, H. A. Huang, and T. Lee, 2013: Gpu acceleration experience
3568 with rrtmg long wave radiation model. *High-Performance Computing in Remote Sensing III*,
3569 International Society for Optics and Photonics, Vol. 8895, 88950H.

3570 Prince, S. D., and Coauthors, 1995: Geographical, biological and remote sensing aspects of the
3571 hydrologic atmospheric pilot experiment in the sahel (hapex-sahel). *Remote Sensing of Environ-*
3572 *ment*, **51 (1)**, 215–234.

3573 Pruppacher, H., and J. Klett, 1997: Microphysics of clouds and precipitation. atmospheric and
3574 oceanographic sciences library, vol. 18. Kluwer Academic Publishers, Dordrecht.

3575 Pury, D. d., and G. Farquhar, 1997: Simple scaling of photosynthesis from leaves to canopies
3576 without the errors of big-leaf models. *Plant, Cell & Environment*, **20 (5)**, 537–557.

3577 Putman, W. M., and S.-J. Lin, 2007: Finite-volume transport on various cubed-sphere grids. *Jour-*
3578 *nal of Computational Physics*, **227 (1)**, 55–78.

3579 Putman, W. M., and M. Suarez, 2011: Cloud-system resolving simulations with the nasa god-
3580 dard earth observing system global atmospheric model (geos-5). *Geophysical Research Letters*,
3581 **38 (16)**.

3582 Qaddouri, A., and V. Lee, 2011: The Canadian Global Environmental Multiscale model on the
3583 Yin-Yang grid system. *Quart. J. Roy. Meteor. Soc.*, **137**, 1913–1926.

3584 Qian, J.-H., F. H. Semazzi, and J. S. Scroggs, 1998: A global nonhydrostatic semi-lagrangian
3585 atmospheric model with orography. *Monthly weather review*, **126 (3)**, 747–771.

3586 Ramanathan, V., R. Cess, E. Harrison, P. Minnis, B. Barkstrom, E. Ahmad, and D. Hartmann,
3587 1989: Cloud-radiative forcing and climate: Results from the earth radiation budget experiment.
3588 *Science*, **243 (4887)**, 57–63.

3589 Ramanathan, V., E. J. Pitcher, R. C. Malone, and M. L. Blackmon, 1983: The Response of a Spec-
3590 tral General Circulation Model to Refinements in Radiative Processes. *J. Atmos. Sci.*, **40 (3)**,
3591 605–630.

- 3592 Randall, D., C. DeMott, C. Stan, M. Khairoutdinov, J. Benedict, R. McCrary, K. Thayer-Calder,
3593 and M. Branson, 2016: Simulations of the tropical general circulation with a multiscale global
3594 model. *Meteorological Monographs*, **56**, 15–1.
- 3595 Randall, D., and Coauthors, 1996a: A revised land surface parameterization (sib2) for gcms.
3596 part iii: The greening of the colorado state university general circulation model. *Jour-
3597 nal of Climate*, **9** (4), 738–763, doi:10.1175/1520-0442(1996)009<0738:ARLSPF>2.0.CO;
3598 2, URL [https://doi.org/10.1175/1520-0442\(1996\)009<0738:ARLSPF>2.0.CO;2](https://doi.org/10.1175/1520-0442(1996)009<0738:ARLSPF>2.0.CO;2), [https://doi.org/
3599 10.1175/1520-0442\(1996\)009<0738:ARLSPF>2.0.CO;2](https://doi.org/10.1175/1520-0442(1996)009<0738:ARLSPF>2.0.CO;2).
- 3600 Randall, D., and Coauthors, 2003: Confronting models with data: The gewex cloud systems study.
3601 *Bulletin of the American Meteorological Society*, **84** (4), 455–469.
- 3602 Randall, D. A., 1976: The interaction of the planetary boundary layer with large-scale circulations.
- 3603 Randall, D. A., 1987: Turbulent fluxes of liquid water and buoyancy in partly cloudy layers.
3604 *Journal of the atmospheric sciences*, **44** (5), 850–858.
- 3605 Randall, D. A., 1994: Geostrophic adjustment and the finite-difference shallow-water equations.
3606 *Monthly Weather Review*, **122** (6), 1371–1377.
- 3607 Randall, D. A., J. A. Abeles, and T. G. Corsetti, 1985: Seasonal simulations of the planetary
3608 boundary layer and boundary-layer stratocumulus clouds with a general circulation model. *Jour-
3609 nal of the atmospheric sciences*, **42** (7), 641–676.
- 3610 Randall, D. A., Harshvardhan, D. A. Dazlich, and T. G. Corsetti, 1989: Interactions among Ra-
3611 diation, Convection, and Large-Scale Dynamics in a General Circulation Model. *J. Atmos. Sci.*,
3612 **46** (13), 1943–1970.

- 3613 Randall, D. A., Q. Shao, and C.-H. Moeng, 1992: A second-order bulk boundary-layer model.
3614 *Journal of the atmospheric sciences*, **49 (20)**, 1903–1923.
- 3615 Randall, D. A., K.-M. Xu, R. J. Somerville, and S. Iacobellis, 1996b: Single-column models and
3616 cloud ensemble models as links between observations and climate models. *Journal of Climate*,
3617 **9 (8)**, 1683–1697.
- 3618 Rauscher, S. A., and T. D. Ringler, 2014: Impact of variable-resolution meshes on midlatitude
3619 baroclinic eddies using cam-mpas-a. *Monthly Weather Review*, **142 (11)**, 4256–4268.
- 3620 Raymond, D. J., and A. M. Blyth, 1986: A stochastic mixing model for nonprecipitating cumulus
3621 clouds. *Journal of the atmospheric sciences*, **43 (22)**, 2708–2718.
- 3622 Redi, M. H., 1982: Oceanic isopycnal mixing by coordinate rotation. *Journal of Physical*
3623 *Oceanography*, **12 (10)**, 1154–1158.
- 3624 Reed, B. C., J. F. Brown, D. VanderZee, T. R. Loveland, J. W. Merchant, and D. O. Ohlen, 1994:
3625 Measuring phenological variability from satellite imagery. *Journal of vegetation science*, **5 (5)**,
3626 703–714.
- 3627 Richardson, L. F., 1911: IX. the approximate arithmetical solution by finite differences of physical
3628 problems involving differential equations, with an application to the stresses in a masonry dam.
3629 *Phil. Trans. R. Soc. Lond. A*, **210 (459-470)**, 307–357.
- 3630 Richardson, L. F., 1922: *Weather prediction by numerical process*. Cambridge University Press.
- 3631 Richter, J. H., A. Solomon, and J. T. Bacmeister, 2014: Effects of vertical resolution and nonoro-
3632 graphic gravity wave drag on the simulated climate in the community atmosphere model, ver-
3633 sion 5. *Journal of Advances in Modeling Earth Systems*, **6 (2)**, 357–383.

- 3634 Riehl, H., and J. Malkus, 1958: On the heat balance of the equatorial trough zone. *Geophysica*, **6**,
3635 503–538.
- 3636 Rienecker, M. M., and Coauthors, 2011: Merra: Nasa’s modern-era retrospective analysis for
3637 research and applications. *Journal of climate*, **24 (14)**, 3624–3648.
- 3638 Ringler, T., M. Petersen, R. L. Higdon, D. Jacobsen, P. W. Jones, and M. Maltrud, 2013: A multi-
3639 resolution approach to global ocean modeling. *Ocean Modelling*, **69**, 211–232.
- 3640 Ritchie, H., 1991: Application of the semi-lagrangian method to a multilevel spectral primitive-
3641 equations model. *Quarterly Journal of the Royal Meteorological Society*, **117 (497)**, 91–106.
- 3642 Ritchie, H., C. Temperton, A. Simmons, M. Hortal, T. Davies, D. Dent, and M. Hamrud, 1995: Im-
3643 plementation of the semi-lagrangian method in a high-resolution version of the ecmwf forecast
3644 model. *Monthly Weather Review*, **123 (2)**, 489–514.
- 3645 Roach, L., C. Horvat, S. Dean, and C. M. Bitz, 2018: An emergent sea ice floe size distribution in
3646 a global coupled ocean-sea ice model.
- 3647 Roach, W. T., and A. Slingo, 1979: A high resolution infrared radiative transfer scheme to study
3648 the interaction of radiation with cloud. *Quart. J. Royal Met. Soc.*, **105 (445)**, 603–614.
- 3649 Robert, A., 1969: The integration of a spectral model of the atmosphere by the implicit method.
3650 *Proc. of WMO/IUGG Symposium on NWP in Tokyo, Japan*, Tokyo, Japan, Japan Meteorol.
3651 Agency, VII.19–VII.24.
- 3652 Robert, A., 1981: A stable numerical integration scheme for the primitive meteorological equa-
3653 tions. *Atmosphere-Ocean*, **19 (1)**, 35–46.

- 3654 Robert, A., 1982: A semi-lagrangian and semi-implicit numerical integration scheme for the prim-
3655 itive meteorological equations. *Journal of the Meteorological Society of Japan. Ser. II*, **60** (1),
3656 319–325.
- 3657 Robert, A., J. Henderson, and C. Turnbull, 1972: An implicit time integration scheme for baro-
3658 clinic models of the atmosphere. *Mon. Wea. Rev.*, **100**, 329–335.
- 3659 Robert, A. J., 1966: The integration of a low order spectral form of the primitive meteorological
3660 equations. *METEOROLOGICAL SOCIETY OF JAPAN, JOURNAL*, **44**, 237–245.
- 3661 Rodgers, C. D., and C. D. Walshaw, 1966: The computation of infra-red cooling rate in planetary
3662 atmospheres. *Quart. J. Royal Met. Soc.*, **92** (391), 67–92.
- 3663 Roeckner, E., L. Dümenil, E. Kirk, F. Lunkeit, M. Ponater, B. Rockel, R. Sausen, and U. Schlese,
3664 1989: The hamburg version of the ecmwf model (echam), research activities in atmospheric and
3665 oceanic modelling. *WMO Tech. Document*, **322**.
- 3666 Rossby, C.-G., 1937: Isentropic analysis. *Bulletin of the american meteorological society*, **18** (6/7),
3667 201–209.
- 3668 Rossow, W. B., C. Delo, and B. Cairns, 2002: Implications of the Observed Mesoscale Variations
3669 of Clouds for the Earth’s Radiation Budget. *J. Climate*, **15** (6), 557–585.
- 3670 Rothman, L. S., and Coauthors, 1987: The HITRAN database: 1986 edition. *Applied Opt.*, **26** (19),
3671 4058–4097.
- 3672 Rotstajn, L. D., 2000a: On the ”tuning” of autoconversion parameterizations in climate models.
3673 *J. Geophys. Res.*, **105** (D12), 15 495–15 507.
- 3674 Rotstajn, L. D., 2000b: On the “tuning” of autoconversion parameterizations in climate models.
3675 *Journal of Geophysical Research: Atmospheres*, **105** (D12), 15 495–15 507.

3676 Rotstayn, L. D., B. F. Ryan, and J. J. Katzfey, 2000: A scheme for calculation of the liquid fraction
3677 in mixed-phase stratiform clouds in large-scale models. *Monthly weather review*, **128 (4)**, 1070–
3678 1088.

3679 Rowntree, P., 1976: Response of the atmosphere to a tropical atlantic ocean temperature anomaly.
3680 *Quarterly Journal of the Royal Meteorological Society*, **102 (433)**, 607–625.

3681 Rowntree, P., and J. Walker, 1978: The effects of doubling the co 2 concentration on radiative-
3682 convective equilibrium. *Carbon dioxide, climate and society*, Elsevier, 181–191.

3683 Rutledge, S. A., and P. V. Hobbs, 1984: The mesoscale and microscale structure and organization
3684 of clouds and precipitation in midlatitude cyclones. xii: A diagnostic modeling study of pre-
3685 cipitation development in narrow cold-frontal rainbands. *Journal of the Atmospheric Sciences*,
3686 **41 (20)**, 2949–2972.

3687 Sadourny, R., 1972: Conservative finite-difference approximations of the primitive equa-
3688 tions on quasi-uniform spherical grids. *Monthly Weather Review*, **100 (2)**, 136–144,
3689 doi:10.1175/1520-0493(1972)100<0136:CFAOTP>2.3.CO;2, URL [https://doi.org/10.1175/
3690 1520-0493\(1972\)100<0136:CFAOTP>2.3.CO;2](https://doi.org/10.1175/1520-0493(1972)100<0136:CFAOTP>2.3.CO;2), [https://doi.org/10.1175/1520-0493\(1972\)
3691 100<0136:CFAOTP>2.3.CO;2](https://doi.org/10.1175/1520-0493(1972)100<0136:CFAOTP>2.3.CO;2).

3692 Sadourny, R., 1975: The dynamics of finite-difference models of the shallow-water equations.
3693 *Journal of the Atmospheric Sciences*, **32 (4)**, 680–689.

3694 Sadourny, R., 1984: January and july performances of the lmd general circulation model. *New
3695 Perspectives in Climate Modeling*.

3696 Sadourny, R., A. Arakawa, and Y. Mintz, 1968: Integration of the nondivergent
3697 barotropic vorticity equation with an icosahedral-hexagonal grid for the sphere. *Monthly*

3698 *Weather Review*, **96 (6)**, 351–356, doi:10.1175/1520-0493(1968)096<0351:IOTNBV>2.0.CO;
3699 2, URL [https://doi.org/10.1175/1520-0493\(1968\)096<0351:IOTNBV>2.0.CO;2](https://doi.org/10.1175/1520-0493(1968)096<0351:IOTNBV>2.0.CO;2), [https://doi.org/](https://doi.org/10.1175/1520-0493(1968)096<0351:IOTNBV>2.0.CO;2)
3700 [10.1175/1520-0493\(1968\)096<0351:IOTNBV>2.0.CO;2](https://doi.org/10.1175/1520-0493(1968)096<0351:IOTNBV>2.0.CO;2).

3701 Saha, S., and Coauthors, 2010a: The ncep climate forecast system reanalysis. *Bulletin of the*
3702 *American Meteorological Society*, **91 (8)**, 1015–1058.

3703 Saha, S., and Coauthors, 2010b: The ncep climate forecast system reanalysis. *Bulletin of the*
3704 *American Meteorological Society*, **91 (8)**, 1015–1058, doi:10.1175/2010BAMS3001.1, URL
3705 <https://doi.org/10.1175/2010BAMS3001.1>, <https://doi.org/10.1175/2010BAMS3001.1>.

3706 Sandbach, S., J. Thuburn, D. Vassilev, and M. G. Duda, 2015: A semi-implicit version of the
3707 mpas-atmosphere dynamical core. *Monthly Weather Review*, **143 (9)**, 3838–3855.

3708 Sasamori, T., 1968: The Radiative Cooling Calculation for Application to General Circulation
3709 Experiments. *J. Appl. Meteor.*, **7 (5)**, 721–729.

3710 Satoh, M., T. Matsuno, H. Tomita, H. Miura, T. Nasuno, and S. Iga, 2008a: Nonhydrostatic icosahedral atmospheric model (NICAM) for global cloud resolving simulations. **227**, 3486–3514.

3711

3712 Satoh, M., T. Matsuno, H. Tomita, H. Miura, T. Nasuno, and S.-i. Iga, 2008b: Nonhydrostatic
3713 icosahedral atmospheric model (nicam) for global cloud resolving simulations. *Journal of Com-*
3714 *putational Physics*, **227 (7)**, 3486–3514.

3715 Satoh, M., and Coauthors, 2014: The non-hydrostatic icosahedral atmospheric model: Description
3716 and development. *Progress in Earth and Planetary Science*, **1 (1)**, 18.

3717 Sausen, R., K. Barthel, and K. Hasselmann, 1988: Coupled ocean-atmosphere models with flux
3718 correction. *Climate Dynamics*, **2 (3)**, 145–163.

3719 Schäfer, S. A., R. J. Hogan, C. Klinger, J. C. Chiu, and B. Mayer, 2016: Representing 3-d cloud
3720 radiation effects in two-stream schemes: 1. longwave considerations and effective cloud edge
3721 length. *Journal of Geophysical Research: Atmospheres*, **121** (14), 8567–8582.

3722 Schiffer, R. A., and W. B. Rossow, 1983: The international satellite cloud climatology project
3723 (isccp): The first project of the world climate research programme. *Bulletin of the American*
3724 *Meteorological Society*, **64** (7), 779–784.

3725 Schiller, A., P. R. Oke, G. Brassington, M. Entel, R. Fiedler, D. A. Griffin, and J. Mansbridge,
3726 2008: Eddy-resolving ocean circulation in the asian–australian region inferred from an ocean
3727 reanalysis effort. *Progress in oceanography*, **76** (3), 334–365.

3728 Schlesinger, M. E., 1976: A numerical simulation of the general circulation of atmospheric ozone.

3729 Schlesinger, M. E., and Y. Mintz, 1979: Numerical simulation of ozone production, transport and
3730 distribution with a global atmospheric general circulation model. *Journal of the Atmospheric*
3731 *Sciences*, **36** (7), 1325–1361.

3732 Schneider, T., J. Teixeira, C. S. Bretherton, F. Brient, K. G. Pressel, C. Schär, and A. P. Siebesma,
3733 2017: Climate goals and computing the future of clouds. *Nature Climate Change*, **7** (1), 3.

3734 Schoenberg Ferrier, B., 1994: A double-moment multiple-phase four-class bulk ice scheme. part
3735 i: Description. *Journal of the Atmospheric Sciences*, **51** (2), 249–280.

3736 Schubert, S. D., R. B. Rood, and J. Pfaendtner, 1993: An assimilated dataset for earth science
3737 applications. *Bulletin of the American meteorological Society*, **74** (12), 2331–2342.

3738 Schuster, A., 1905: Radiation Through a Foggy Atmosphere. *Ap. J.*, **21** (1), 1–22.

3739 Seifert, A., and K. D. Beheng, 2001: A double-moment parameterization for simulating autocon-
3740 version, accretion and selfcollection. *Atmospheric research*, **59**, 265–281.

- 3741 Seland, Ø., T. Iversen¹, A. Kirkevåg, and T. Storelvmo^{1, 2}, 2008: Aerosol-climate interactions
3742 in the cam-oslo atmospheric gcm and investigation of associated basic shortcomings. *Tellus A:
3743 Dynamic Meteorology and Oceanography*, **60** (3), 459–491.
- 3744 Sellers, P., J. Berry, G. Collatz, C. Field, and F. Hall, 1992: Canopy reflectance, photosynthesis,
3745 and transpiration. iii. a reanalysis using improved leaf models and a new canopy integration
3746 scheme. *Remote sensing of environment*, **42** (3), 187–216.
- 3747 Sellers, P., Y. Mintz, Y. e. a. Sud, and A. Dalcher, 1986: A simple biosphere model (sib) for use
3748 within general circulation models. *Journal of the Atmospheric Sciences*, **43** (6), 505–531.
- 3749 Sellers, P., and Coauthors, 1996a: A revised land surface parameterization (sib2) for at-
3750 mospheric gcms. part i: Model formulation. *Journal of Climate*, **9** (4), 676–705, doi:
3751 10.1175/1520-0442(1996)009<0676:ARLSPF>2.0.CO;2, URL [https://doi.org/10.1175/
3752 1520-0442\(1996\)009<0676:ARLSPF>2.0.CO;2](https://doi.org/10.1175/1520-0442(1996)009<0676:ARLSPF>2.0.CO;2), [https://doi.org/10.1175/1520-0442\(1996\)
3753 009<0676:ARLSPF>2.0.CO;2](https://doi.org/10.1175/1520-0442(1996)009<0676:ARLSPF>2.0.CO;2).
- 3754 Sellers, P. J., 1985: Canopy reflectance, photosynthesis and transpiration. *International Journal of
3755 Remote Sensing*, **6** (8), 1335–1372.
- 3756 Sellers, P. J., C. J. Tucker, G. J. Collatz, S. O. Los, C. O. Justice, D. A. Dazlich, and D. A.
3757 Randall, 1996b: A revised land surface parameterization (sib2) for atmospheric gcms. part
3758 ii: The generation of global fields of terrestrial biophysical parameters from satellite data.
3759 *Journal of Climate*, **9** (4), 706–737, doi:10.1175/1520-0442(1996)009<0706:ARLSPF>2.0.CO;
3760 2, URL [https://doi.org/10.1175/1520-0442\(1996\)009<0706:ARLSPF>2.0.CO;2](https://doi.org/10.1175/1520-0442(1996)009<0706:ARLSPF>2.0.CO;2), [https://doi.org/
3761 10.1175/1520-0442\(1996\)009<0706:ARLSPF>2.0.CO;2](https://doi.org/10.1175/1520-0442(1996)009<0706:ARLSPF>2.0.CO;2).

- 3762 Sellers, P. J., and Coauthors, 1997: Boreas in 1997: Experiment overview, scientific results, and
3763 future directions. *Journal of Geophysical Research: Atmospheres*, **102 (D24)**, 28 731–28 769.
- 3764 Sellers, W. D., 1969: A global climate model based on the energy balance of the earth-atmosphere
3765 system. *J. Appl. Meteor.*, **8**, 392–400.
- 3766 Semtner, A. J., Jr., 1974: An oceanic general circulation model with bottom topography. Tech. rep.
- 3767 Semtner, A. J., Jr., 1976: A model for the thermodynamic growth of sea ice in numerical investi-
3768 gations of climate. *J. Phys. Oceanogr.*, **6**, 379–389.
- 3769 Semtner, A. J., Jr., and R. M. Chervin, 1992: Ocean general circulation from a global eddy-
3770 resolving model. *Journal of Geophysical Research: Oceans*, **97 (C4)**, 5493–5550.
- 3771 Semtner, A. J., Jr., and Y. Mintz, 1977: Numerical simulation of the gulf stream and mid-ocean
3772 eddies. *Journal of Physical Oceanography*, **7 (2)**, 208–230.
- 3773 Senior, C., and Coauthors, 2010: Synergies between numerical weather prediction and general
3774 circulation climate models. *The development of atmospheric general circulation models, edited*
3775 *by: Donner, L., Schubert, W., and Somerville, R., Cambridge University Press, Cambridge, UK.*
- 3776 Senior, C. A., and J. F. B. Mitchell, 2000: The time-dependence of climate sensitivity. *Geophys.*
3777 *Res. Lett.*, **27**, 2685–2688.
- 3778 Shabecoff, P., 1988: Global warming has begun, expert tells senate. *New York Times*, **24 (1988)**,
3779 A1.
- 3780 Shchepetkin, A. F., and J. C. McWilliams, 2005: The regional oceanic modeling system (roms): a
3781 split-explicit, free-surface, topography-following-coordinate oceanic model. *Ocean modelling*,
3782 **9 (4)**, 347–404.

- 3783 Shevliakova, E., and Coauthors, 2009: Carbon cycling under 300 years of land use change: Im-
3784 portance of the secondary vegetation sink. *Global Biogeochemical Cycles*, **23** (2).
- 3785 Shima, S.-i., K. Kusano, A. Kawano, T. Sugiyama, and S. Kawahara, 2009: The super-droplet
3786 method for the numerical simulation of clouds and precipitation: A particle-based and prob-
3787 abilistic microphysics model coupled with a non-hydrostatic model. *Quarterly Journal of the*
3788 *Royal Meteorological Society*, **135** (642), 1307–1320.
- 3789 Shonk, J. K. P., and R. J. Hogan, 2008: Tripleclouds: An Efficient Method for Representing
3790 Horizontal Cloud Inhomogeneity in 1D Radiation Schemes by Using Three Regions at Each
3791 Height. *J. Climate*, **21** (11), 2352–2370.
- 3792 Shukla, J., and Y. Mintz, 1982: Influence of land-surface evapotranspiration on the earth's climate.
3793 *Science*, **215** (4539), 1498–1501.
- 3794 Shuman, F. G., and J. B. Hoovermale, 1968: An operational six-layer primitive equation model.
3795 *Journal of Applied Meteorology*, **7** (4), 525–547.
- 3796 Silberman, I., 1954: Planetary waves in the atmosphere. *Journal of Meteorology*, **11** (1), 27–34.
- 3797 Simmons, A., D. Burridge, M. Jarraud, C. Girard, and W. Wergen, 1989: The ecmwf medium-
3798 range prediction models development of the numerical formulations and the impact of increased
3799 resolution. *Meteorology and atmospheric physics*, **40** (1-3), 28–60.
- 3800 Simmons, A. J., and D. M. Burridge, 1981: An energy and angular-momentum conserving verti-
3801 cal finite-difference scheme and hybrid vertical coordinates. *Monthly Weather Review*, **109** (4),
3802 758–766.
- 3803 Simpson, J., R. H. Simpson, D. A. Andrews, and M. A. Eaton, 1965: Experimental cumulus
3804 dynamics. *Reviews of Geophysics*, **3** (3), 387–431.

3805 Simpson, J., and V. Wiggert, 1969: Models of precipitating cumulus towers. *Mon. Wea. Rev.*,
3806 **97 (7)**, 471–489.

3807 Sitch, S., V. Brovkin, W. von Bloh, D. van Vuuren, B. Eickhout, and A. Ganopolski, 2005: Impacts
3808 of future land cover changes on atmospheric co2 and climate. *Global Biogeochemical Cycles*,
3809 **19 (2)**.

3810 Sitch, S., and Coauthors, 2008: Evaluation of the terrestrial carbon cycle, future plant geogra-
3811 phy and climate-carbon cycle feedbacks using five dynamic global vegetation models (dgvms).
3812 *Global Change Biology*, **14 (9)**, 2015–2039.

3813 Skamarock, W. C., and J. B. Klemp, 1993: Adaptive grid refinement for two-dimensional and
3814 three-dimensional nonhydrostatic atmospheric flow. *Monthly Weather Review*, **121 (3)**, 788–
3815 804.

3816 Skamarock, W. C., J. B. Klemp, M. G. Duda, L. D. Fowler, and S.-H. Park, 2012a: A multiscale
3817 nonhydrostatic atmospheric model using centroidal voronoi tessellations and C-grid staggering.
3818 *Mon. Wea. Rev.*, **140**, 3090–3105.

3819 Skamarock, W. C., J. B. Klemp, M. G. Duda, L. D. Fowler, S.-H. Park, and T. D. Ringler, 2012b:
3820 A multiscale nonhydrostatic atmospheric model using centroidal voronoi tessellations and c-grid
3821 staggering. *Monthly Weather Review*, **140 (9)**, 3090–3105.

3822 Slingo, A., 1985: *Handbook of the Meteorological Office 11-layer atmospheric general circulation*
3823 *model*. Met 0 20 (Dynamical Climatology Branch), Meteorological Office.

3824 Slingo, A., and H. M. Schrecker, 1982: On the shortwave radiative properties of stratiform water
3825 clouds. *Quart. J. Royal Met. Soc.*, **108 (456)**, 407–426.

- 3826 Smagorinsky, J., 1958: On the numerical integration of the primitive equations of motion for
3827 baroclinic flow in a closed region. *Monthly Weather Review*, **86 (12)**, 457–466.
- 3828 Smagorinsky, J., 1960: On the dynamical prediction of large-scale condensation by numerical
3829 methods. *Physics of Precipitation: Proceedings of the Cloud Physics Conference, Woods Hole,*
3830 *Massachusetts, June 3-5, 1959*, Wiley Online Library, 71–78.
- 3831 Smagorinsky, J., 1963: General circulation experiments with the primitive equations: I. the basic
3832 experiment. *Monthly weather review*, **91 (3)**, 99–164.
- 3833 Smagorinsky, J., 1983: The beginnings of numerical weather prediction and general circulation
3834 modeling: early recollections. *Advances in Geophysics*, Vol. 25, Elsevier, 3–37.
- 3835 Smagorinsky, J., and G. O. Collins, 1955: On the numerical prediction of precipitation. *Monthly*
3836 *Weather Review*, **83 (3)**, 53–68, doi:10.1175/1520-0493(1955)083<0053:OTNPOP>2.0.CO;2.
- 3837 Smagorinsky, J., S. Manabe, and J. L. Holloway, Jr., 1965: Numerical results from a nine-level
3838 general circulation model of the atmosphere. *Mon. Wea. Rev.*, **93 (12)**, 727–768.
- 3839 Smagorinsky, J., R. Strickler, W. Sangster, S. Manabe, J. Holloway Jr, and G. Hembree, 1967:
3840 Prediction experiments with a general circulation model. *Proc. Int. Symp. on Dynamics of Large*
3841 *Scale Atmospheric Processes*, 70–134.
- 3842 Small, R. J., and Coauthors, 2014: A new synoptic scale resolving global climate simulation using
3843 the community earth system model. *Journal of Advances in Modeling Earth Systems*, **6 (4)**,
3844 1065–1094.
- 3845 Smith, R., J. Dukowicz, and R. Malone, 1992: Parallel ocean general circulation modeling. *Phys-*
3846 *ica D: Nonlinear Phenomena*, **60 (1-4)**, 38–61.

3847 Smith, R., S. Kortas, and B. Meltz, 1995: Curvilinear coordinates for global ocean models, los
3848 alamos preprint. Tech. rep., LA-UR-95-1146.

3849 Smith, R., and Coauthors, 2010: The parallel ocean program (pop) reference manual ocean com-
3850 ponent of the community climate system model (ccsm) and community earth system model
3851 (cesm). *Rep. LAUR-01853*, **141**, 1–140.

3852 Solomon, H., 1971: On the representation of isentropic mixing in ocean circulation models. *Jour-
3853 nal of Physical Oceanography*, **1 (3)**, 233–234.

3854 Somerville, R. C. J., and Coauthors, 1974: The GISS Model of the Global Atmosphere. *J. Atmos.
3855 Sci.*, **31 (1)**, 84–117.

3856 Sommeria, G., and J. Deardorff, 1977: Subgrid-scale condensation in models of nonprecipitating
3857 clouds. *Journal of the Atmospheric Sciences*, **34 (2)**, 344–355.

3858 Song, X., and G. J. Zhang, 2011: Microphysics parameterization for convective clouds in a global
3859 climate model: Description and single-column model tests. *Journal of Geophysical Research:
3860 Atmospheres*, **116 (D2)**.

3861 St-Cyr, A., C. Jablonowski, J. M. Dennis, H. M. Tufo, and S. J. Thomas, 2008: A comparison
3862 of two shallow-water models with nonconforming adaptive grids. *Monthly Weather Review*,
3863 **136 (6)**, 1898–1922.

3864 Stacey, M. W., S. Pond, and Z. P. Nowak, 1995: A numerical model of the circulation in knight
3865 inlet, british columbia, canada. *Journal of Physical Oceanography*, **25 (6)**, 1037–1062.

3866 Stackpole, J. D., 1978: The nmc 9-layer global primitive equation model on a latitude-longitude
3867 grid.

- 3868 Stamnes, K., S.-C. Tsay, W. Wiscombe, and K. Jayaweera, 1988: Numerically stable algorithm for
3869 discrete-ordinate-method radiative transfer in multiple scattering and emitting layered media.
3870 *Applied Opt.*, **27** (12), 2502–2509.
- 3871 Stan, C., M. Khairoutdinov, C. A. DeMott, V. Krishnamurthy, D. M. Straus, D. A. Randall, J. L.
3872 Kinter, and J. Shukla, 2010: An ocean-atmosphere climate simulation with an embedded cloud
3873 resolving model. *Geophys. Res. Lett.*, **37**, L01 702, doi:10.1029/2009gl040822, URL [http://dx.
3874 doi.org/10.1029/2009GL040822](http://dx.doi.org/10.1029/2009GL040822).
- 3875 Starr, V. P., 1945: A quasi-lagrangian system of hydrodynamical equations. *Journal of Meteorol-
3876 ogy*, **2** (4), 227–237.
- 3877 Starr, V. P., 1948: An essay on the general circulation of the earth's atmosphere. *Journal of Mete-
3878 orology*, **5** (2), 39–43.
- 3879 Starr, V. P., and R. White, 1951: A hemispherical study of the atmospheric angular-momentum
3880 balance. *Quarterly Journal of the Royal Meteorological Society*, **77** (332), 215–225.
- 3881 Starr Malkus, J., 1954: Some results of a trade-cumulus cloud investigation. *Journal of Meteorol-
3882 ogy*, **11** (3), 220–237.
- 3883 Starr Malkus, J., 1955: On the formation and structure of downdrafts in cumulus clouds. *Journal
3884 of Meteorology*, **12** (4), 350–354.
- 3885 Stephens, G. L., 1978: Radiation profiles in extended water clouds. II: Parameterization schemes.
3886 *J. Atmos. Sci.*, **35** (11), 2123–2132.
- 3887 Stephens, G. L., 1984: The Parameterization of Radiation for Numerical Weather Prediction and
3888 Climate Models. *Mon. Wea. Rev.*, **112** (4), 826–867.

- 3889 Stevens, B., G. Feingold, W. R. Cotton, and R. L. Walko, 1996: Elements of the microphysical
3890 structure of numerically simulated nonprecipitating stratocumulus. *Journal of the atmospheric*
3891 *sciences*, **53** (7), 980–1006.
- 3892 Stevens, B., and Coauthors, 2013: Atmospheric component of the mpi-m earth system model:
3893 Echem6. *Journal of Advances in Modeling Earth Systems*, **5** (2), 146–172.
- 3894 Stier, P., and Coauthors, 2005: The aerosol-climate model echam5-ham. *Atmospheric Chemistry*
3895 *and Physics*, **5** (4), 1125–1156.
- 3896 Stocker, T., Q. Dahe, and G. Plattner, 2013: Working group i contribution to the ipcc fifth assess-
3897 ment report climate change 2013, the physical science basis. *Final draft underlying scientific-*
3898 *technical assessment IPCC, Stockholm*.
- 3899 Stöckli, R., T. Rutishauser, I. Baker, M. A. Liniger, and A. S. Denning, 2011: A global reanalysis
3900 of vegetation phenology. *Journal of Geophysical Research: Biogeosciences*, **116** (G3).
- 3901 Stöckli, R., T. Rutishauser, D. Dragoni, J. O’keefe, P. Thornton, M. Jolly, L. Lu, and A. Den-
3902 ning, 2008a: Remote sensing data assimilation for a prognostic phenology model. *Journal of*
3903 *Geophysical Research: Biogeosciences*, **113** (G4).
- 3904 Stöckli, R., and Coauthors, 2008b: Use of fluxnet in the community land model development.
3905 *Journal of Geophysical Research: Biogeosciences*, **113** (G1).
- 3906 Stokes, G. M., and S. E. Schwartz, 1994: The atmospheric radiation measurement (arm) pro-
3907 gram: Programmatic background and design of the cloud and radiation test bed. *Bulletin of the*
3908 *American Meteorological Society*, **75** (7), 1201–1221.
- 3909 Stommel, H., 1951: Entrainment of air into a cumulus cloud. *Journal of Me-*
3910 *teorology*, **8** (2), 127–129, doi:10.1175/1520-0469(1951)008<0127:EOAIAC>2.0.CO;2,

3911 URL [https://doi.org/10.1175/1520-0469\(1951\)008<0127:EOAIAC>2.0.CO;2](https://doi.org/10.1175/1520-0469(1951)008<0127:EOAIAC>2.0.CO;2), [https://doi.org/](https://doi.org/10.1175/1520-0469(1951)008<0127:EOAIAC>2.0.CO;2)
3912 [10.1175/1520-0469\(1951\)008<0127:EOAIAC>2.0.CO;2](https://doi.org/10.1175/1520-0469(1951)008<0127:EOAIAC>2.0.CO;2).

3913 Stowe, L. L., C. Wellemeyer, H. Yeh, and T. Eck, 1988: Nimbus-7 global cloud climatology. part
3914 i: Algorithms and validation. *Journal of Climate*, **1** (5), 445–470.

3915 Suarez, M. J., A. Arakawa, and D. A. Randall, 1983: The parameterization of the planetary bound-
3916 ary layer in the ucla general circulation model: Formulation and results. *Monthly weather re-*
3917 *view*, **111** (11), 2224–2243.

3918 Sullivan, W., 1961: *Assault on the unknown: the International Geophysical Year*. McGraw-Hill.

3919 Sulsky, D., H. Schreyer, K. Peterson, R. Kwok, and M. Coon, 2007: "using the material-point
3920 method to model sea ice dynamics". *J. Geophys. Res.*, **112**, 10.1029/2005JC003329.

3921 Sun, S., and R. Bleck, 2001: Thermohaline circulation studies with an isopycnic coordinate ocean
3922 model. *Journal of physical oceanography*, **31** (9), 2761–2782.

3923 Sun, S., and R. Bleck, 2006: Multi-century simulations with the coupled giss–hycom climate
3924 model: control experiments. *Climate dynamics*, **26** (4), 407–428.

3925 Sun, S., R. Bleck, S. G. Benjamin, B. W. Green, and G. A. Grell, 2018: Subseasonal forecasting
3926 with an icosahedral, vertically quasi-lagrangian coupled model. part i: Model overview and
3927 evaluation of systematic errors. *Monthly Weather Review*, **146** (5), 1601–1617, doi:10.1175/
3928 MWR-D-18-0006.1.

3929 Sundqvist, H., 1975: On truncation errors in sigma-system models. *Atmosphere*, **13** (3), 81–95.

3930 Sundqvist, H., E. Berge, and J. E. Kristjánsson, 1989: Condensation and cloud parameteriza-
3931 tion studies with a mesoscale numerical weather prediction model. *Monthly Weather Review*,
3932 **117** (8), 1641–1657.

3933 Swinbank, W., 1951: The measurement of vertical transfer of heat and water vapor by eddies in
3934 the lower atmosphere. *Journal of Meteorology*, **8 (3)**, 135–145.

3935 Tans, P. P., I. Y. Fung, and T. Takahashi, 1990: Observational constraints on the global atmospheric
3936 CO₂ budget. *Science*, **247 (4949)**, 1431–1438.

3937 Tapp, M., and P. White, 1976: A non-hydrostatic mesoscale model. *Quarterly Journal of the Royal*
3938 *Meteorological Society*, **102 (432)**, 277–296.

3939 Taylor, K. E., and J. E. Penner, 1994: Response of the climate system to atmospheric aerosols and
3940 greenhouse gases. *Nature*, **369 (6483)**, 734.

3941 Temperton, C., and A. Staniforth, 1987: An efficient two-time-level semi-lagrangian semi-implicit
3942 integration scheme. *Quarterly Journal of the Royal Meteorological Society*, **113 (477)**, 1025–
3943 1039.

3944 Thayer-Calder, K., and Coauthors, 2015: A unified parameterization of clouds and turbulence
3945 using CLUBB and subcolumns in the community atmosphere model. *Geoscientific Model Devel-*
3946 *opment*, **8 (12)**, 3801.

3947 Thomas, L., A. Tandon, A. Mahadevan, M. Hecht, and H. Hasumi, 2008: Ocean modeling in
3948 an eddying regime. *Geophysical Monograph Series*, Vol. 177, American Geophysical Union,
3949 17–38.

3950 Thompson, G., and T. Eidhammer, 2014: A study of aerosol impacts on clouds and precipitation
3951 development in a large winter cyclone. *Journal of the Atmospheric Sciences*, **71 (10)**, 3636–
3952 3658.

3953 Thorndike, A. S., D. S. Rothrock, G. A. Maykut, and R. Colony, 1975: The thickness distribution
3954 of sea ice. *J. Geophys. Res.*, **80**, 4501–4513.

3955 Thornton, P. E., J.-F. Lamarque, N. A. Rosenbloom, and N. M. Mahowald, 2007: Influence of
3956 carbon-nitrogen cycle coupling on land model response to co2 fertilization and climate variabil-
3957 ity. *Global biogeochemical cycles*, **21** (4).

3958 Thornton, P. E., and Coauthors, 2009: Carbon-nitrogen interactions regulate climate-carbon cycle
3959 feedbacks: results from an atmosphere-ocean general circulation model. *Biogeosciences*, **6** (10),
3960 2099–2120.

3961 Thuburn, J., 2008: Some conservation issues for the dynamical cores of NWP and climate models.
3962 **227**, 3715–3730.

3963 Thuburn, J., and T. J. Woollings, 2005: Vertical discretizations for compressible Euler equation
3964 atmospheric models giving optimal representation of normal modes. **203**, 386–404.

3965 Tiedtke, M., 1989: A comprehensive mass flux scheme for cumulus parameterization in large-
3966 scale models. *Monthly Weather Review*, **117** (8), 1779–1800.

3967 Tiedtke, M., 1993: Representation of clouds in large-scale models. *Monthly Weather Review*,
3968 **121** (11), 3040–3061.

3969 Tokioka, T., 1978: Some considerations on vertical differencing. *Meteorological Society of Japan*
3970 *Journal*, **56**, 98–111.

3971 Tomita, H., H. Miura, S. Iga, T. Nasuno, and M. Satoh, 2005: A global cloud-resolving simulation:
3972 Preliminary results from an aqua planet experiment. *Geophysical Research Letters*, **32** (8).

3973 Tomita, H., and M. Satoh, 2004: A new dynamical framework of nonhydrostatic global model
3974 using the icosahedral grid. *Fluid Dynamics Research*, **34** (6), 357–400.

- 3975 Tompkins, A. M., 2002: A prognostic parameterization for the subgrid-scale variability of water
3976 vapor and clouds in large-scale models and its use to diagnose cloud cover. *J. Atmos. Sci.*,
3977 **59 (12)**, 1917–1942.
- 3978 Toy, M. D., and D. A. Randall, 2009: Design of a nonhydrostatic atmospheric model based on a
3979 generalized vertical coordinate. *Monthly Weather Review*, **137 (7)**, 2305–2330.
- 3980 Trenberth, K. E., 1999: Atmospheric moisture recycling: Role of advection and local evaporation.
3981 *Journal of Climate*, **12 (5)**, 1368–1381.
- 3982 Trenberth, K. E., and C. J. Guillemot, 1996: Physical processes involved in the 1988 drought and
3983 1993 floods in north america. *Journal of Climate*, **9 (6)**, 1288–1298.
- 3984 Troen, I., and L. Mahrt, 1986: A simple model of the atmospheric boundary layer; sensitivity to
3985 surface evaporation. *Boundary-Layer Meteorology*, **37 (1-2)**, 129–148.
- 3986 Tsamados, M., D. L. Feltham, and A. V. Wilchinsky, 2013: "impact of a new anisotropic rheology
3987 on simulations of arctic sea ice". *J. Geophys. Res.*, **118**, 91–107, 10.1029/2012JC007990.
- 3988 Tucker, C., I. Fung, C. Keeling, and R. Gammon, 1986: Relationship between atmospheric co2
3989 variations and a satellite-derived vegetation index. *Nature*, **319 (6050)**, 195.
- 3990 Tucker, C. J., 1979: Red and photographic infrared linear combinations for monitoring vegetation.
3991 *Remote sensing of Environment*, **8 (2)**, 127–150.
- 3992 Turner, A. K., E. C. Hunke, and C. M. Bitz, 2013: Two modes of sea-ice gravity drainage: A
3993 parameterization for large-scale modeling. *J. Geophys. Res.*, **118**, 2279–2294.
- 3994 Turner, D., and R. Ellingson, 2017: *The Atmospheric Radiation Measurement (ARM) Program:
3995 The First 20 Years*. American Meteorological Society.

- 3996 Untch, A., and M. Hortal, 2004: A finite-element scheme for the vertical discretization of the semi-
3997 lagrangian version of the ecmwf forecast model. *Quarterly Journal of the Royal Meteorological*
3998 *Society*, **130 (599)**, 1505–1530.
- 3999 Unterstrasser, S., and I. Sölch, 2010: Study of contrail microphysics in the vortex phase with
4000 a lagrangian particle tracking model. *Atmospheric Chemistry and Physics*, **10 (20)**, 10 003–
4001 10 015.
- 4002 Uppala, S. M., and Coauthors, 2005: The era-40 re-analysis. *Quarterly Journal of the royal mete-*
4003 *orological society*, **131 (612)**, 2961–3012.
- 4004 Vancoppenolle, M., T. Fichefet, and H. Goosse, 2009: "simulating the mass balance and salinity
4005 of arctic and antarctic sea ice. 2. importance of sea ice salinity variations". *Ocean Modelling*,
4006 **27**, 54–69.
- 4007 Veronis, G., 1975: The role of models in tracer studies. *Numerical models of ocean circulation*,
4008 133–146.
- 4009 Viterbo, P., and A. C. Beljaars, 1995: An improved land surface parameterization scheme in the
4010 ecmwf model and its validation. *Journal of Climate*, **8 (11)**, 2716–2748.
- 4011 Volodin, E., N. Dianskii, and A. Gusev, 2010: Simulating present-day climate with the inmcm4. 0
4012 coupled model of the atmospheric and oceanic general circulations. *Izvestiya, Atmospheric and*
4013 *Oceanic Physics*, **46 (4)**, 414–431.
- 4014 Von Humboldt, A., B. H. Paul, and W. S. Dallas, 1859: *Cosmos: a sketch of a physical description*
4015 *of the universe*, Vol. 5.

4016 Wan, H., and Coauthors, 2013: The icon-1.2 hydrostatic atmospheric dynamical core on trian-
4017 gular grids, part i: formulation and performance of the baseline version. *Geoscientific Model*
4018 *Development*, **6**, 735–763.

4019 Washington, W., 2007: *Odyssey in Climate Modeling, Global Warming, and Advising Five Presi-*
4020 *dents*. Lulu. com.

4021 Washington, W., and Coauthors, 2000: Parallel climate model (pcm) control and transient simula-
4022 tions. *Climate Dynamics*, **16 (10-11)**, 755–774.

4023 Washington, W. M., and A. Kasahara, 1970: A january simulation experiment with the two-layer
4024 version of the near global circulation model. *Monthly Weather Review*, **98 (8)**, 559–580.

4025 Washington, W. M., and G. A. Meehl, 1983: General circulation model experiments on the cli-
4026 matic effects due to a doubling and quadrupling of carbon dioxide concentration. *Journal of*
4027 *Geophysical Research: Oceans*, **88 (C11)**, 6600–6610.

4028 Washington, W. M., and G. A. Meehl, 1984: Seasonal cycle experiment on the climate sensitivity
4029 due to a doubling of co2 with an atmospheric general circulation model coupled to a simple
4030 mixed-layer ocean model. *Journal of Geophysical Research: Atmospheres*, **89 (D6)**, 9475–
4031 9503.

4032 Washington, W. M., and G. A. Meehl, 1989: Climate sensitivity due to increased co 2: experiments
4033 with a coupled atmosphere and ocean general circulation model. *Climate dynamics*, **4 (1)**, 1–38.

4034 Washington, W. M., and D. L. Williamson, 1977: A description of the near global circulation
4035 models. *Methods in Computational Physics: Advances in Research and Applications*, Vol. 17,
4036 Elsevier, 111–172.

- 4037 Weart, S., 2010: The development of general circulation models of climate. *Studies in History and*
4038 *Philosophy of Science Part B: Studies in History and Philosophy of Modern Physics*, **41 (3)**,
4039 208–217.
- 4040 Weart, S. R., 2008: *The discovery of global warming*. Harvard University Press.
- 4041 Webb, D. J., B. A. De Cuevas, and A. C. Coward, 1998: The first main run of the occam global
4042 ocean model. *Internal document*, **34**.
- 4043 Weller, H., S.-J. Lock, and N. Wood, 2013: Runge–kutta imex schemes for the horizontally ex-
4044 plicit/vertically implicit (hevi) solution of wave equations. *Journal of Computational Physics*,
4045 **252**, 365–381.
- 4046 Wenzel, S., P. M. Cox, V. Eyring, and P. Friedlingstein, 2014: Emergent constraints on climate-
4047 carbon cycle feedbacks in the cmip5 earth system models. *Journal of Geophysical Research:*
4048 *Biogeosciences*, **119 (5)**, 794–807.
- 4049 Wetherald, R., and S. Manabe, 1988: Cloud feedback processes in a general circulation model.
4050 *Journal of the Atmospheric Sciences*, **45 (8)**, 1397–1416.
- 4051 White, M. A., P. E. Thornton, and S. W. Running, 1997: A continental phenology model for mon-
4052 itoring vegetation responses to interannual climatic variability. *Global biogeochemical cycles*,
4053 **11 (2)**, 217–234.
- 4054 Wiin-Nielsen, A., 1991: The birth of numerical weather prediction. *Tellus A*, **43 (4)**, 36–52.
- 4055 Williamson, D., 1983: Description of the near community climate model (ccm0b). ncartechnical
4056 report ncar/tn-210+ str. *Boulder, Colo.: National Center for Atmospheric Research*.
- 4057 Williamson, D. L., 1968: Integration of the barotropic vorticity equation on a spherical geodesic
4058 grid. *Tellus*, **20 (4)**, 642–653.

- 4059 Williamson, D. L., 1997: Climate simulations with a spectral, semi-lagrangian model with linear
4060 grids. *Atmosphere-Ocean*, **35 (sup1)**, 279–292.
- 4061 Williamson, D. L., 2007: The evolution of dynamical cores for global atmospheric models. *Journal*
4062 *of the Meteorological Society of Japan. Ser. II*, **85**, 241–269.
- 4063 Williamson, D. L., L. M. Bath, R. K. Sato, T. A. Mayer, and M. L. Kuhn, 1983: Documentation
4064 of ncar ccm0b program modules. Tech. rep., Technical Report NCAR/TN-212+ IA, National
4065 Center for Atmospheric Research, Boulder, Colorado, NTIS No. PB83 263996, 198 pp.
- 4066 Williamson, D. L., and P. J. Rasch, 1994: Water vapor transport in the ncar ccm2. *Tellus A*, **46 (1)**,
4067 34–51.
- 4068 Willis, E. P., and W. H. Hooke, 2006: Cleveland abbe and american meteorology, 1871–1901.
4069 *Bulletin of the American Meteorological Society*, **87 (3)**, 315–326.
- 4070 Wing, A. A., K. A. Reed, M. Satoh, B. Stevens, S. Bony, and T. Ohno, 2018: Radiative-convective
4071 equilibrium model intercomparison project. *Geoscientific Model Development*, **11**, 793–813.
- 4072 Winninghoff, F. J., 1968: On the adjustment toward a geostrophic balance in a simple primitive
4073 equation model with application to the problems of initialization and objective analysis. *Ph.D.*
4074 *thesis, UCLA*.
- 4075 Winton, M., 2000: A reformulated three-layer sea ice model. *J. Atmos. Ocean. Technol.*, **17**, 525–
4076 531.
- 4077 Wiscombe, W. J., 1980: Improved Mie scattering algorithms. *Applied Opt.*, **19 (9)**, 1505–1509.
- 4078 Wood, N., and Coauthors, 2014: An inherently mass-conserving semi-implicit semi-Lagrangian
4079 discretisation of the deep-atmosphere global nonhydrostatic equations. *Quart. J. Roy. Meteor.*
4080 *Soc.*, **140**, 1505–1520, doi:10.1002/qj.2235.

- 4081 Woods, A., 2006: Medium range weather prediction. USA: Springer Publications.
- 4082 Woodward, F., and M. Lomas, 2004: Vegetation dynamics—simulating responses to climatic
4083 change. *Biological reviews*, **79** (3), 643–670.
- 4084 Yamaguchi, T., G. Feingold, and V. E. Larson, 2017: Framework for improvement by vertical
4085 enhancement: A simple approach to improve representation of low and high-level clouds in
4086 large-scale models. *Journal of Advances in Modeling Earth Systems*, **9** (1), 627–646.
- 4087 Yeh, K.-S., J. Côté, S. Gravel, A. Méthot, A. Patoine, M. Roch, and A. Staniforth, 2002: The CMC-
4088 MRB Global Environmental Multiscale (GEM) model. Part III: Nonhydrostatic formulation.
4089 *Mon. Wea. Rev.*, **130**, 339–356.
- 4090 Yuan, H., Y. Dai, R. E. Dickinson, B. Pinty, W. Shangguan, S. Zhang, L. Wang, and S. Zhu,
4091 2017: Reexamination and further development of two-stream canopy radiative transfer models
4092 for global land modeling. *Journal of Advances in Modeling Earth Systems*, **9** (1), 113–129.
- 4093 Zängl, G., D. Reinert, P. Rípodas, and M. Baldauf, 2015: The icon (icosahedral non-hydrostatic)
4094 modelling framework of dwd and mpi-m: Description of the non-hydrostatic dynamical core.
4095 *Quarterly Journal of the Royal Meteorological Society*, **141** (687), 563–579.
- 4096 Zapotocny, T. H., D. R. Johnson, and F. M. Reames, 1994: Development and initial test of the
4097 university of wisconsin global isentropic–sigma model. *Monthly weather review*, **122** (9), 2160–
4098 2178.
- 4099 Zarzycki, C. M., and C. Jablonowski, 2015: Experimental tropical cyclone forecasts using a
4100 variable-resolution global model. *Monthly Weather Review*, **143** (10), 4012–4037.

4101 Zdunkowski, W. G., R. M. Welch, and G. J. Korb, 1980: An investigation of the structure of typical
4102 two-stream methods for the calculation of solar fluxes and heating rates in clouds. *Beiträge zur*
4103 *Physik Atmosphäre*, **53**, 147–166.

4104 Zhang, J., and W. D. Hibler III, 1997: On an efficient numerical method for modeling sea ice
4105 dynamics. *J. Geophys. Res.*, **102**, 8691–8702.

4106 Zhang, X., M. A. Friedl, C. B. Schaaf, A. H. Strahler, J. C. Hodges, F. Gao, B. C. Reed, and
4107 A. Huete, 2003: Monitoring vegetation phenology using modis. *Remote sensing of environment*,
4108 **84 (3)**, 471–475.

4109 Zhao, M., and Coauthors, 2016: Uncertainty in model climate sensitivity traced to representations
4110 of cumulus precipitation microphysics. *Journal of Climate*, **29 (2)**, 543–560.

4111 Zhao, Q., T. L. Black, and M. E. Baldwin, 1997: Implementation of the cloud prediction scheme
4112 in the eta model at ncep. *Weather and forecasting*, **12 (3)**, 697–712.

4113 Zhu, Z., J. Thuburn, B. J. Hoskins, and P. H. Haynes, 1992: A vertical finite-difference scheme
4114 based on a hybrid σ - θ - p coordinate. *Monthly weather review*, **120 (5)**, 851–862.

4115 Ziegler, C. L., 1985: Retrieval of thermal and microphysical variables in observed convective
4116 storms. part 1: Model development and preliminary testing. *Journal of the atmospheric sciences*,
4117 **42 (14)**, 1487–1509.

4118 FIGURES

4119 **LIST OF FIGURES**

4120 **Fig. 1.** Left: Cleveland Abbe (1838-1916). Centre: Vilhelm Bjerknes (1862-1951). Right: Lewis
4121 Fry Richardson (1881-1953) 184

4122 **Fig. 2.** The Electronic Numerical Integrator and Computer (ENIAC)) 185

4123 **Fig. 3.** Schematic showing the vertical placement of the horizontal velocity components u and v and
4124 potential temperature θ on the Charney-Phillips and Lorenz grids. 186

4125 **Fig. 4.** A schematic of the early GFDL model from Manabe (1969b). 187

4126 **Fig. 5.** a) Diagram of the Kessler microphysics parameterization. b) Diagram of a typical two-
4127 moment parameterization with multiple ice classes. 188

4128 **Fig. 6.** Some examples of spherical harmonics. Spherical harmonics are wavelike functions defined
4129 on the surface of a sphere. They are spherical analogues of the sines and cosines that provide
4130 a basis for Fourier series in one dimension. 189

4131 **Fig. 7.** Schematic showing the horizontal distribution of variables on the B- grid (left), C-grid (cen-
4132 ter), and Z-grid (right). Here, u is the eastward velocity component, v is the northward
4133 velocity component, p is the pressure, ζ is the vertical component of vorticity, and δ is the
4134 horizontal velocity divergence. 190

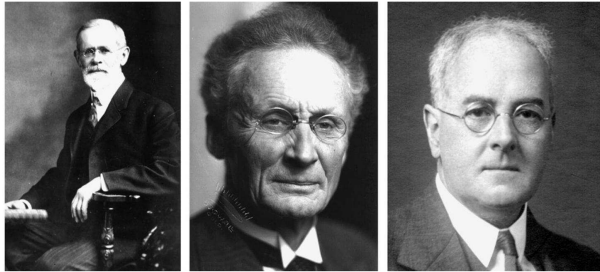
4135 **Fig. 8.** Flow diagram (courtesy of Albert Semtner, Jr.) showing relationships among numerical
4136 ocean codes originating from the methods of Bryan (1969b). The Bryan (1969b) algorithm
4137 was the basis for Cox’s code at GFDL and the starting point for extensions made by Semtner
4138 (1974) at UCLA. The Semtner (1974) branch on the left led to the Parallel Ocean Climate
4139 Model (POCM) used at NCAR and the Naval Postgraduate School (NPS). It also fostered the
4140 Parallel Ocean Program (POP) developed at the Los Alamos National Laboratory (LANL).
4141 The Cox (1984) code formed the basis of the Fine Resolution Antarctic Model (FRAM)
4142 developed in the UK by Peter Killworth and David Webb. The OCCAM project in the UK
4143 (Webb et al. 1998) was among the first global models with active mesoscale eddy variability
4144 (using resolutions as fine as $1/12^\circ$). On the right side of the diagram are Modular Ocean
4145 Model versions 1 and 2 (MOM1 and MOM2), representing the GFDL descendants of the
4146 Bryan-Cox code. On the far right are the NCAR efforts with NCOM (Gent et al. 1998,
4147 NCAR CSM Ocean Model) and CSM (Climate System Model). 191

4148 **Fig. 9.** The treatments of radiation in global models have been compared to benchmark “line-by-
4149 line” calculations for many decades. Panel a) shows results for longwave fluxes at the sur-
4150 face and the tropopause in a single idealized but quasi-realistic atmosphere. The line-by-line
4151 models, shown as plus signs, agree with each other quite well, partly because they share the
4152 same spectroscopic data; by comparison both narrow- and wide-band models (“NBMs” and
4153 “WBMs” respectively) show significantly more variation. Panel b), published fifteen years
4154 later, focuses on forcing i.e. the change in flux caused by a change in composition, here the
4155 impacts of methane and nitrous oxide. Line-by-line calculations are indistinguishable from
4156 one another while the GCMs show variation of 25% or more of the signal in the longwave
4157 while entirely ignoring the impact in the shortwave. Panel c), appearing almost a decade later
4158 still, shows that errors in GCM parameterizations (circles) still swamp those from line-by-
4159 line models (squares) in calculations of the forcing by quadrupled carbon dioxide concen-
4160 trations. Panel a is Fig. 15 of Ellingson et al. (1991); Panel b is Figure 6 of Collins et al.
4161 (2006b); panel c is redrawn from Figure 3 and supplementary material in Pincus et al. (2015). . . 192

4162 **Fig. 10.** Equivalent resistor networks used to represent surface energy flux in land surface models
4163 of several levels of complexity. T is temperature, e is vapor pressure, and g is conductance
4164 (transfer coefficient). Subscripts a, s, c, v, and g refer to lowest atmospheric layer, surface,
4165 canopy air space, vegetation, and ground surface respectively. Subscripts h and w refer to
4166 sensible and latent heat respectively. From Bonan (2015). 193

4167 **Fig. 11.** Schematic of sea ice state variables and surface fluxes that are predicted within a grid cell of
4168 an Earth system model. It is common for the sea ice thickness distribution to be resolved in
4169 five discrete categories, each with a unique thickness range, and another category for open
4170 water. Schematic redrawn from Notz and Bitz (2017). 194

4171 **Fig. 12.** Three examples of quasi-uniform spherical grids. Left: cubed sphere; center: hexagonal-
4172 icosahedral grid; right: yin-yang grid. In practice the resolutions used would be much finer
4173 than shown here. 195



4174 FIG. 1. Left: Cleveland Abbe (1838-1916). Centre: Vilhelm Bjerknes (1862-1951). Right: Lewis Fry
4175 Richardson (1881-1953)

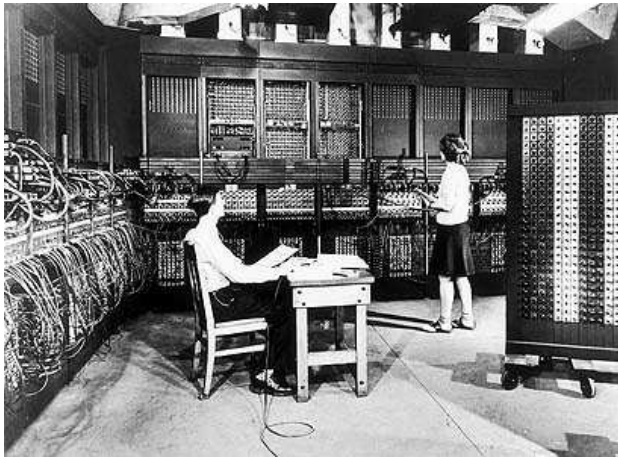
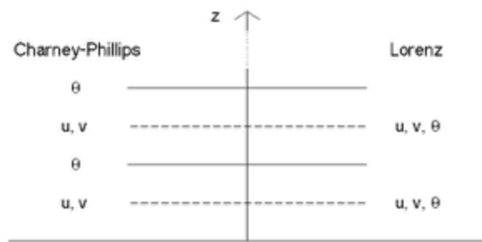


FIG. 2. The Electronic Numerical Integrator and Computer (ENIAC))



4176 FIG. 3. Schematic showing the vertical placement of the horizontal velocity components u and v and potential
 4177 temperature θ on the Charney-Phillips and Lorenz grids.

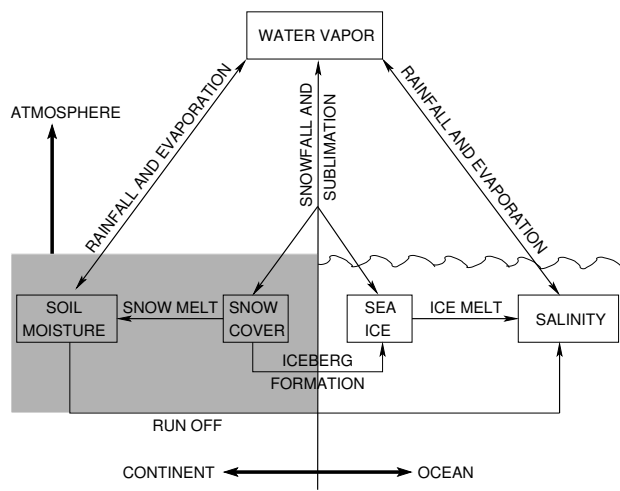
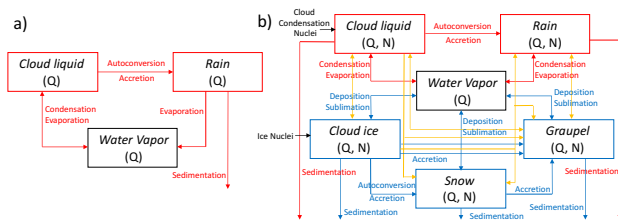
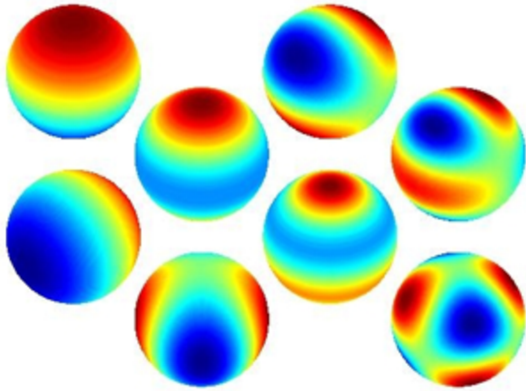


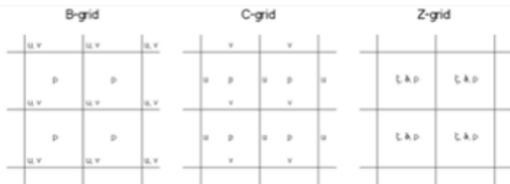
FIG. 4. A schematic of the early GFDL model from Manabe (1969b).



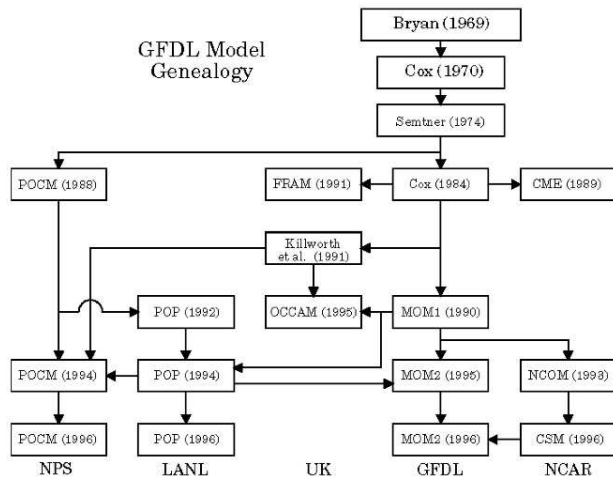
4178 FIG. 5. a) Diagram of the Kessler microphysics parameterization. b) Diagram of a typical two-moment
 4179 parameterization with multiple ice classes.



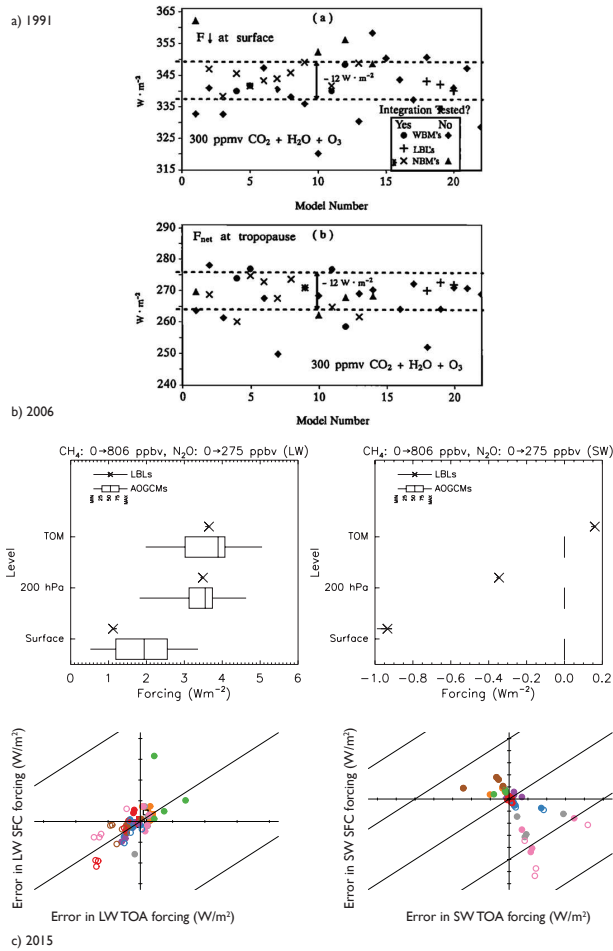
4180 FIG. 6. Some examples of spherical harmonics. Spherical harmonics are wavelike functions defined on the
4181 surface of a sphere. They are spherical analogues of the sines and cosines that provide a basis for Fourier series
4182 in one dimension.



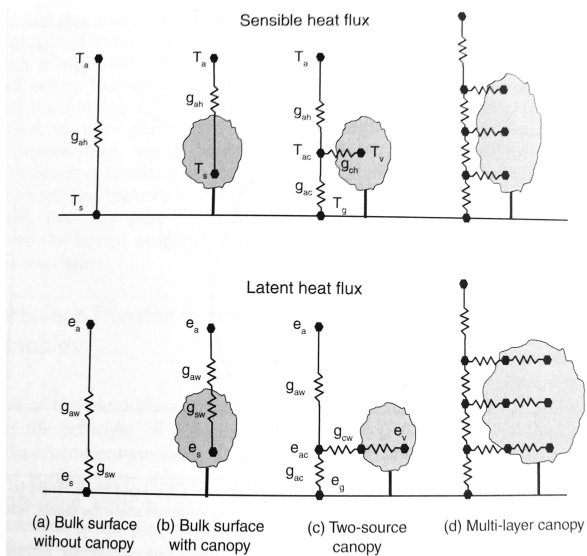
4183 FIG. 7. Schematic showing the horizontal distribution of variables on the B- grid (left), C-grid (center), and
 4184 Z-grid (right). Here, u is the eastward velocity component, v is the northward velocity component, p is the
 4185 pressure, ζ is the vertical component of vorticity, and δ is the horizontal velocity divergence.



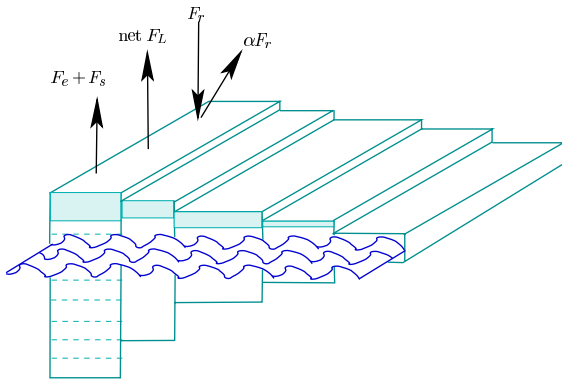
4186 FIG. 8. Flow diagram (courtesy of Albert Semtner, Jr.) showing relationships among numerical ocean codes
 4187 originating from the methods of Bryan (1969b). The Bryan (1969b) algorithm was the basis for Cox's code at
 4188 GFDL and the starting point for extensions made by Semtner (1974) at UCLA. The Semtner (1974) branch on
 4189 the left led to the Parallel Ocean Climate Model (POCM) used at NCAR and the Naval Postgraduate School
 4190 (NPS). It also fostered the Parallel Ocean Program (POP) developed at the Los Alamos National Laboratory
 4191 (LANL). The Cox (1984) code formed the basis of the Fine Resolution Antarctic Model (FRAM) developed in
 4192 the UK by Peter Killworth and David Webb. The OCCAM project in the UK (Webb et al. 1998) was among
 4193 the first global models with active mesoscale eddy variability (using resolutions as fine as $1/12^\circ$). On the right
 4194 side of the diagram are Modular Ocean Model versions 1 and 2 (MOM1 and MOM2), representing the GFDL
 4195 descendants of the Bryan-Cox code. On the far right are the NCAR efforts with NCOM (Gent et al. 1998,
 4196 NCAR CSM Ocean Model) and CSM (Climate System Model).



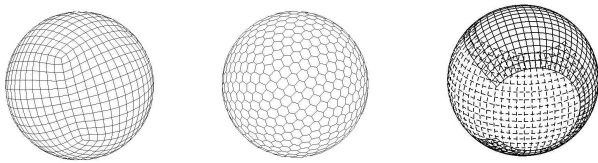
4197 FIG. 9. The treatments of radiation in global models have been compared to benchmark “line-by-line” calcu-
 4198 lations for many decades. Panel a) shows results for longwave fluxes at the surface and the tropopause in a single
 4199 idealized but quasi-realistic atmosphere. The line-by-line models, shown as plus signs, agree with each other
 4200 quite well, partly because they share the same spectroscopic data; by comparison both narrow- and wide-band
 4201 models (“NBMs” and “WBMs” respectively) show significantly more variation. Panel b), published fifteen years
 4202 later, focuses on forcing i.e. the change in flux caused by a change in composition, here the impacts of methane
 4203 and nitrous oxide. Line-by-line calculations are indistinguishable from one another while the GCMs show vari-
 4204 ation of 25% or more of the signal in the longwave while entirely ignoring the impact in the shortwave. Panel
 4205 c, appearing almost a decade later still, shows that errors in GCM parameterizations (circles) still swamp those
 4206 from line-by-line models (squares) in calculations of the forcing by quadrupled carbon dioxide concentrations.
 4207 Panel a is Fig. 15 of Ellingson et al. (1991); Panel b is Figure 6 of Collins et al. (2006b); panel c is redrawn from
 4208 Figure 3 and supplementary material in Pincus et al. (2015).



4209 FIG. 10. Equivalent resistor networks used to represent surface energy flux in land surface models of several
 4210 levels of complexity. T is temperature, e is vapor pressure, and g is conductance (transfer coefficient). Subscripts
 4211 a , s , c , v , and g refer to lowest atmospheric layer, surface, canopy air space, vegetation, and ground surface
 4212 respectively. Subscripts h and w refer to sensible and latent heat respectively. From Bonan (2015).



4213 FIG. 11. Schematic of sea ice state variables and surface fluxes that are predicted within a grid cell of an Earth
 4214 system model. It is common for the sea ice thickness distribution to be resolved in five discrete categories, each
 4215 with a unique thickness range, and another category for open water. Schematic redrawn from Notz and Bitz
 4216 (2017).



4217 FIG. 12. Three examples of quasi-uniform spherical grids. Left: cubed sphere; center: hexagonal-icosahedral
4218 grid; right: yin-yang grid. In practice the resolutions used would be much finer than shown here.